Spectral evolution in GRBs: confronting the predictions of the internal shock model to observations in the *Fermi* era

Bošnjak Željka

University of Rijeka, Croatia & CEA - Saclay, France

in collaboration with:

Frédéric Daigne, ***Institut d'Astrophysique de Paris***

Extreme Universe Laboratory Workshop on Gamma-Ray Bursts - Moscow, October 2013

High energy gamma ray emission

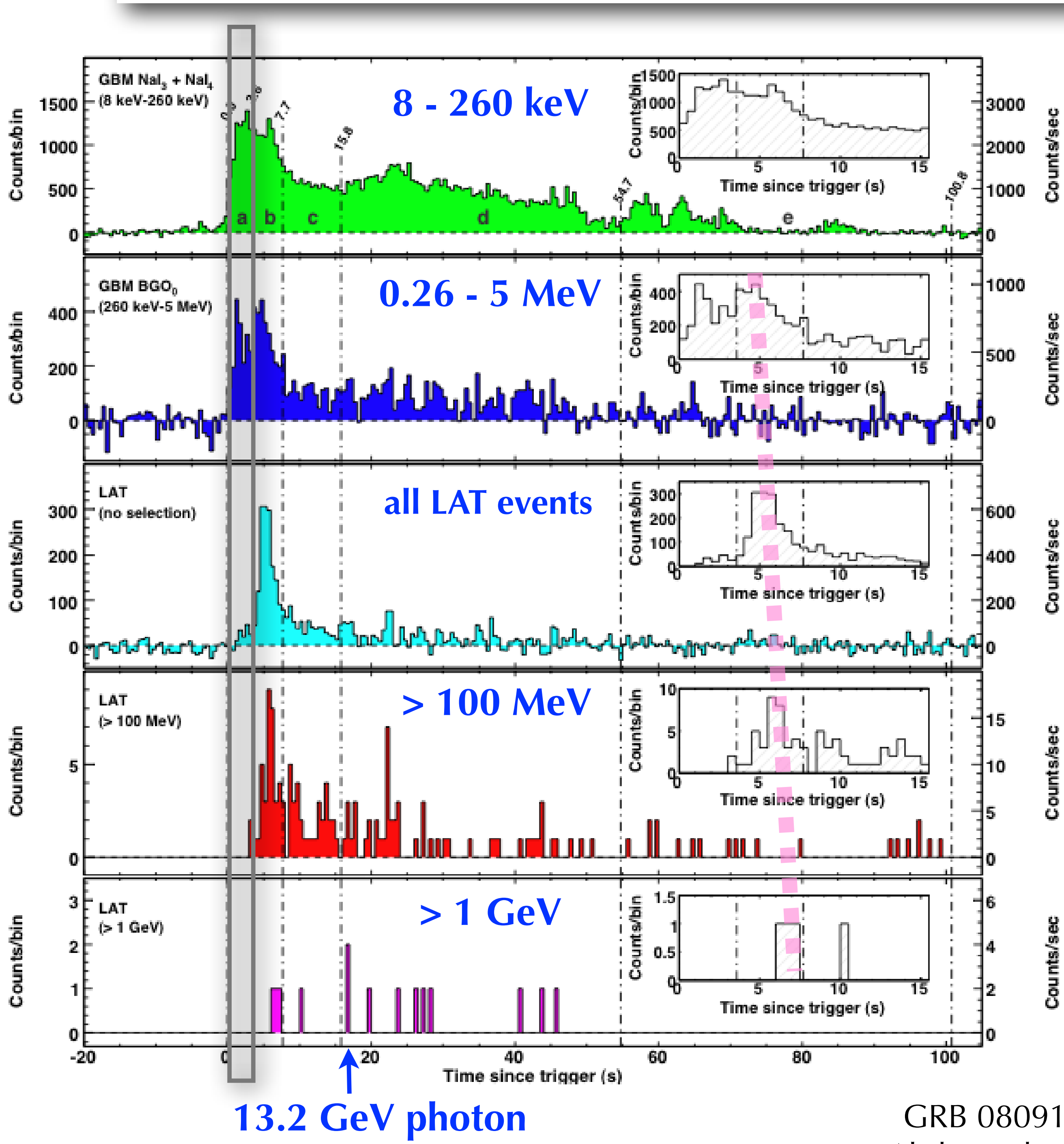

GRB 080916C
Abdo et al. 2008

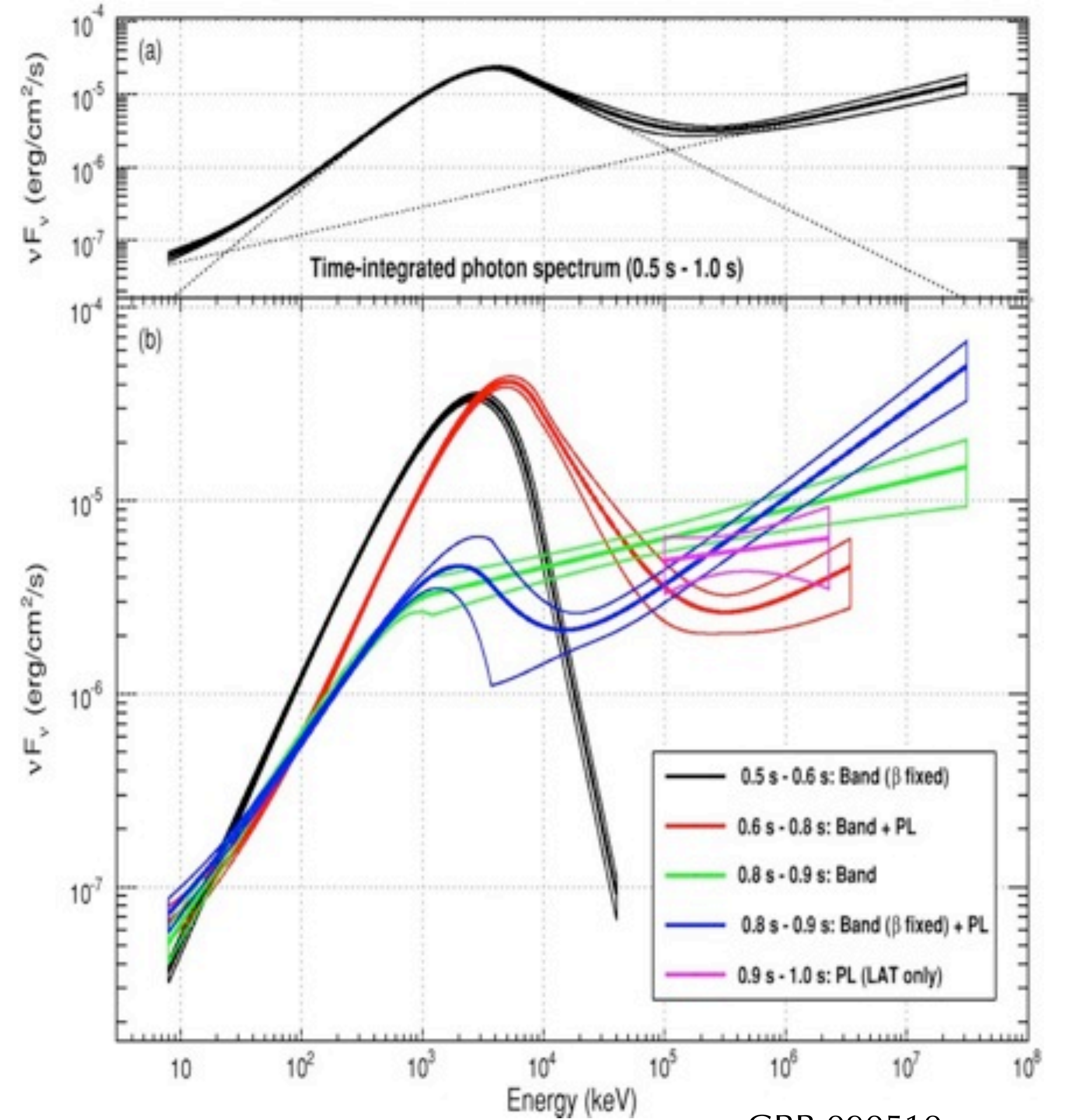

GRB 090510
Ackermann et al. 2010

Fermi/LAT observations:

Delayed onset of high energy (>100 MeV) emission

Long lived high energy emission

Deviation from the usual GRB spectral models: **extra component**

Sub-MeV emission

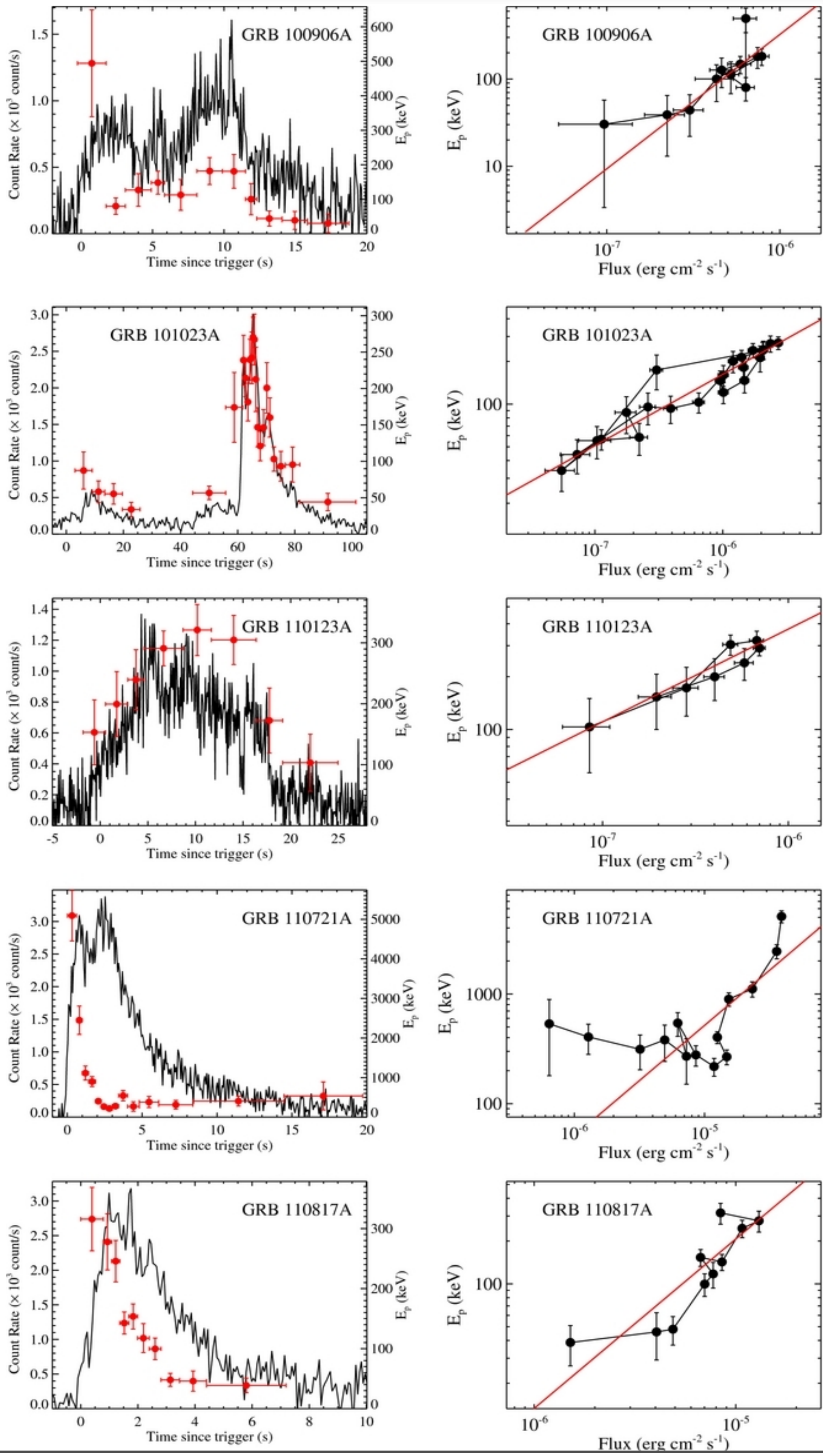

Lu et al. 2012

Ferm/GBM observations:

hard-to-soft evolution

hardness maximum preceding the peak of the intensity

hardness-intensity correlation: $E_{p,obs} \propto F(t)^{\kappa}$, $\kappa \simeq 0.4\text{-}1.2$

energy-dependent pulse asymmetry: $W(E_{obs}) \propto E_{obs}^{-a}$

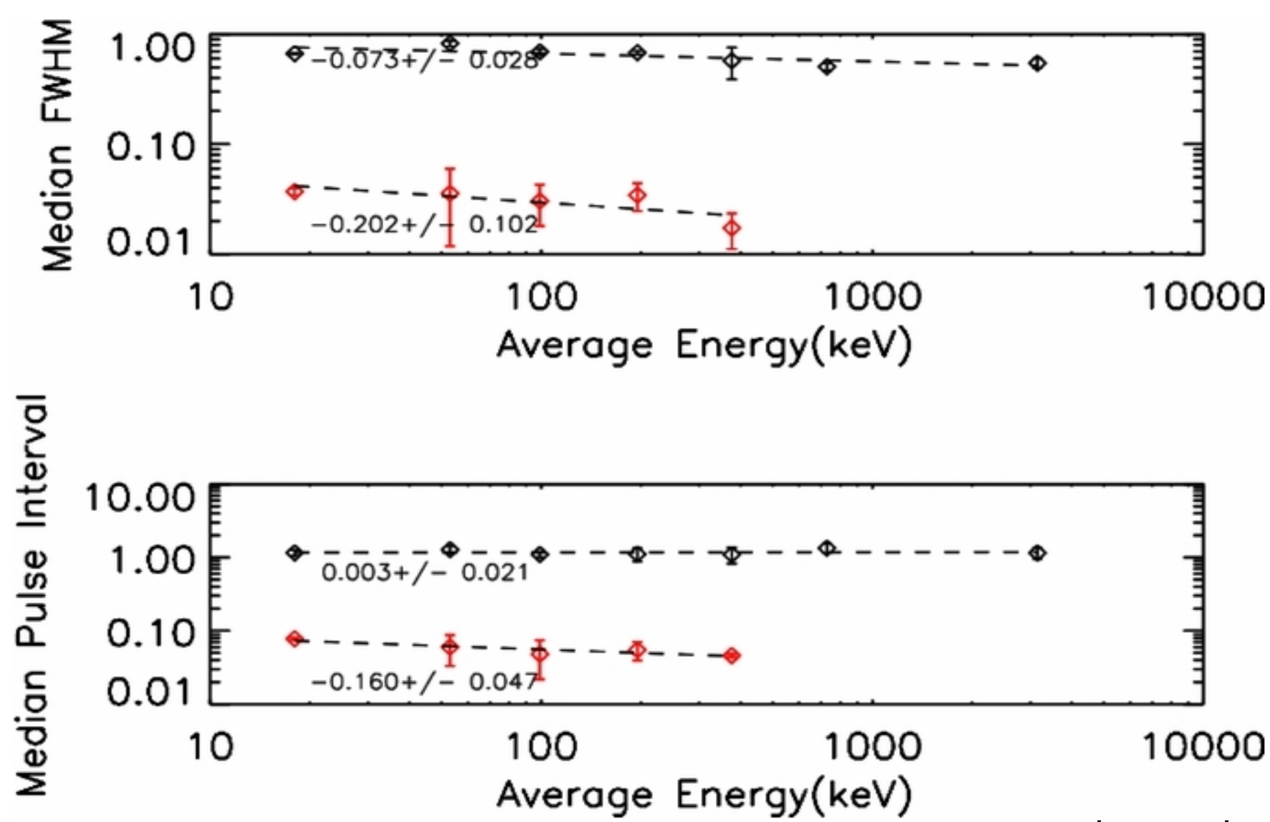

Bhat et al. 2012

Prompt high energy emission in the framework of internal shocks

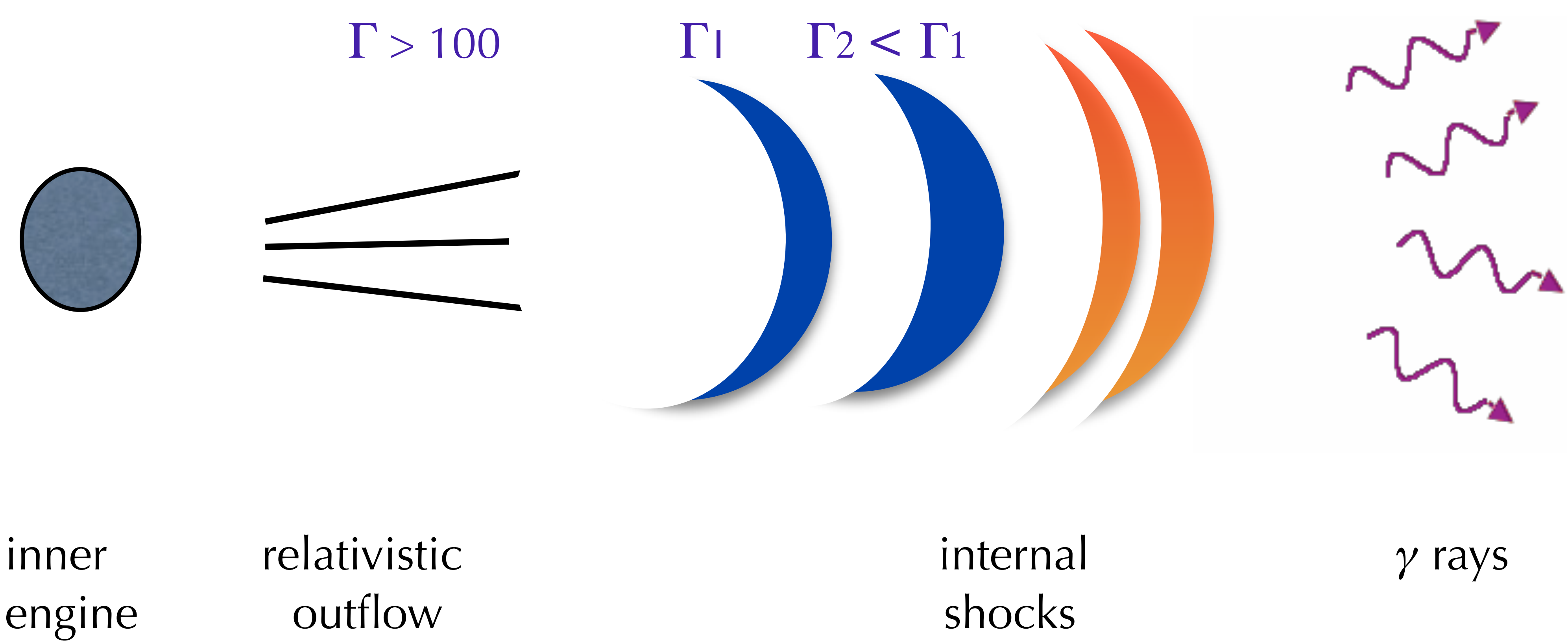

Modeling:

1. dynamics of internal shocks

2. radiative processes in the shocked medium

3. observed spectra and time profiles

Dynamics of the internal shocks

Input parameters: distribution of Lorentz factors **$\Gamma(t)$**, kinetic energy rate **dE/dt** during the relativistic ejection, total duration of the ejection phase **t_w**

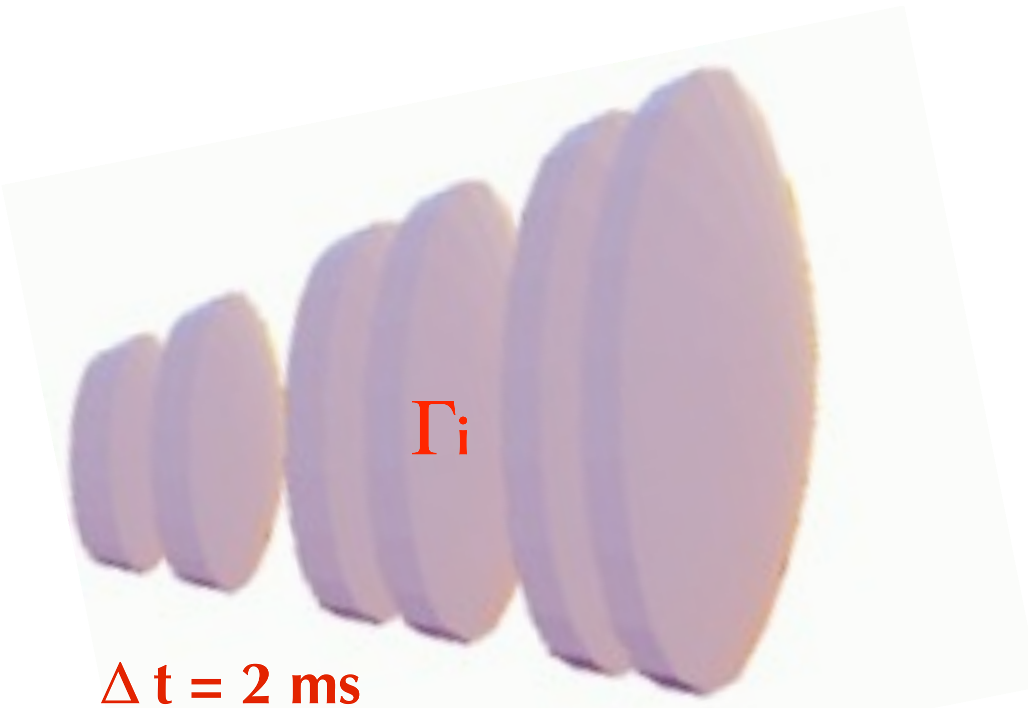

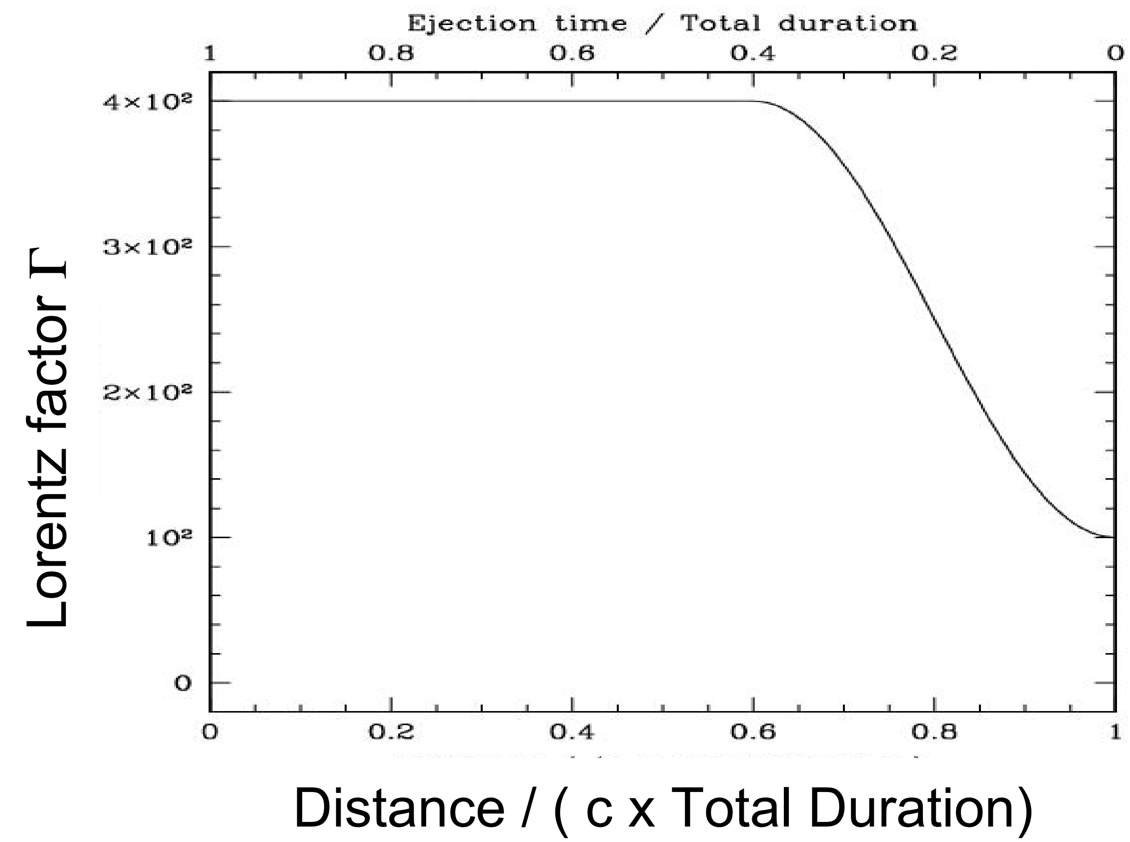

$\Delta t = 2$ ms

$t_w \sim 2$ s, $N = 1000$

$M_i \sim 1 / \Gamma_i$

$$R_{IS,\,start} \sim \Gamma^2 c t_{var} \sim 3 \times 10^{11}\ \mathrm{cm}\ (\Gamma/100)^2 (t_{var}/1\ \mathrm{ms})$$

$$R_{IS,\,end} \sim \Gamma^2 c t_w \sim 3 \times 10^{15}\ \mathrm{cm}\ (\Gamma/100)^2 (t_w/10\ \mathrm{s})$$

Dissipated energy: from 6% ($\Gamma_2 / \Gamma_1 = 2$) to 43 % ($\Gamma_2 / \Gamma_1 = 10$)

Daigne & Mochkovitch 2000: the simplified approach for the dynamics has been confirmed by a comparison with a full hydrodynamical calculation

Dynamics of the internal shocks

Physical conditions in the shocked medium: Lorentz factor Γ_*, comoving density ρ^*, comoving specific energy density ε^*

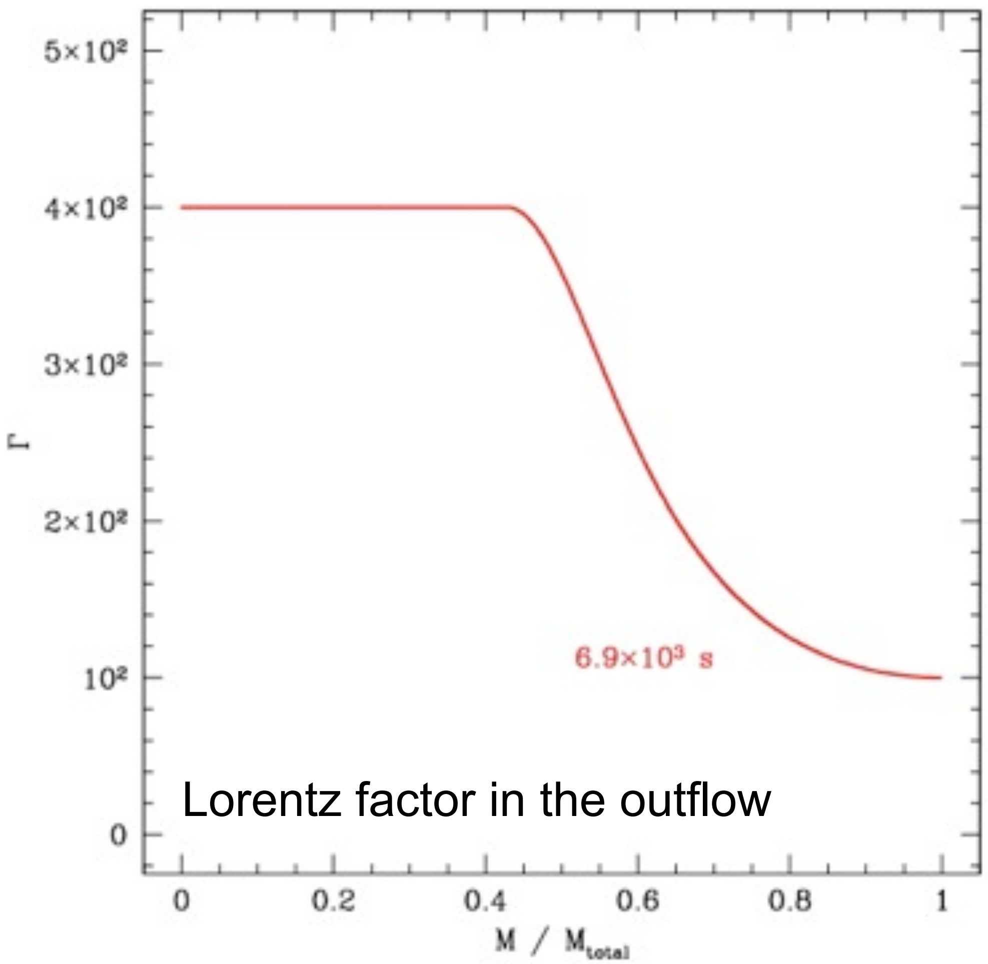

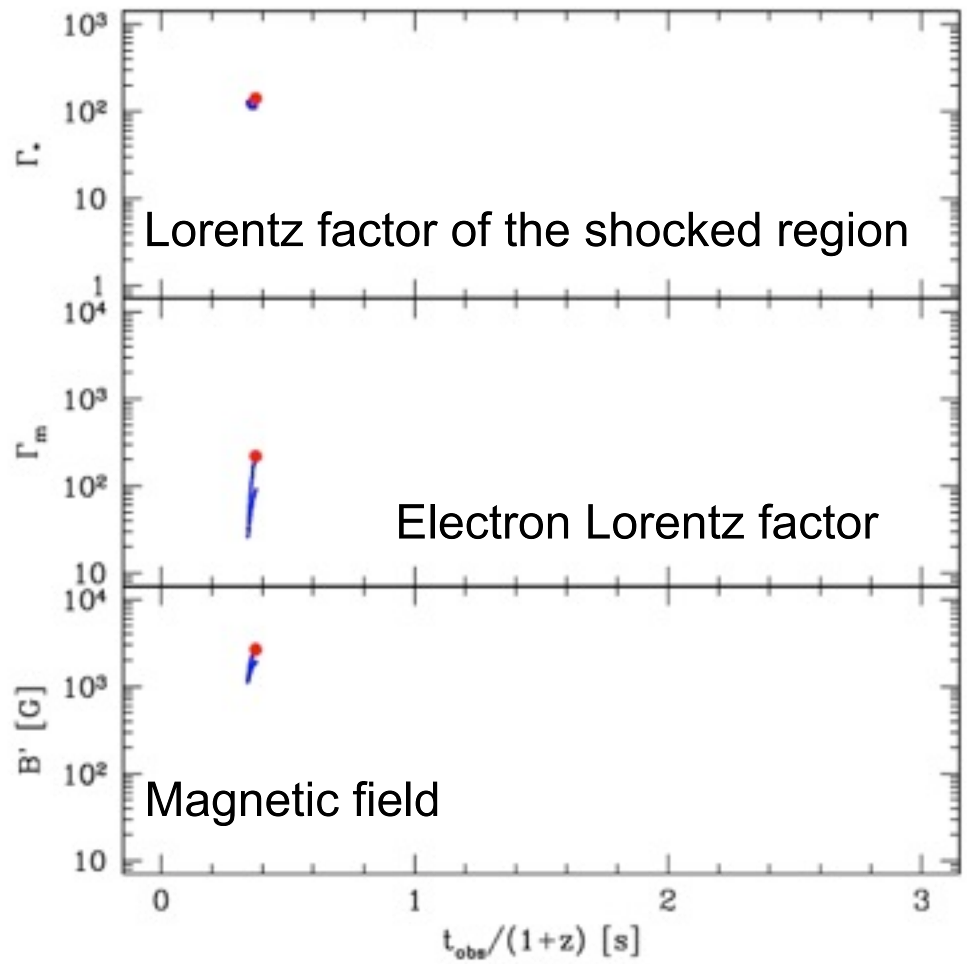

Dissipated energy is distributed between protons, electrons (fraction ε_e) and magnetic field (fraction ε_B)

Dynamics of the internal shocks

Physical conditions in the shocked medium: Lorentz factor Γ_*, comoving density ρ^*, comoving specific energy density ε^*

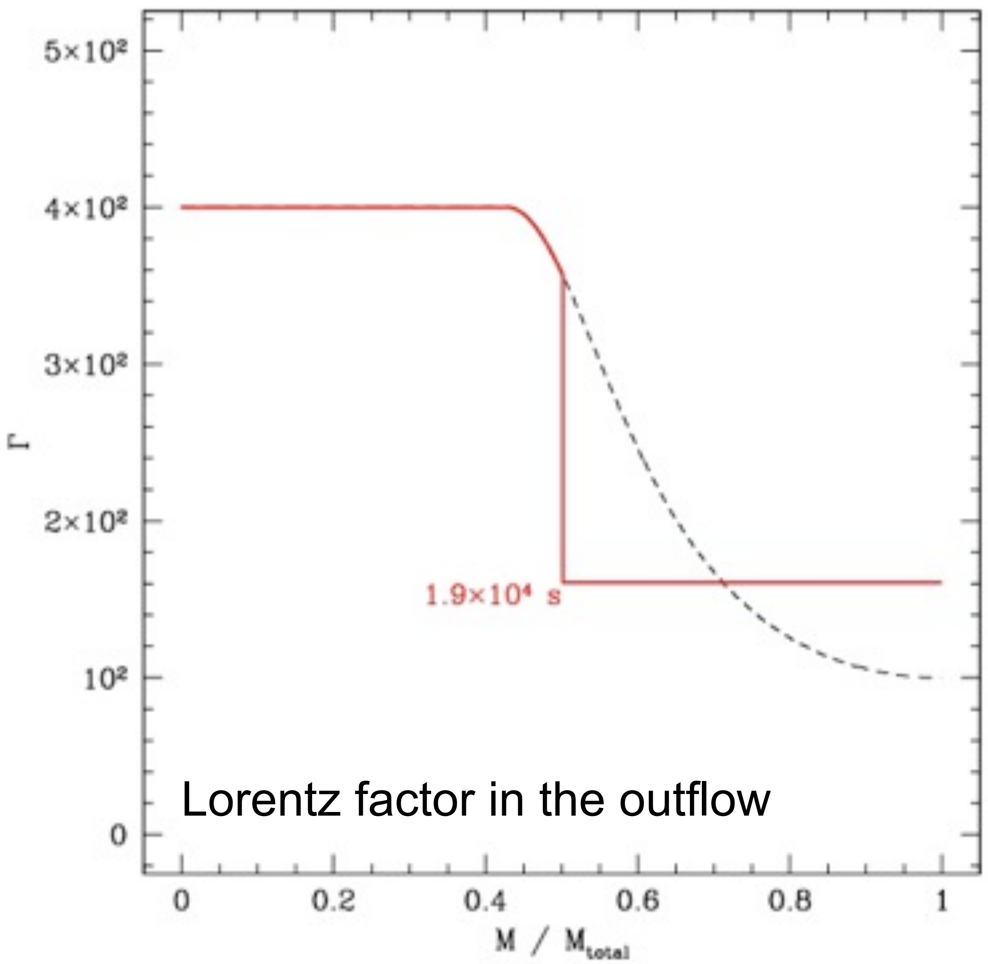

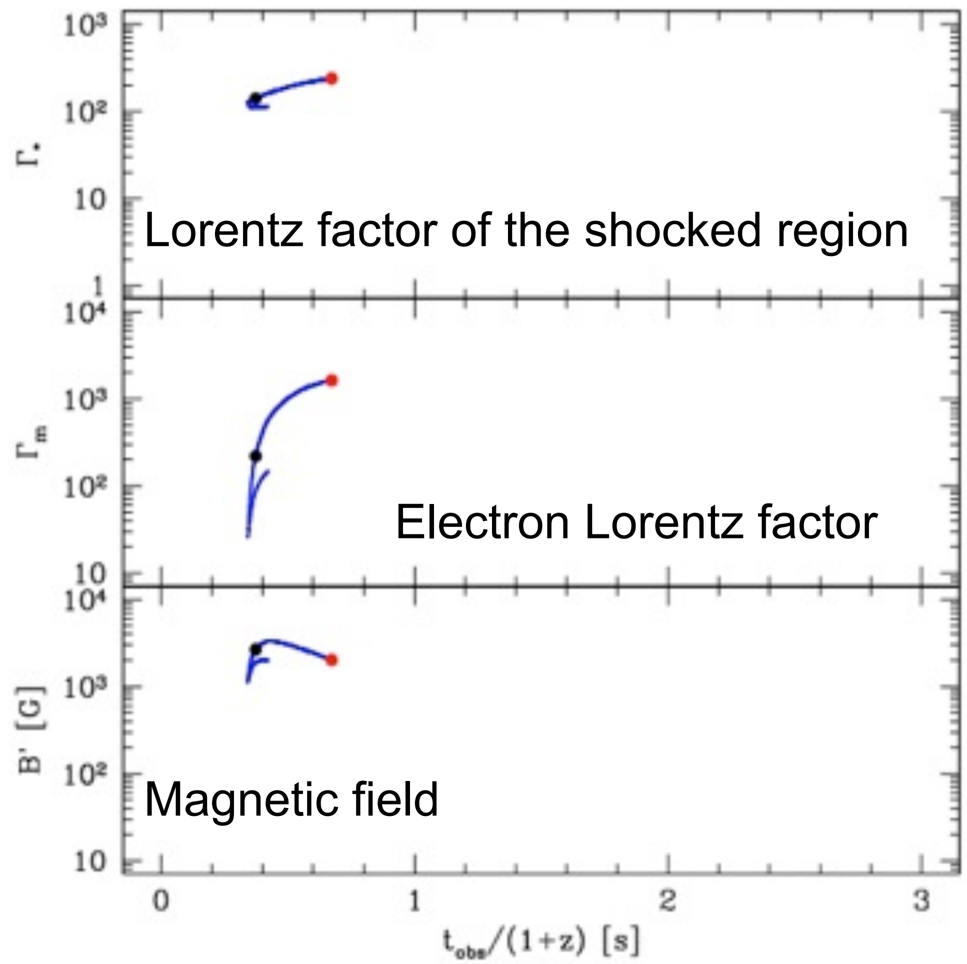

Dissipated energy is distributed between protons, electrons (fraction ε_e) and magnetic field (fraction ε_B)

Dynamics of the internal shocks

Physical conditions in the shocked medium: Lorentz factor Γ_*, comoving density ρ^*, comoving specific energy density ε^*

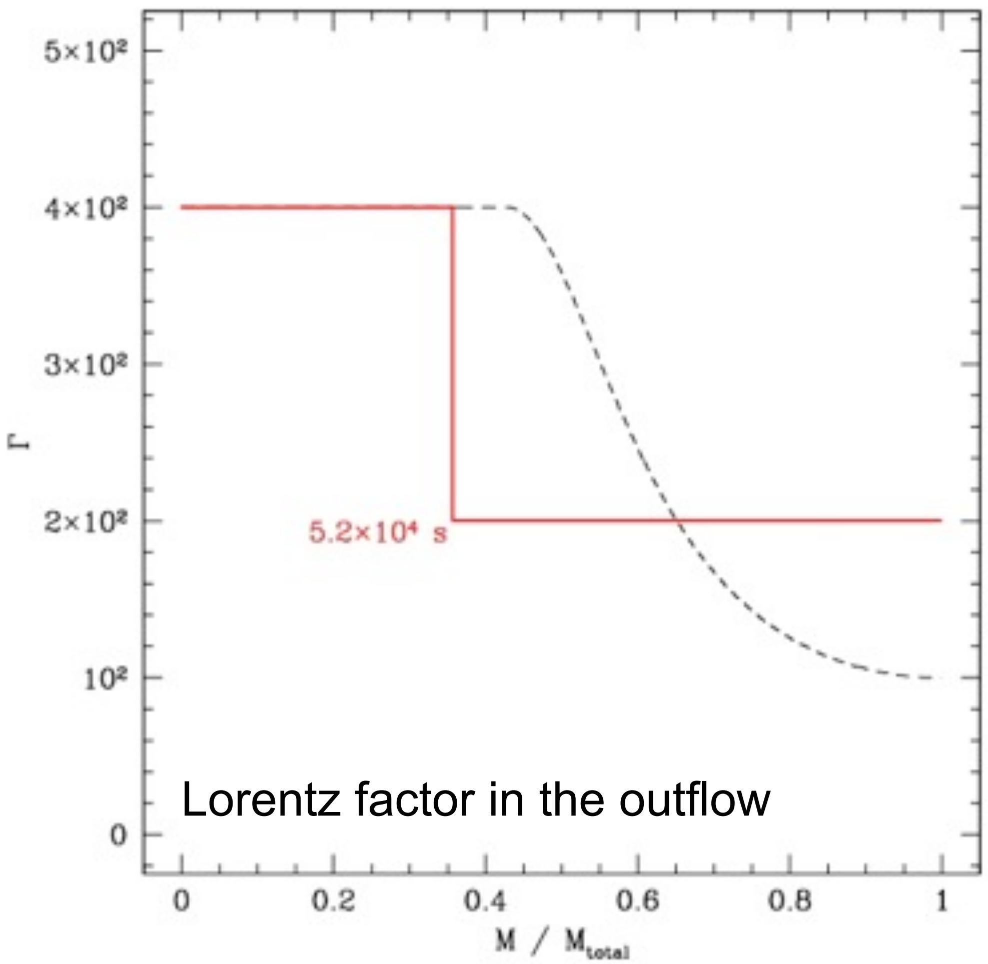

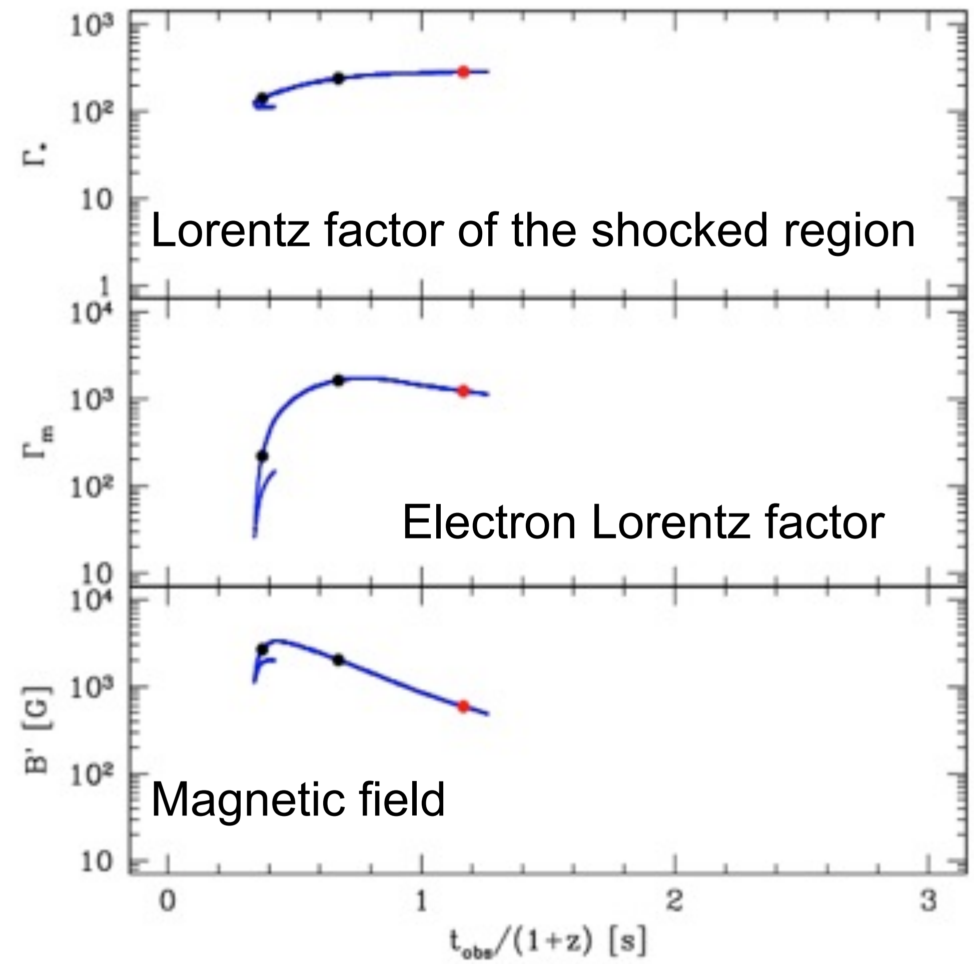

Dissipated energy is distributed between protons, electrons (fraction ε_e) and magnetic field (fraction ε_B)

Dynamics of the internal shocks

Physical conditions in the shocked medium: Lorentz factor Γ_*, comoving density ρ^*, comoving specific energy density ε^*

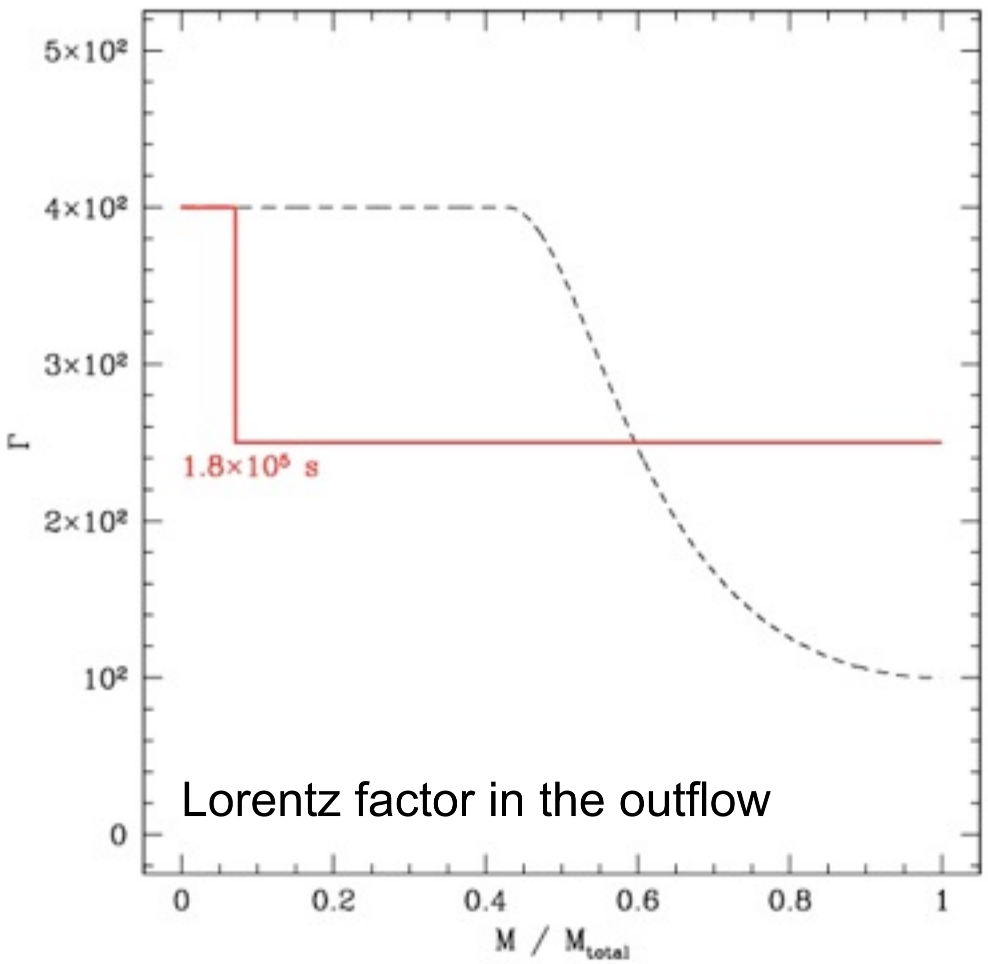

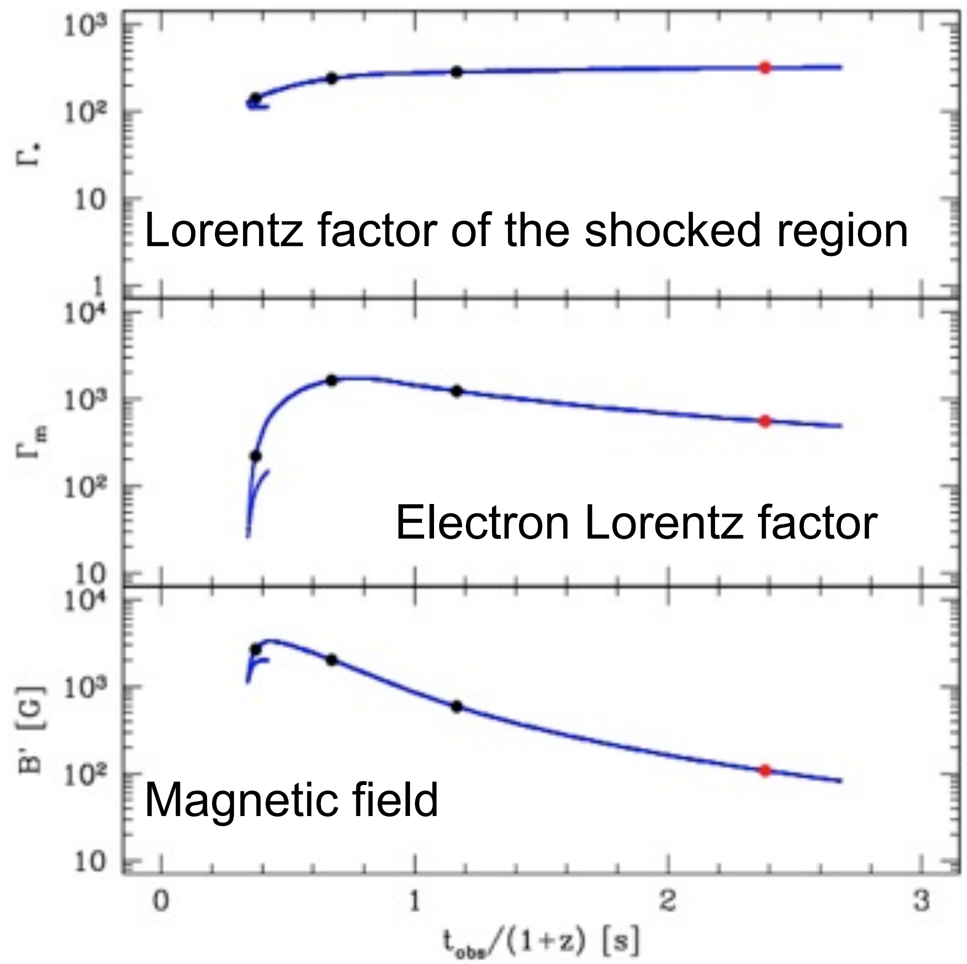

Dissipated energy is distributed between protons, electrons (fraction ε_e) and magnetic field (fraction ε_B)

Dynamics of the internal shocks

Physical conditions in the shocked medium: Lorentz factor Γ_*, comoving density ρ^*, comoving specific energy density ε^*

Relativistic electron density:

$$n'(\Gamma_e, t'=0) \propto \Gamma_e^{-p} \qquad \Gamma_e \geq \Gamma_m$$

$\zeta < 1$ of all electrons is accelerated (e.g. Bykov & Meszaros 1996)

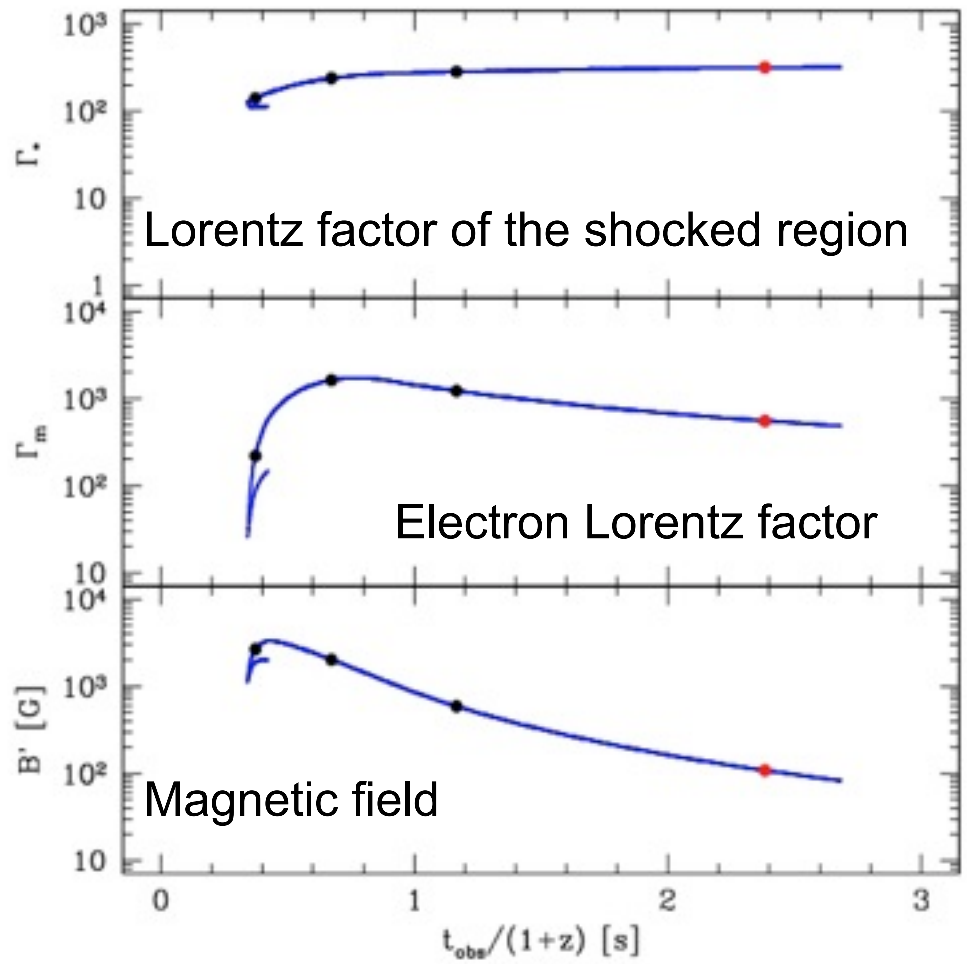

Radiative processes

Assumption: instantaneous shock acceleration

Adiabatic cooling timescale: $t'_{ex} = R / \Gamma^* c$ (comoving frame)

Radiative timescale: t'_{rad}

$t'_{rad} << t'_{ex}$ high radiative efficiency

Electron and photon distributions evolve strongly with time!

Radiative processes

Assumption: instantaneous shock acceleration

Adiabatic cooling timescale: $t'_{ex} = R / \Gamma^* c$ (comoving frame)
Radiative timescale: t'_{rad}

$t'_{rad} << t'_{ex}$ high radiative efficiency

Electron and photon distributions evolve strongly with time!

The present version of the code follows the time evolution of the electron density $n'_e(\Gamma'_e, t')$ and the photon density $n'_{\nu'}(t')$ including the following processes:

- **adiabatic cooling (spherical expansion)**
- **synchrotron**
- **inverse Compton**
- **synchrotron self-absorption**
- **$\gamma\gamma$ annihilation**

Not included:
*** emission from secondary leptons**
*** IC in optically thick regime (Comptonization)**

ELECTRONS:

$$\frac{\partial n'}{\partial t'}(\Gamma'_e, t') = -\frac{\partial}{\partial \Gamma'_e}\left[\left(\frac{d\Gamma'_e}{dt'}\bigg|_{syn+ic} + \frac{d\Gamma'_e}{dt'}\bigg|_{ad}\right) n'(\Gamma'_e, t')\right]$$

PHOTONS:

$$\frac{\partial n'_\nu}{\partial t'} = \int n'(\Gamma'_e, t') P_{syn+ic}(\Gamma'_e) d\Gamma'_e - c n'_\nu \int n'(\Gamma'_e, t') \sigma_{abs}(\Gamma'_e, \nu) d\Gamma'_e - c n'_\nu \int_{\nu' > \frac{(m_e c^2)^2}{h^2 \nu}} n'_{\nu'}(t') \sigma_{\gamma\gamma}(\nu, \nu') d\nu'$$

Radiative processes

Radiation: the time evolution of electrons and photons in **the comoving frame** is solved (time-dependent radiative code)

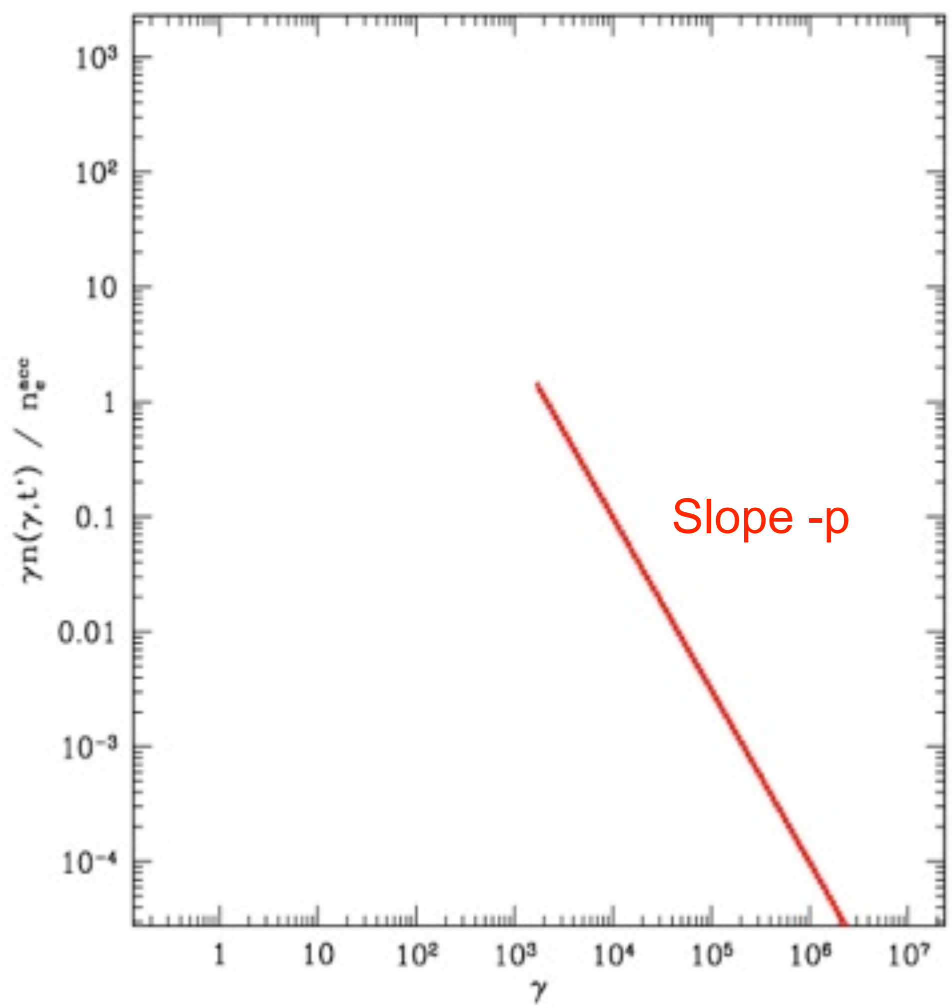

Electron distribution

Radiative processes

Radiation: **the time evolution of electrons and photons** in **the comoving frame** is solved (time-dependent radiative code)

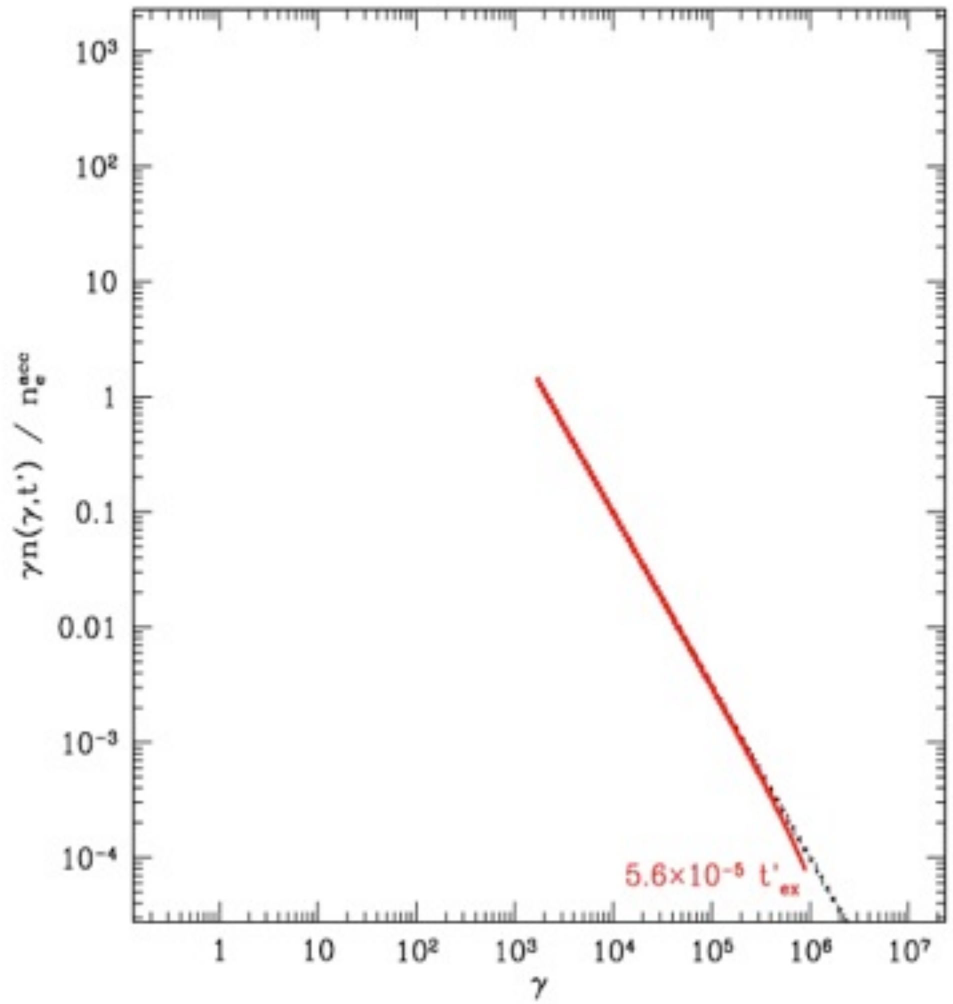

Electron distribution

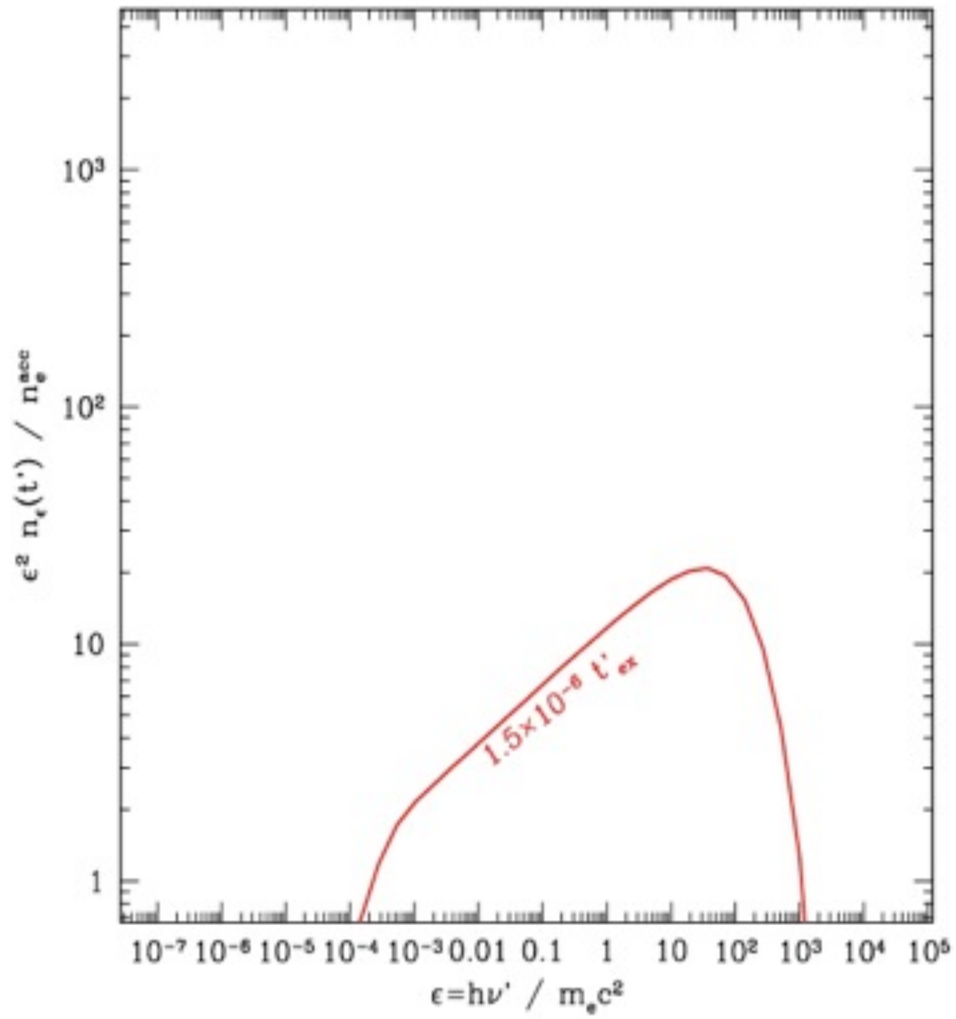

Photon spectrum

Radiative processes

Radiation: **the time evolution of electrons and photons** in **the comoving frame** is solved (time-dependent radiative code)

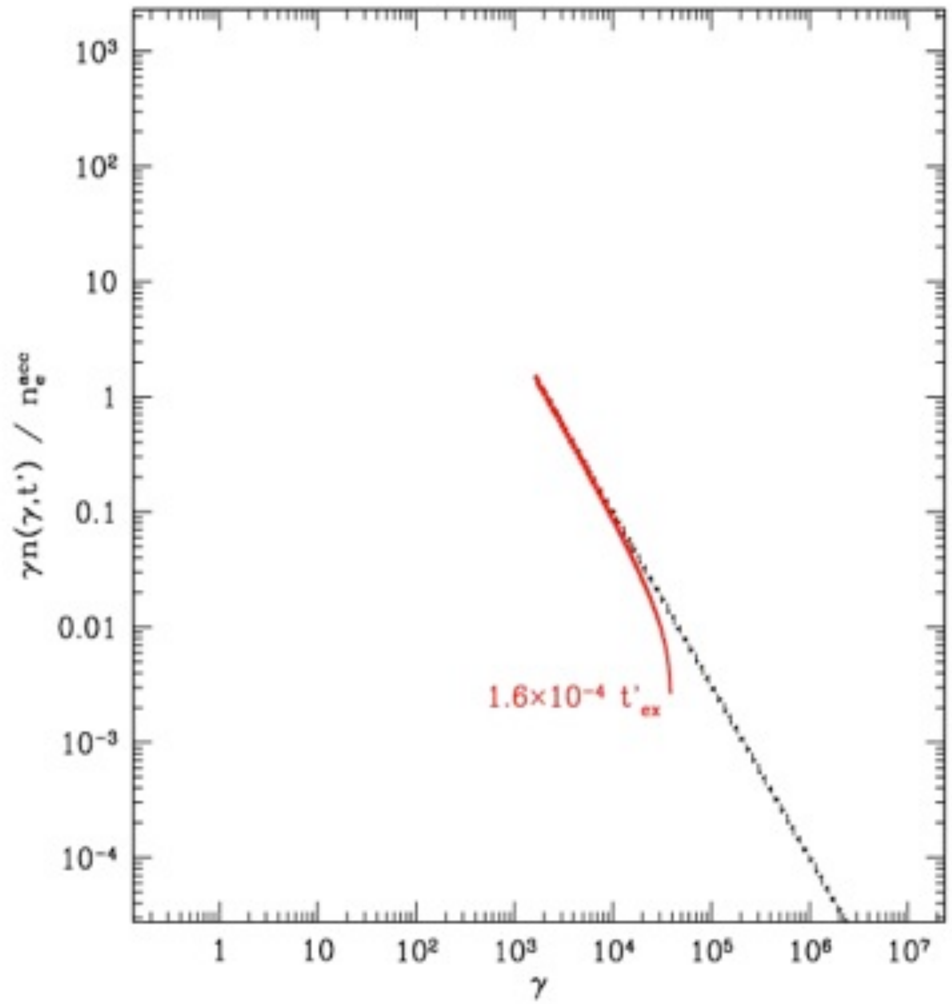

Electron distribution

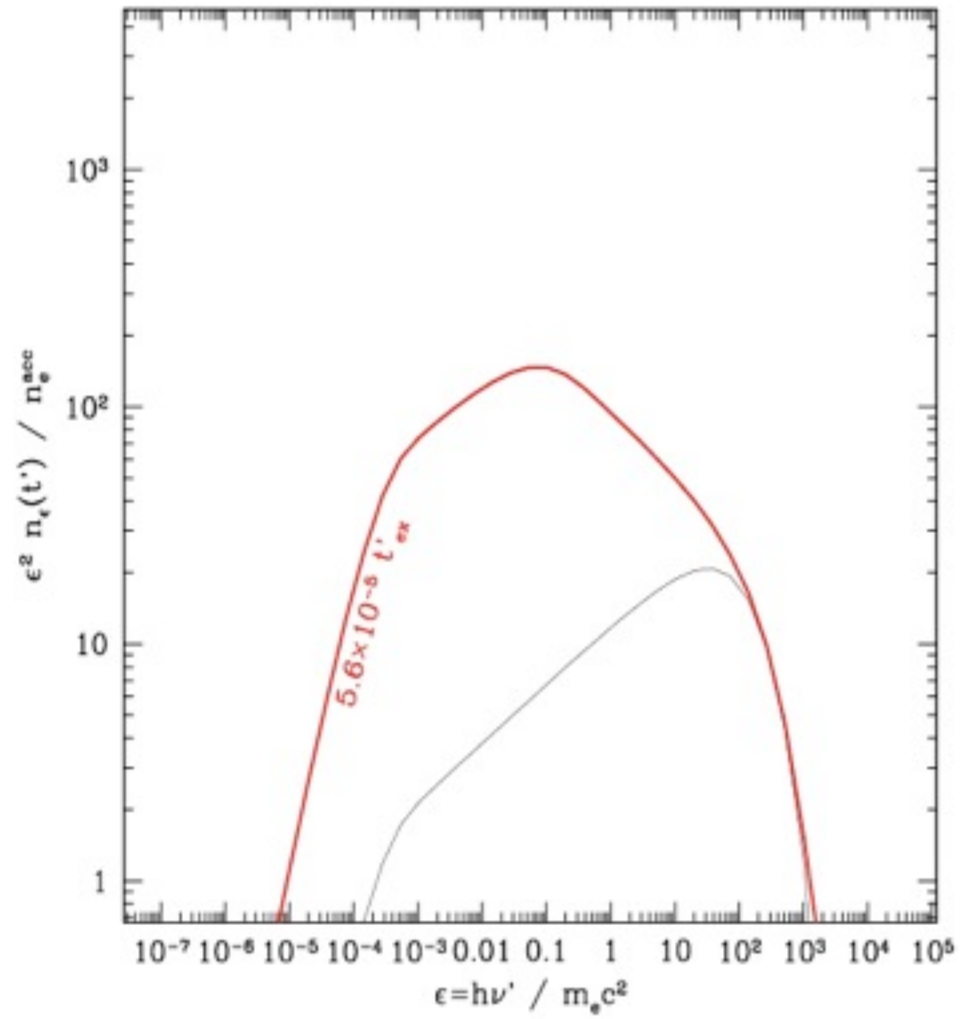

Photon spectrum

Radiative processes

Radiation: **the time evolution of electrons and photons** in **the comoving frame** is solved (time-dependent radiative code)

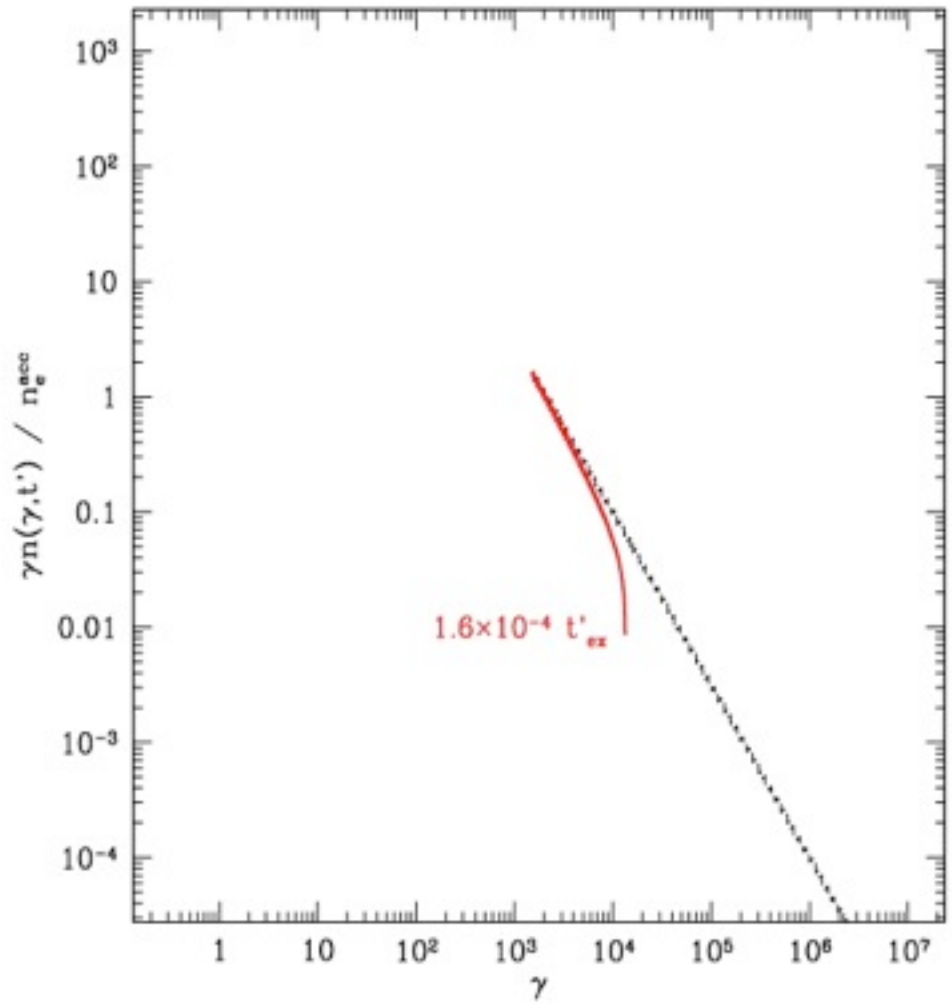

Electron distribution

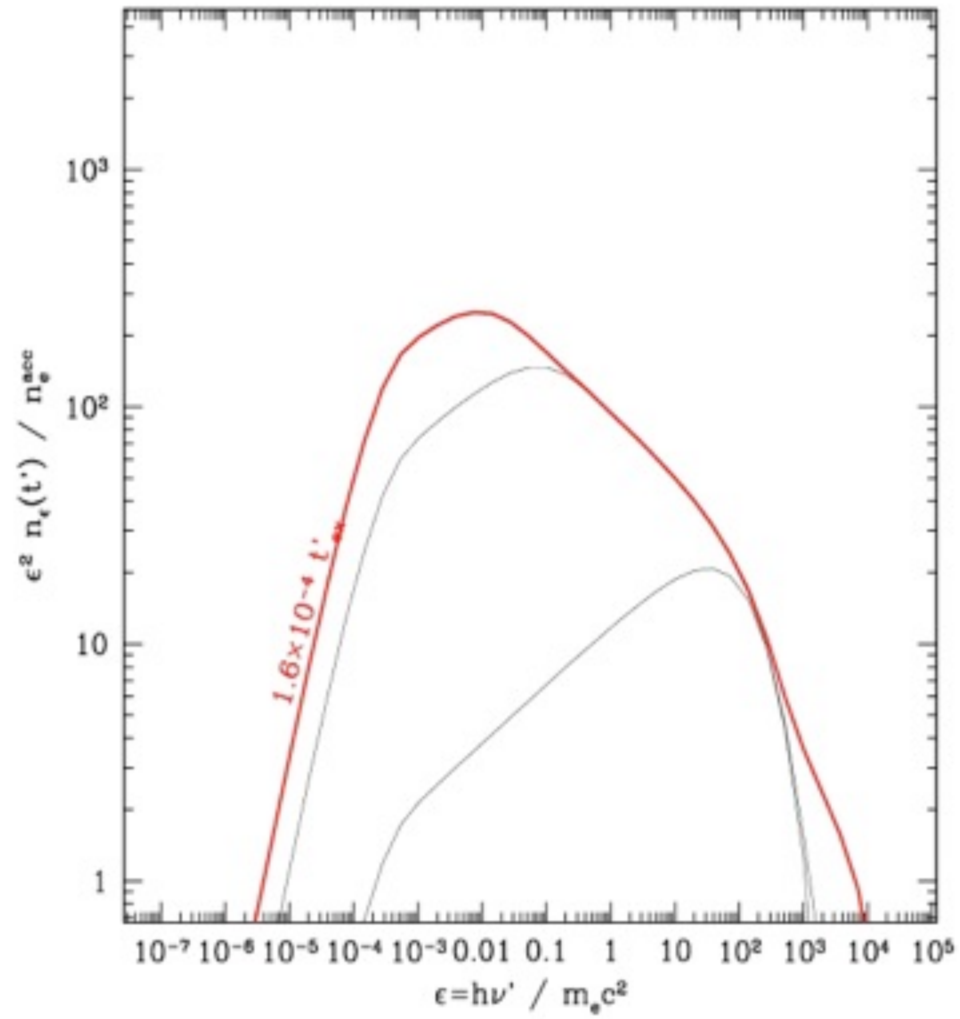

Photon spectrum

Radiative processes

Radiation: **the time evolution of electrons and photons** in **the comoving frame** is solved (time-dependent radiative code)

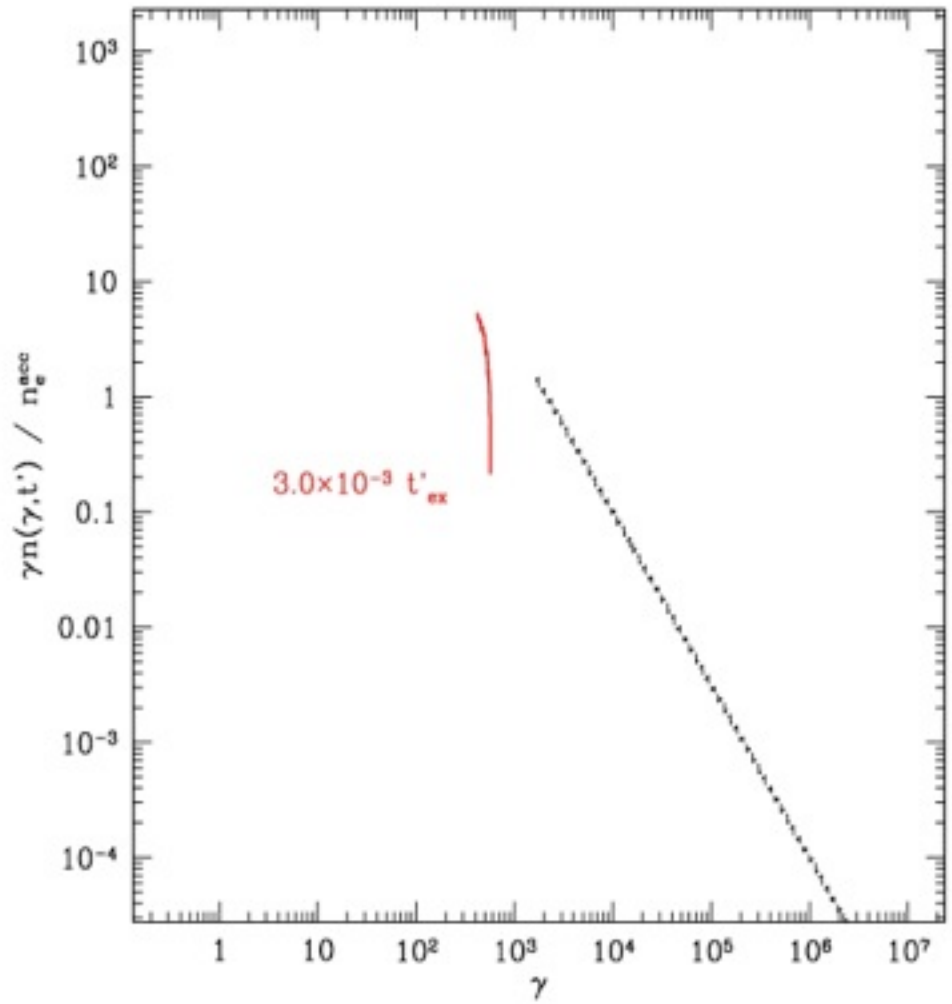

Electron distribution

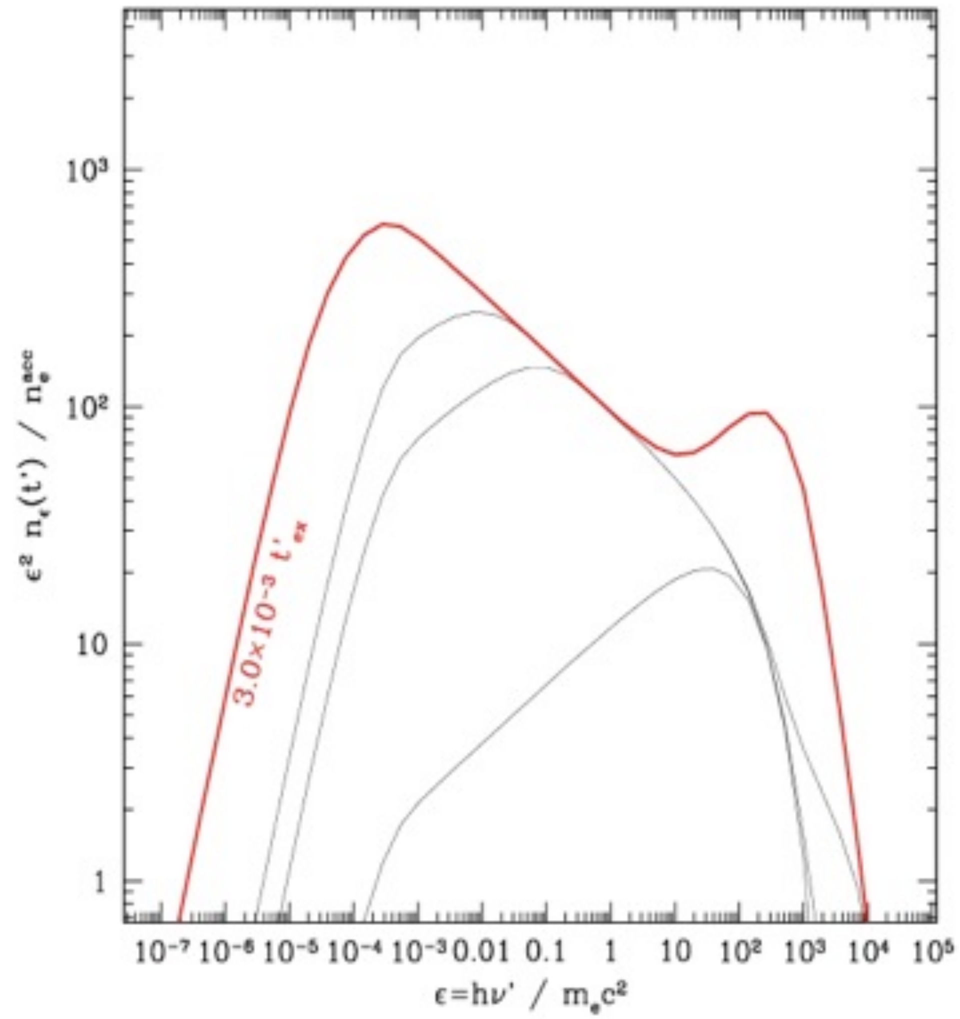

Photon spectrum

Radiation: **the time evolution of electrons and photons** in **the comoving frame** is solved (time-dependent radiative code)

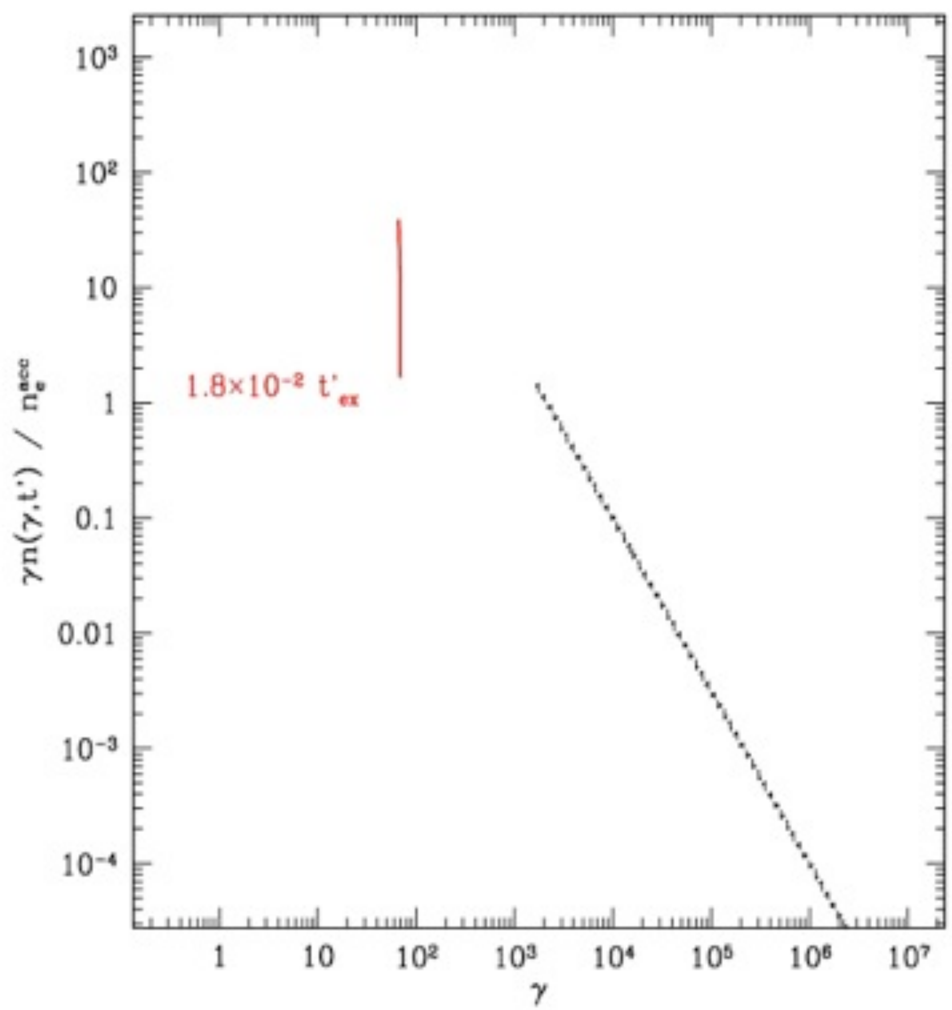

Electron distribution

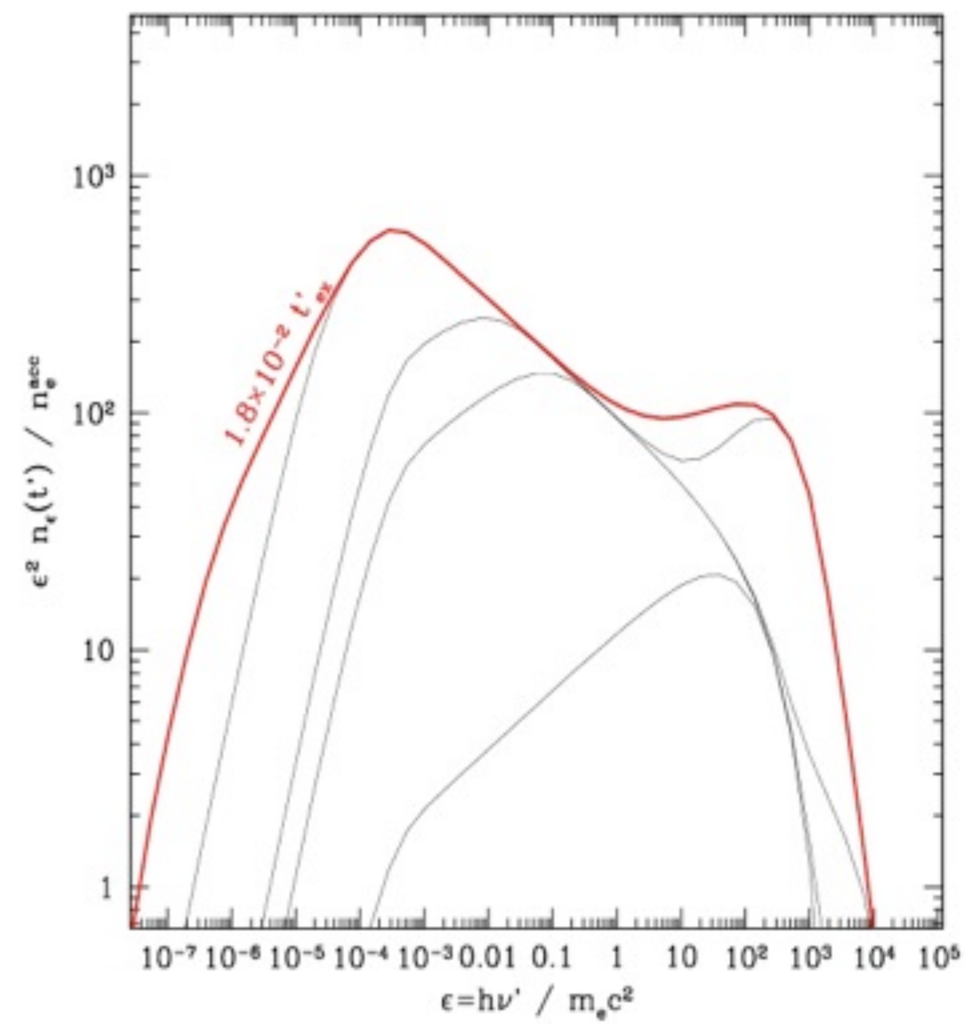

Photon spectrum

Radiative processes

Radiation: **the time evolution of electrons and photons** in **the comoving frame** is solved (time-dependent radiative code)

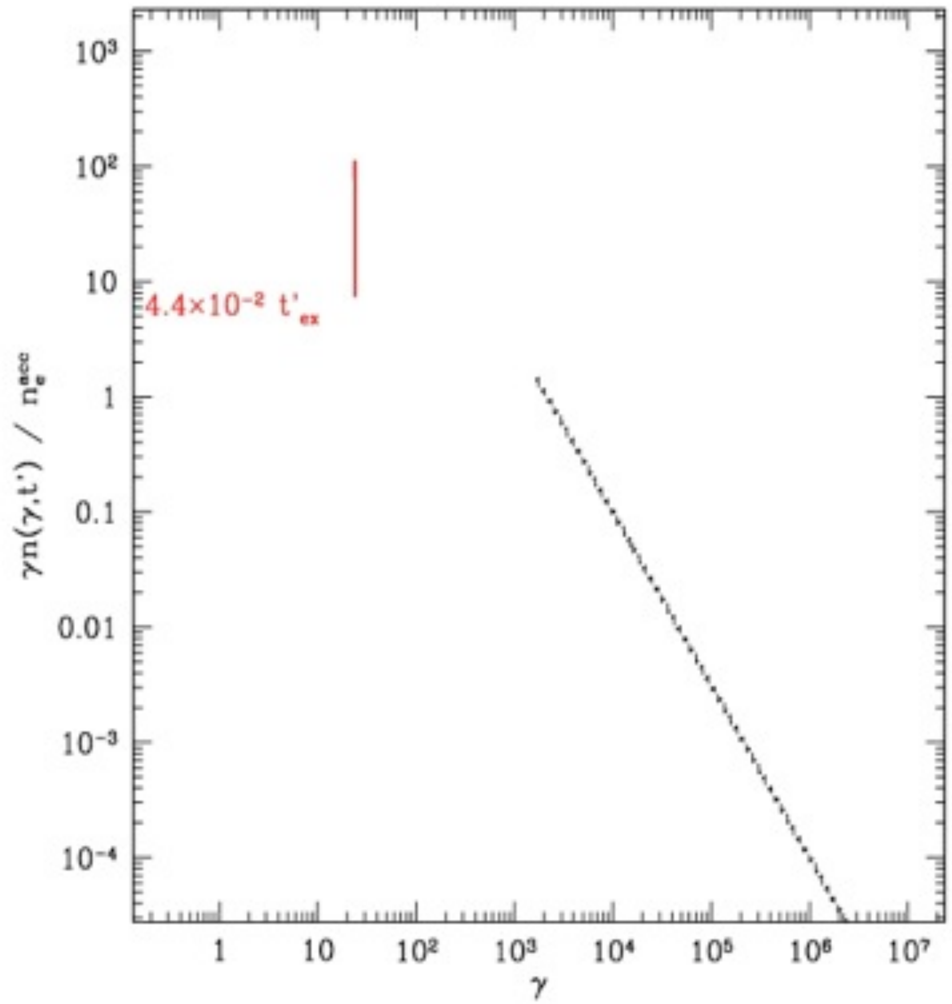

Electron distribution

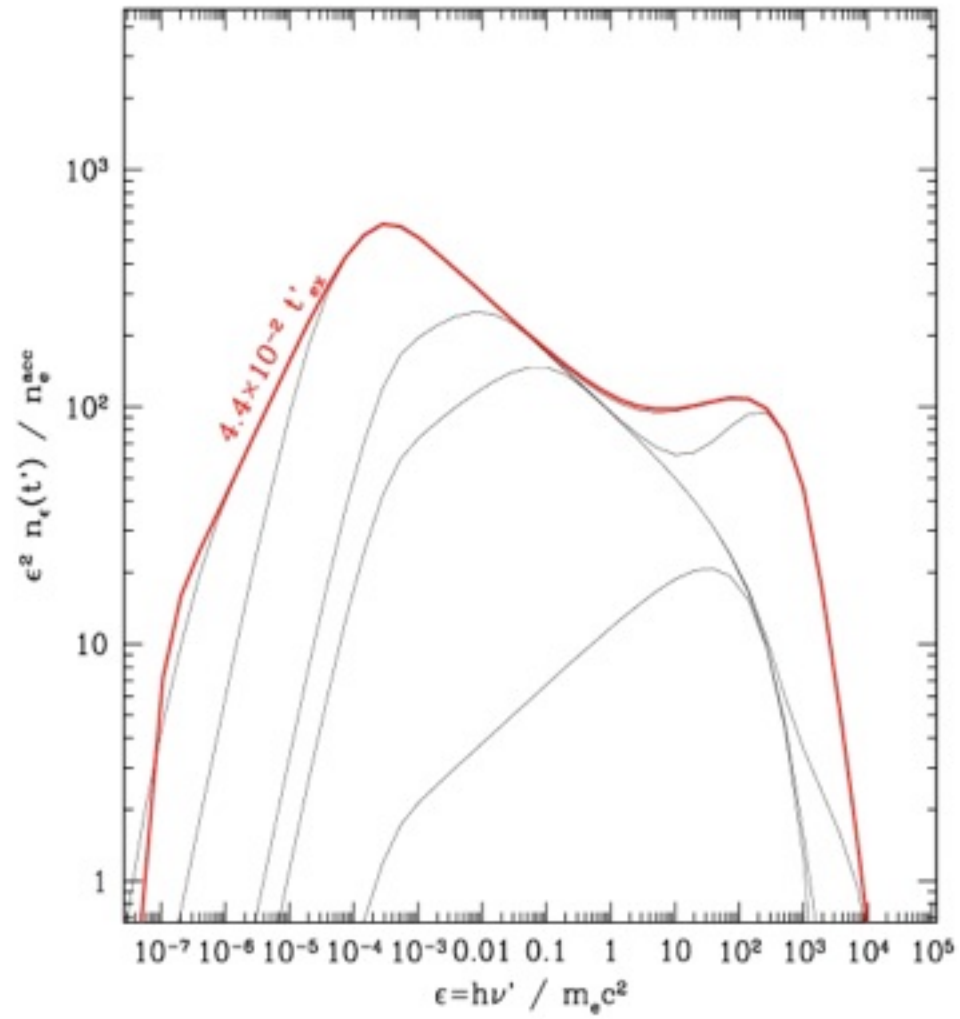

Photon spectrum

Radiative processes

Radiation: **the time evolution of electrons and photons** in **the comoving frame** is solved (time-dependent radiative code)

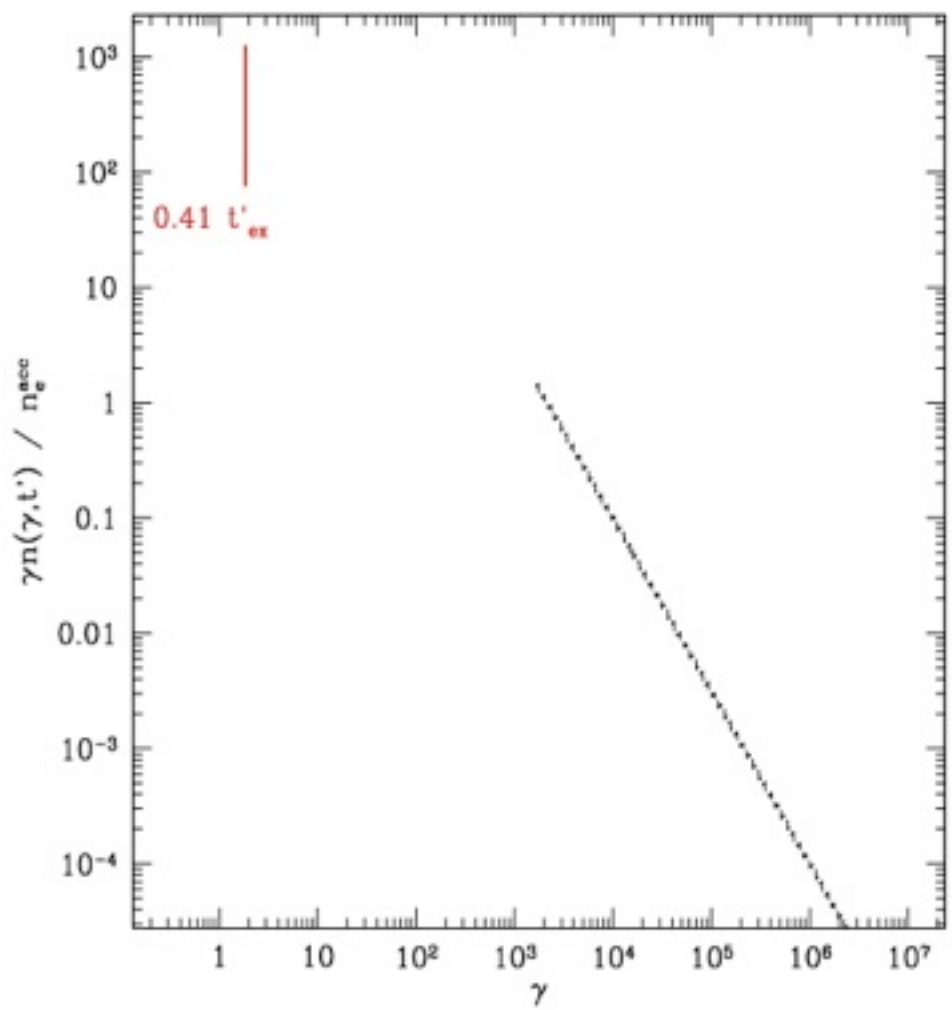

Electron distribution

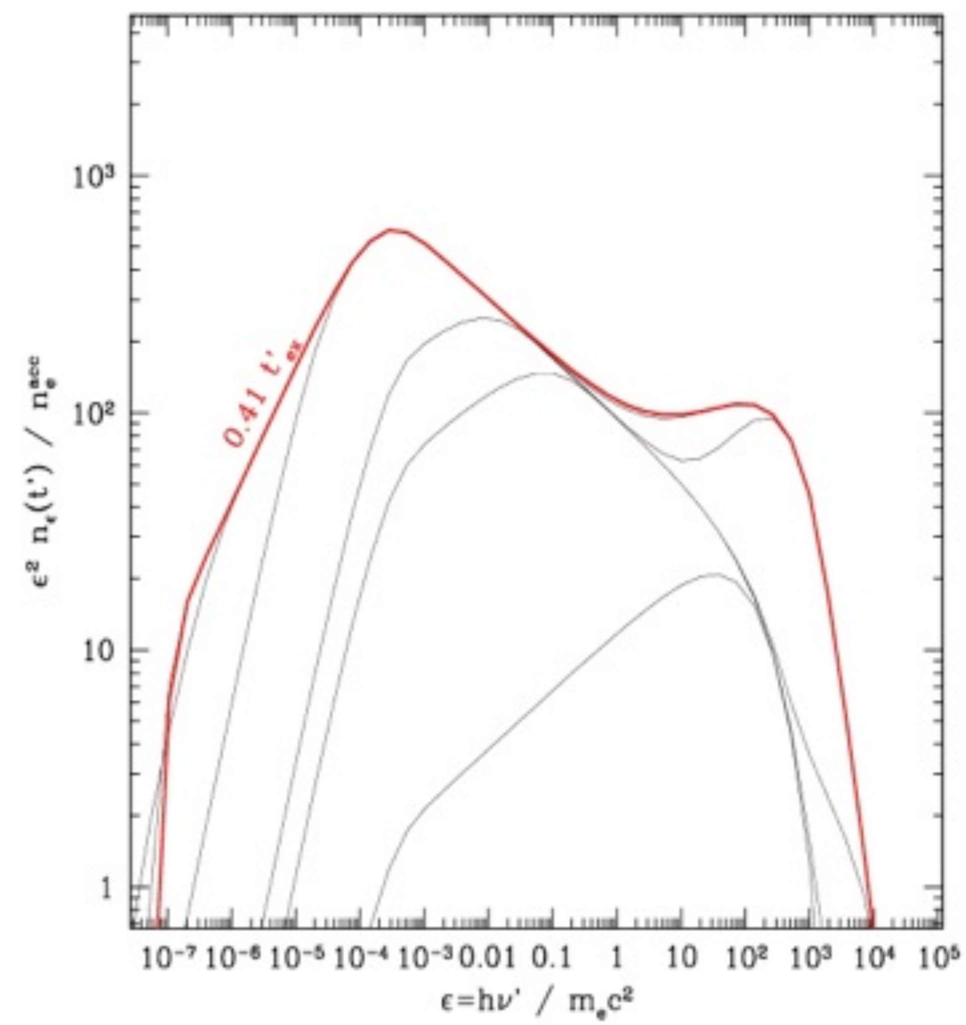

Photon spectrum

Radiative processes

Radiation: **the time evolution of electrons and photons** in **the comoving frame** is solved (time-dependent radiative code)

Comptonization parameter
$Y = L_{IC} / L_{syn}$

IC dominant:
low frequency synchrotron peak
Thomson regime

Synchrotron dominant:
high frequency synchrotron peak
Klein-Nishina regime

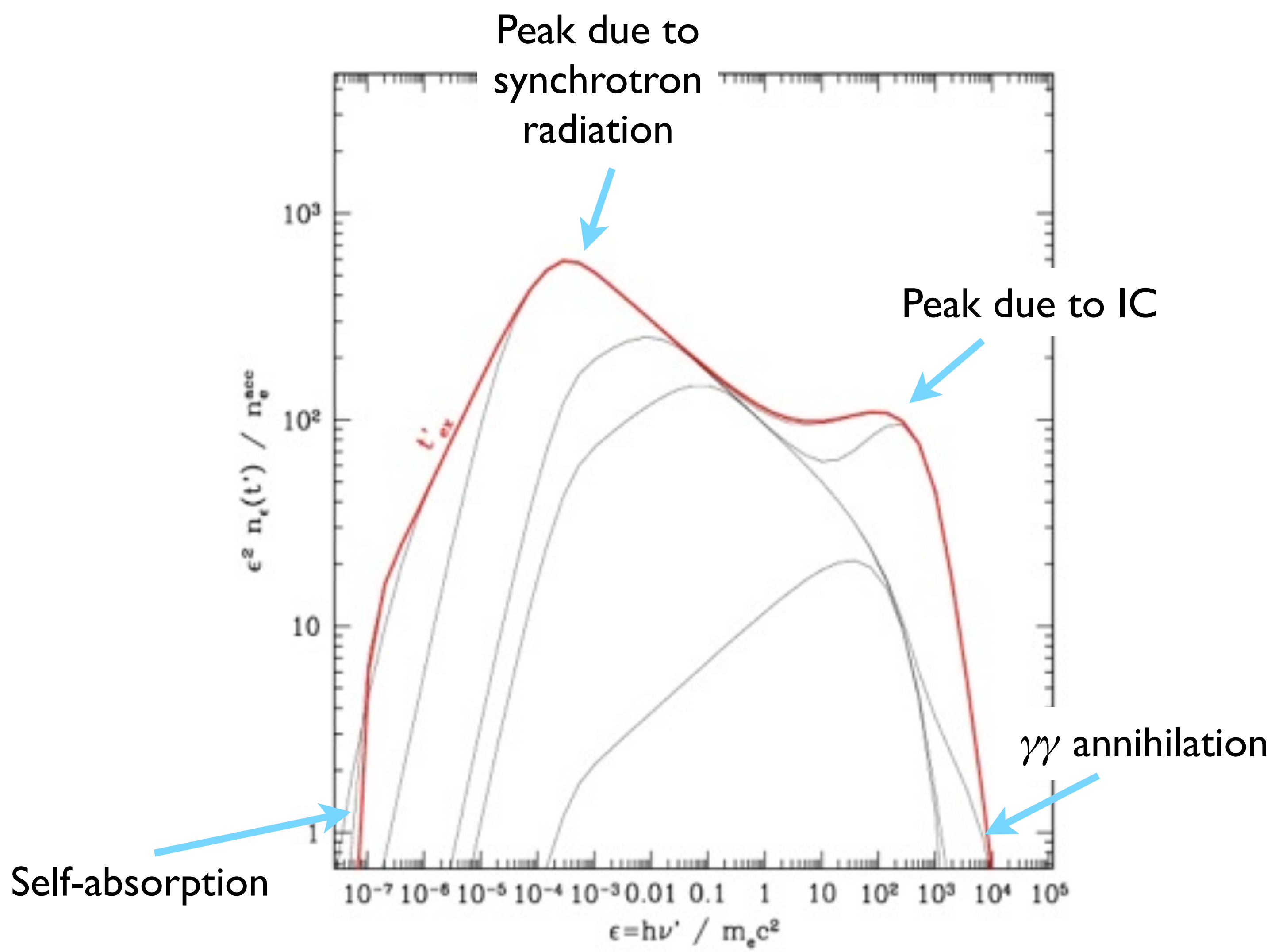

Emitted photon spectrum

Radiative processes

Radiation: **the time evolution of electrons and photons** in **the comoving frame** is solved (time-dependent radiative code)

Comptonization parameter
$Y = L_{ic} / L_{syn}$

IC dominant:
low frequency synchrotron peak
Thomson regime

Synchrotron dominant:
high frequency synchrotron peak
Klein-Nishina regime

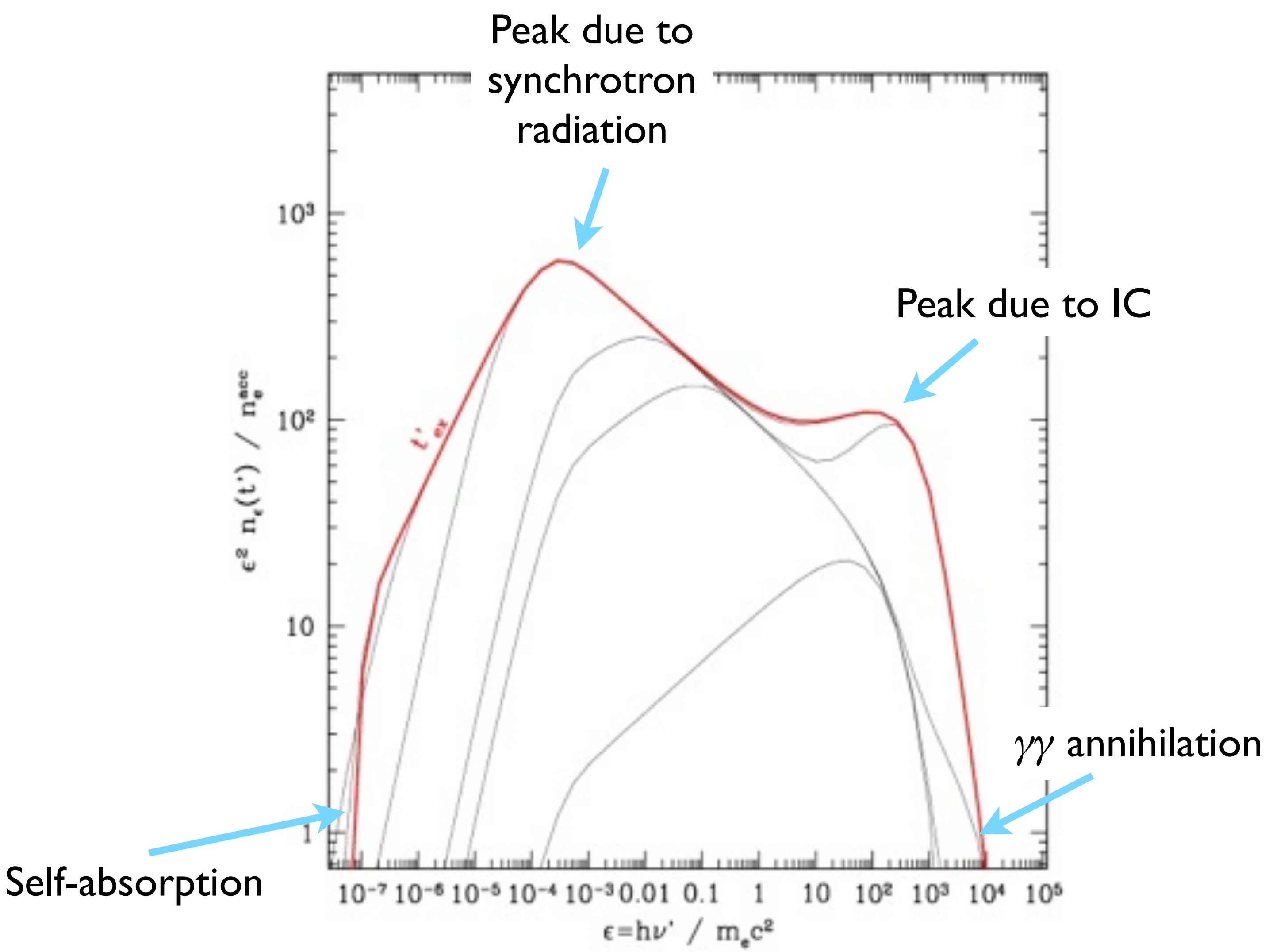

Emitted photon spectrum

This calculation is done at all times along the propagation of each shock wave
All the contributions are added together to produce a synthetic gamma-ray burst (spectrum+lightcurve)

Observed spectra and time profiles

The observed spectra and the light curves are computed from the comoving emission by integration over equal-arrival time surfaces.

relativistic effects (Doppler factor)
geometry (curvature of the emitting surface)
cosmological effect (redshifts)

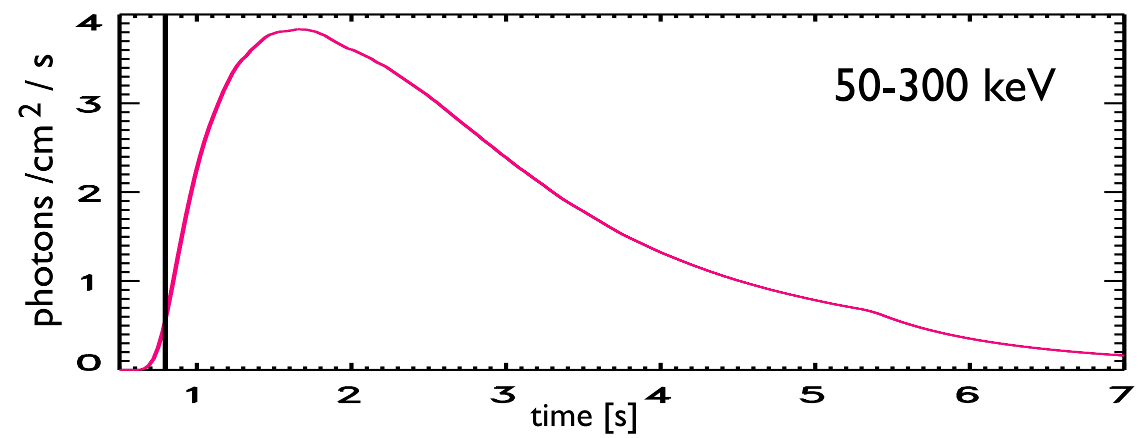

Instantaneous observed spectrum:

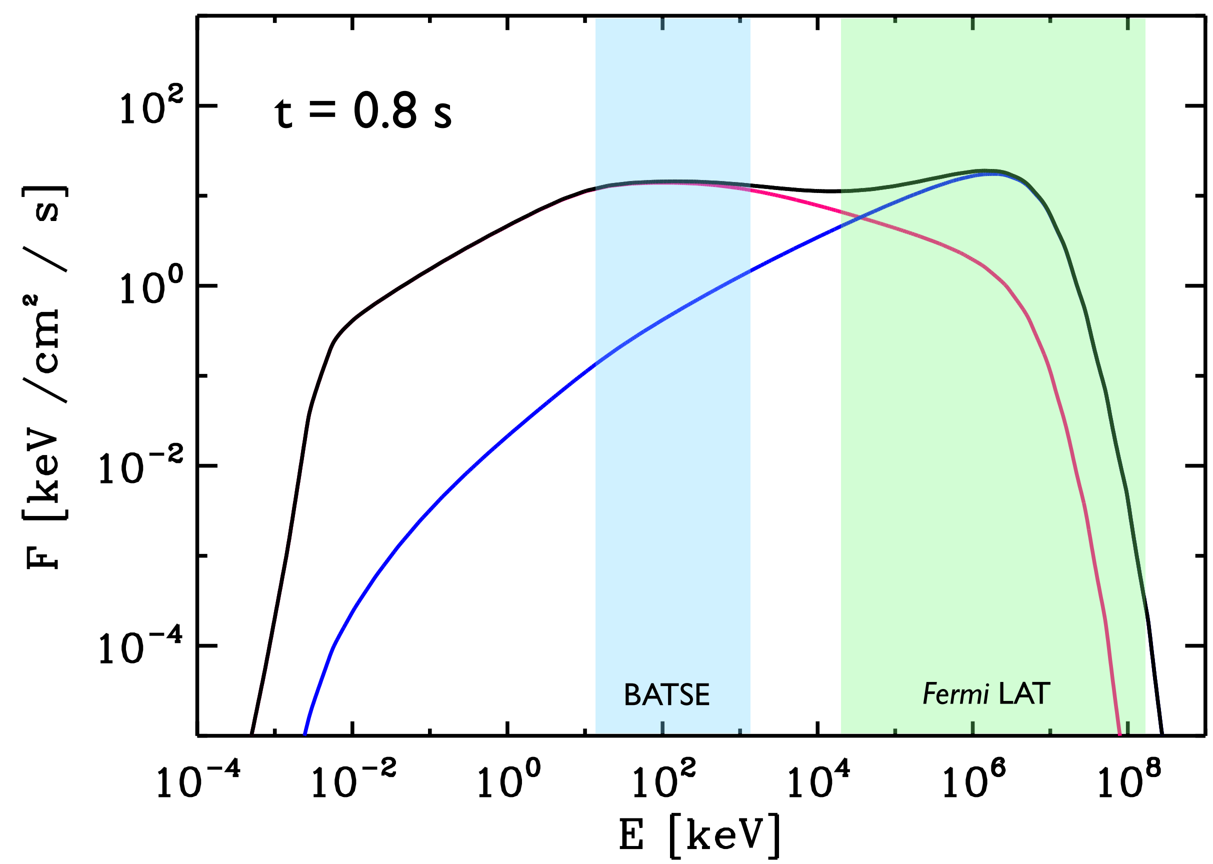

synchrotron
inverse Compton
total

Observed spectra and time profiles

The observed spectra and the light curves are computed from the comoving emission by integration over equal-arrival time surfaces.

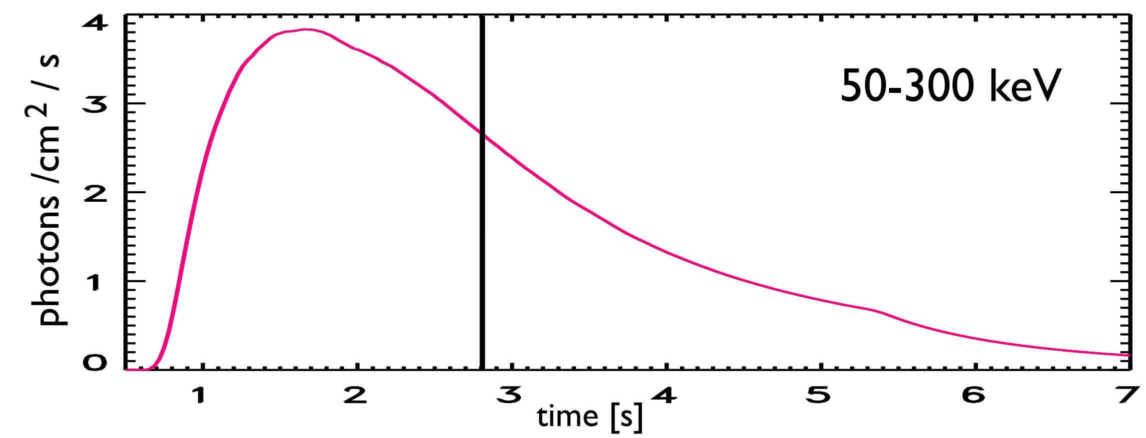

relativistic effects (Doppler factor)
geometry (curvature of the emitting surface)
cosmological effect (redshifts)

Instantaneous observed spectrum:

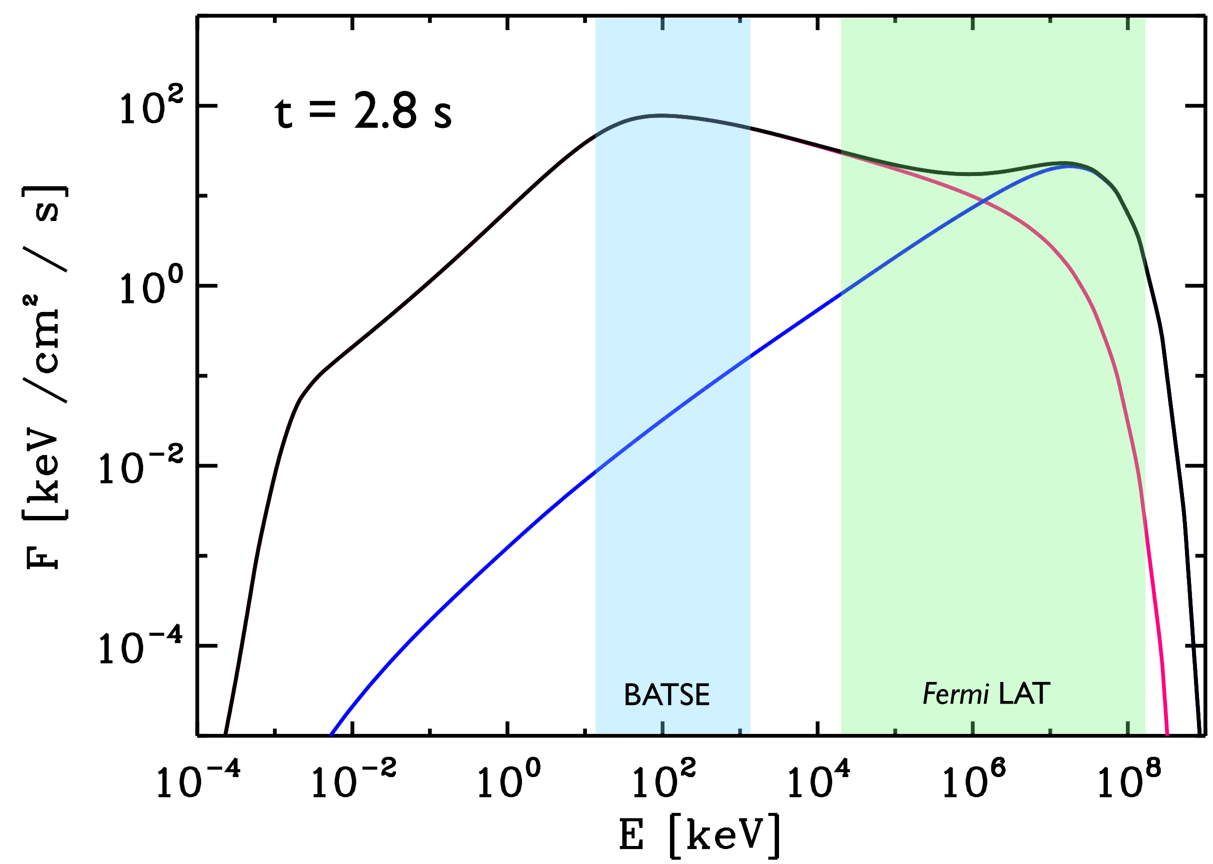

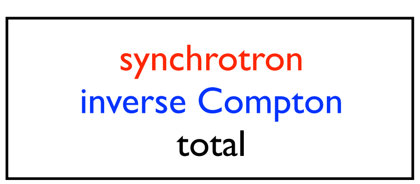

Dominant radiative process in sub-MeV range

2 possibilities for the dominant process in the keV-MeV range

1. SYNCHROTRON

2. INVERSE COMPTON

Dominant radiative process in sub-MeV range

2 possibilities for the dominant process in the keV-MeV range

1. SYNCHROTRON

High Γ_m requires that only a fraction of the electrons is accelerated (<10%)

High B: **no IC component** at high energy

Low B: **IC component** at high energy

2. INVERSE COMPTON

Dominant radiative process in sub-MeV range

2 possibilities for the dominant process in the keV-MeV range

1. SYNCHROTRON

High Γ_m requires that only a fraction of the electrons is accelerated (<10%)

High B: **no IC component** at high energy

Low B: **IC component** at high energy

2. INVERSE COMPTON

All electrons are accelerated

Synchrotron component at low energy

Second inverse Compton peak at high energy

Piran et al. 2008: crisis for the GRB energy budget

A steep electron slope (p>3) is required to have two well defined peaks

Dominant radiative process in sub-MeV range

SYNCHROTRON CASE **(A)**

high magnetic field

$dE/dt = 5 \times 10^{53} \text{erg s}^{-1}$, $\varepsilon_B = \varepsilon_e = 1/3$, $\zeta = 0.003$, $p = 2.5$, $z=1$

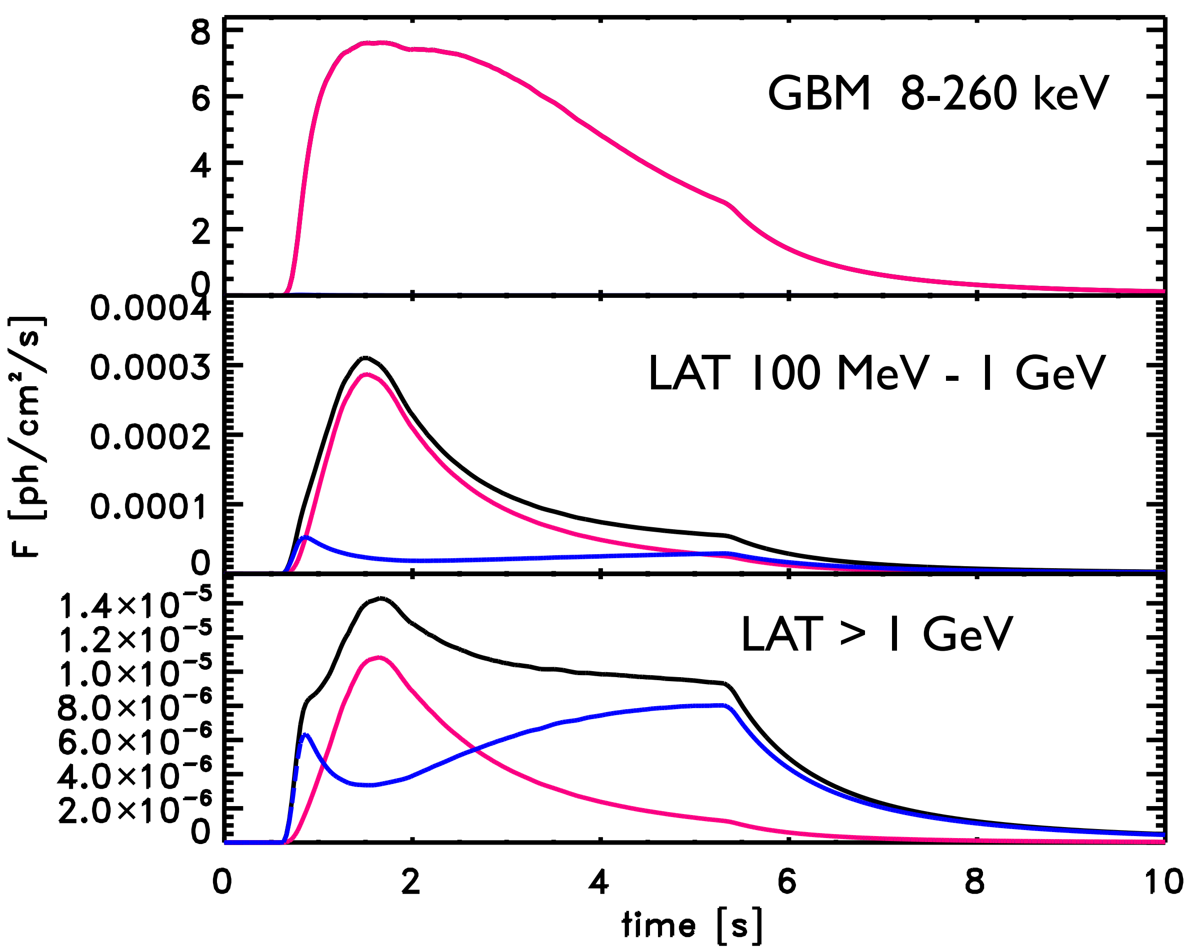

Observed lightcurve

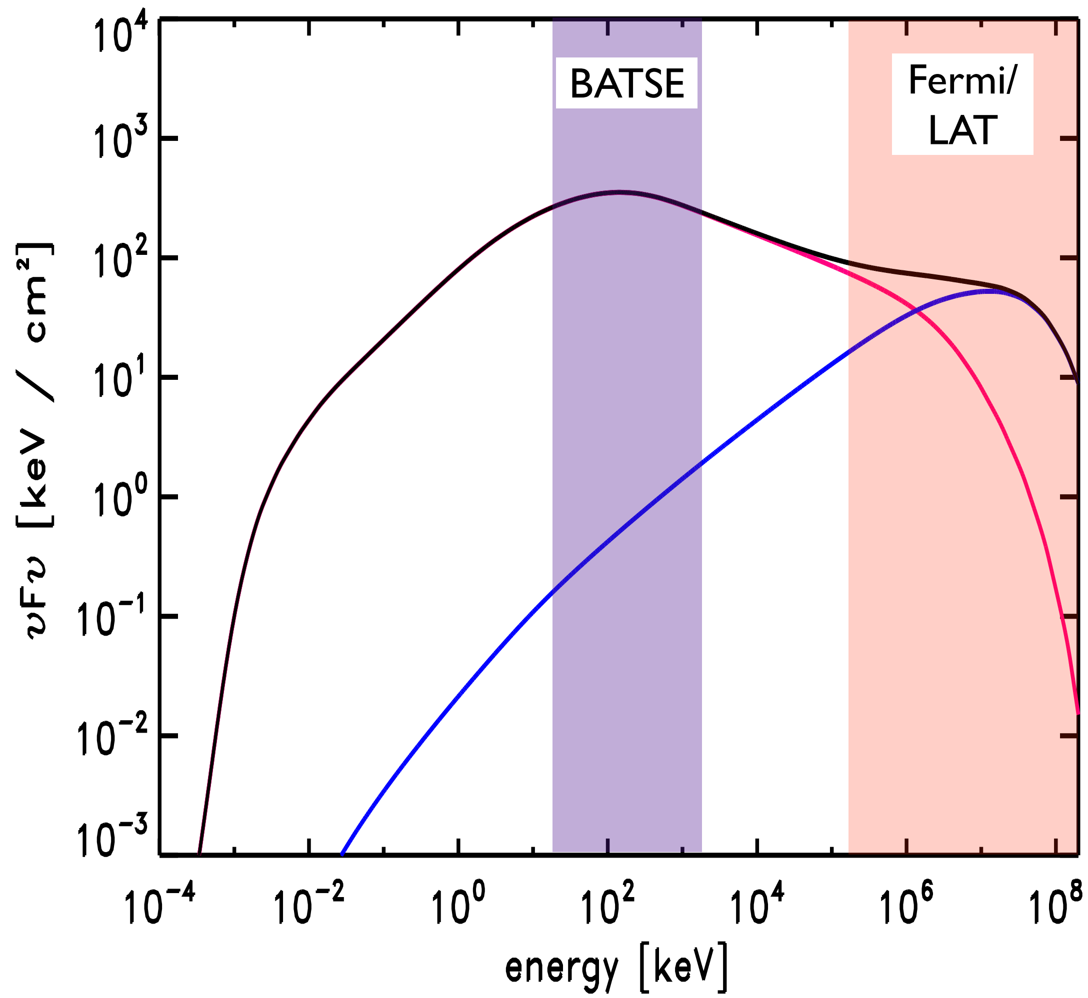

Observed spectrum

synchrotron
inverse Compton
total

Dominant radiative process in sub-MeV range

SYNCHROTRON CASE **(A)**

high magnetic field

$dE/dt = 5 \times 10^{53}$ erg s^{-1}, $\varepsilon_B = \varepsilon_e = 1/3$, $\zeta = 0.003$, $p = 2.5$, $z=1$

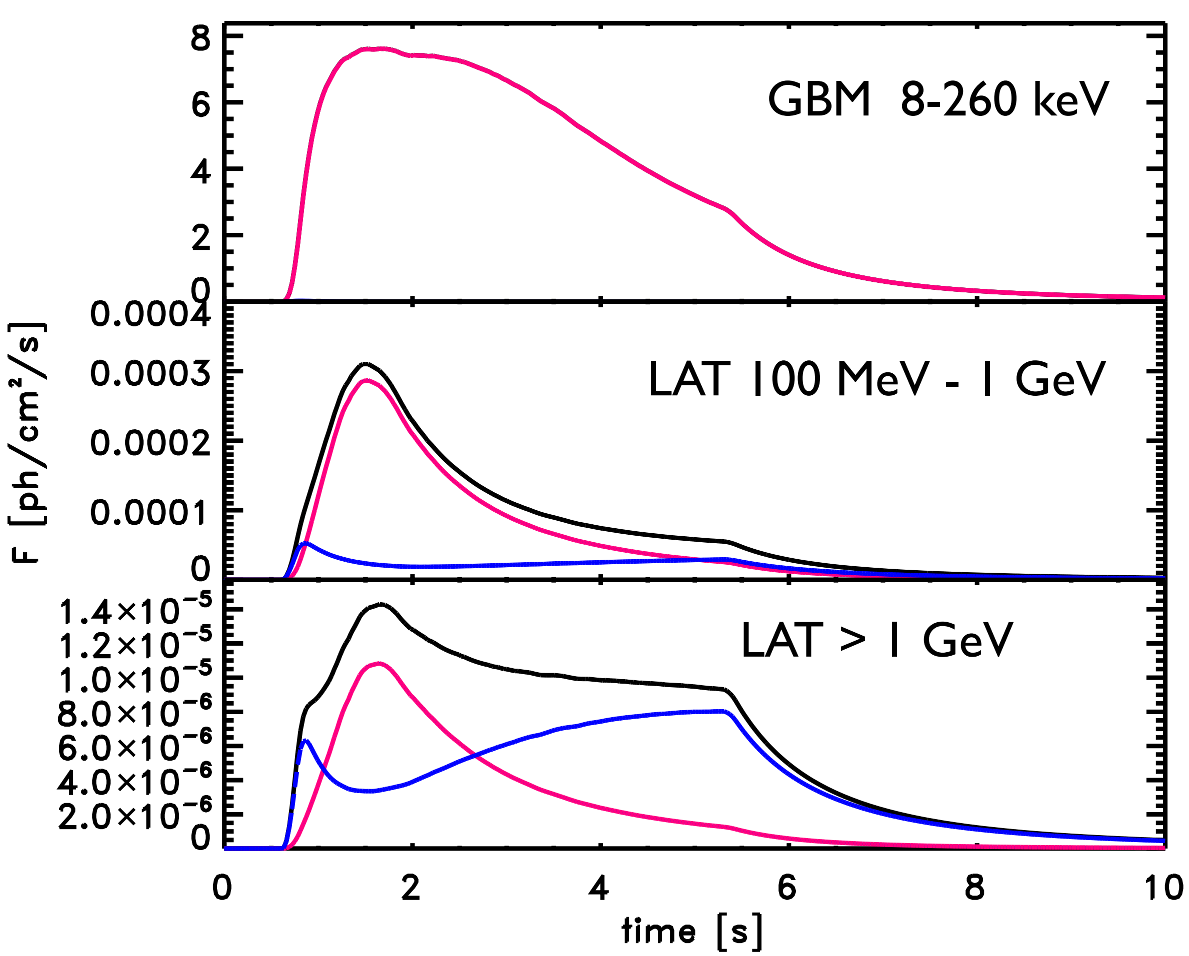

Observed lightcurve

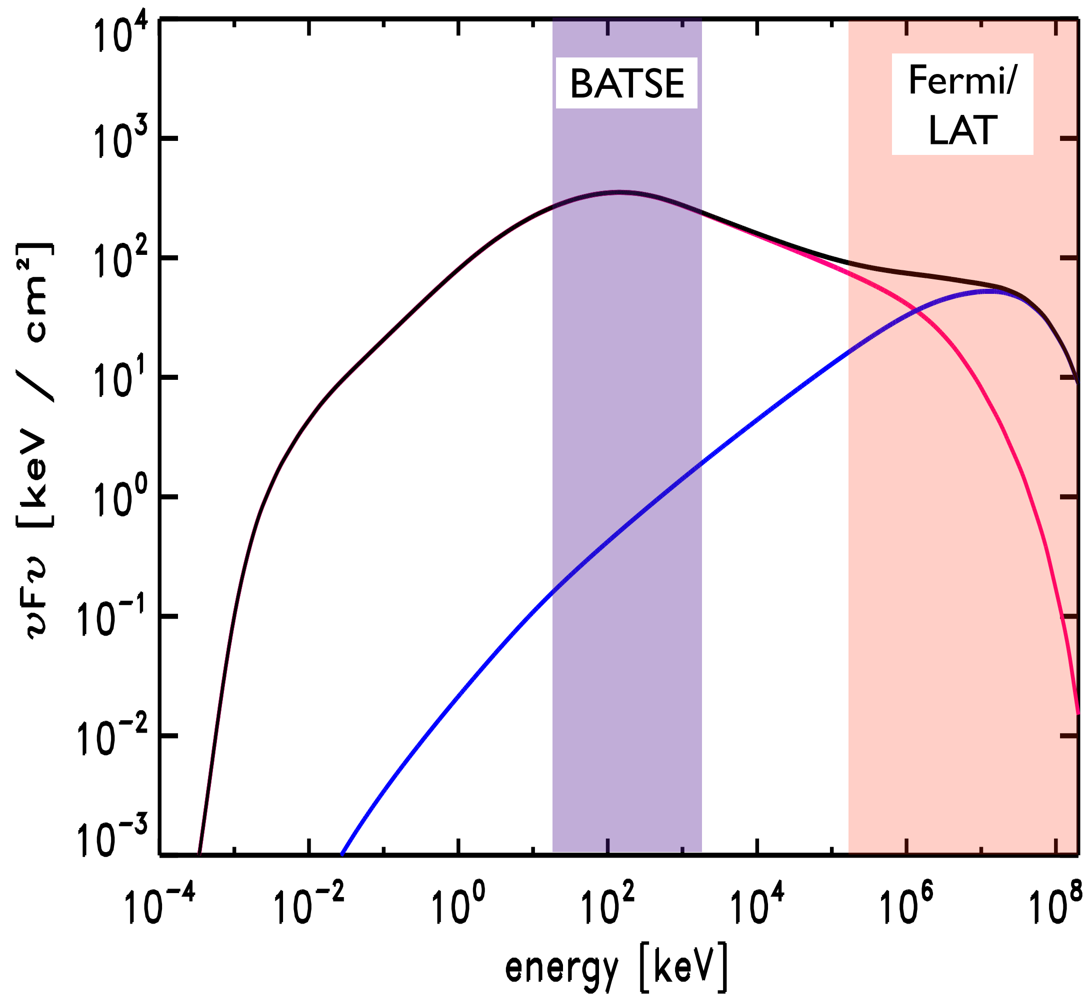

Observed spectrum

synchrotron
inverse Compton
total

Dominant radiative process in sub-MeV range

SYNCHROTRON CASE **(B)**

low magnetic field

dE/dt = 5 x 10^{53} erg s^{-1}, ε_B = 0.003, ε_e = 1/3, ζ = 0.003, p = 2.5, z=1

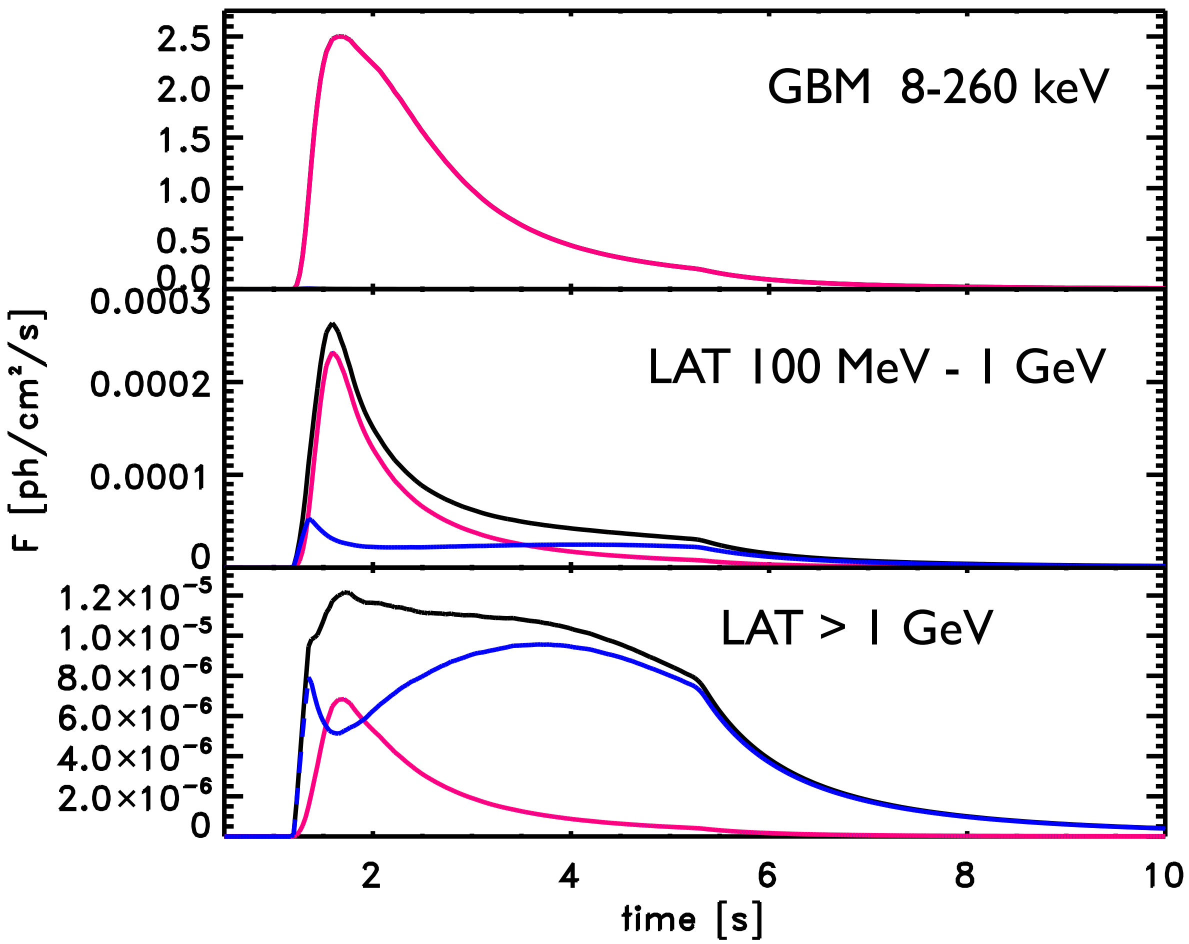

Observed lightcurve

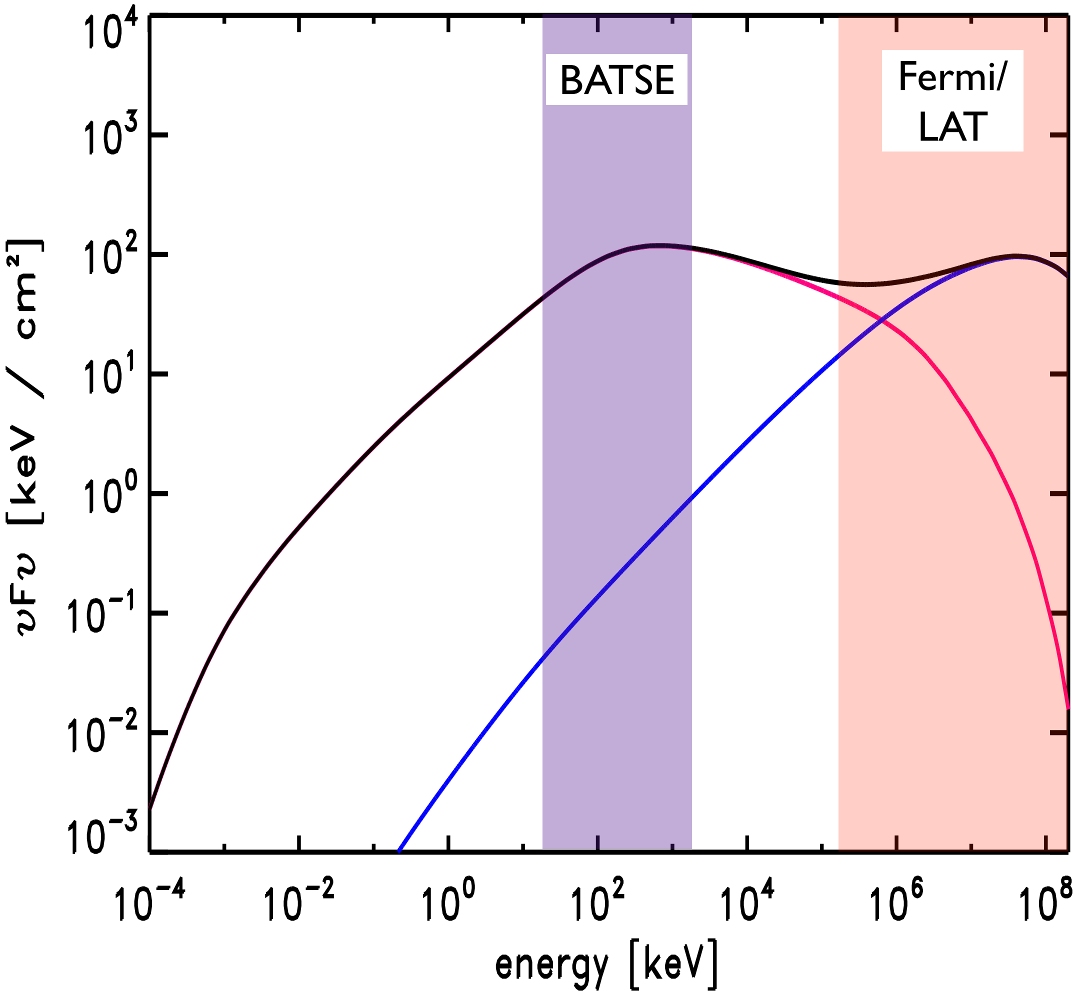

Observed spectrum

synchrotron
inverse Compton
total

A complex electron distribution?

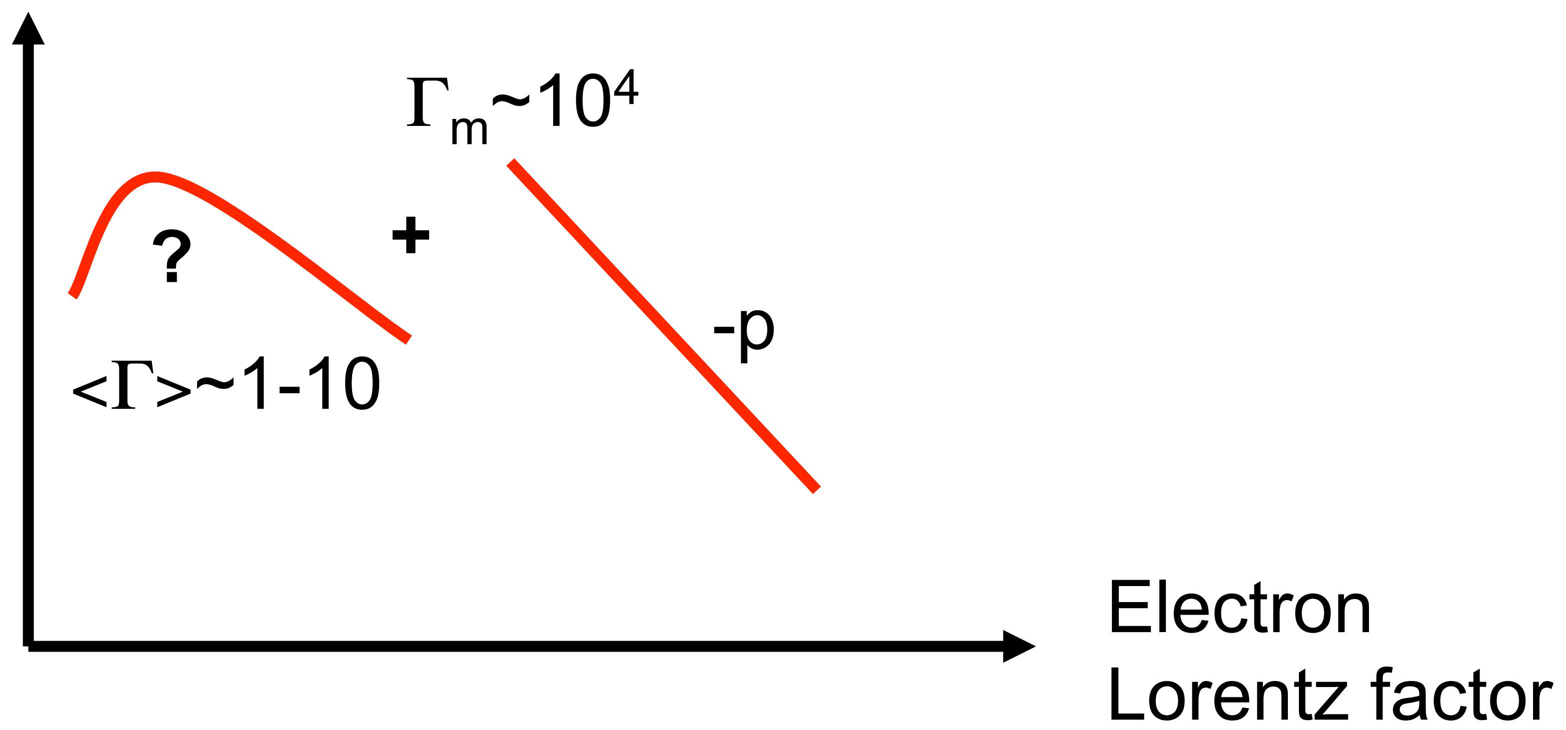

A complex electron distribution?

Observed GRB pulse @ z=1: $E_{\gamma,iso} = 5\times10^{51}$ erg ; E_p = 200 keV ; τ = 2 s

Synchrotron case with high magnetic field (ε_B=1/3)

Assume ε_e is distributed in

- Fraction η for accelerated e^- (high Lorentz factor)
- Fraction $(1-\eta)$ in Maxwellian (low Lorentz factor)

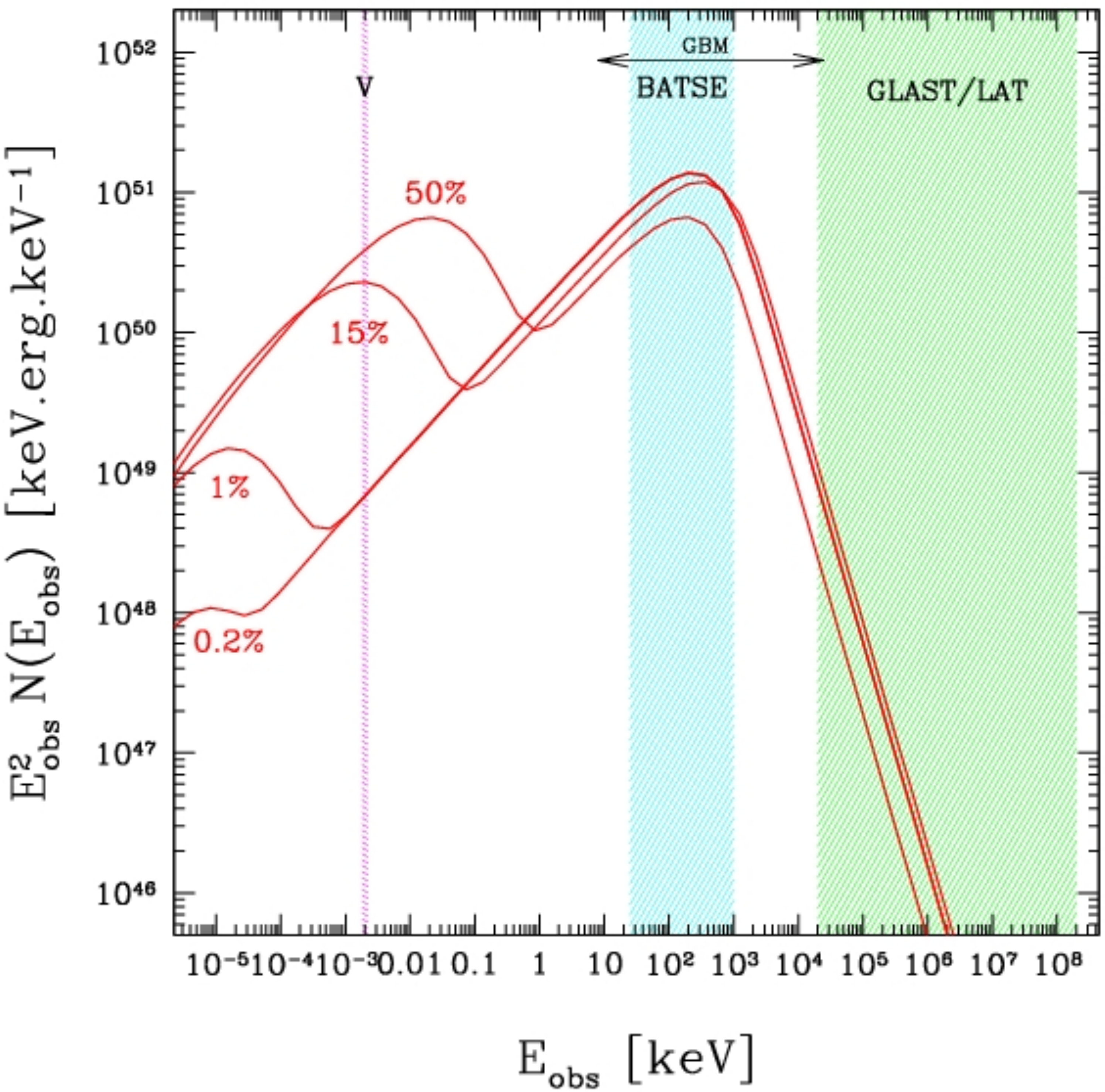

A complex electron distribution?

Observed GRB pulse @ z=1: $E_{\gamma,iso} = 5\times10^{51}$ erg ; E_p = 200 keV ; τ = 2 s

Synchrotron case with high magnetic field (ε_B=1/3)

Assume ε_e is distributed in

- Fraction η for accelerated e^- (high Lorentz factor)
- Fraction $(1-\eta)$ in Maxwellian (low Lorentz factor)

The low-energy emission (optical) from the thermal electrons is usually self-absorbed…

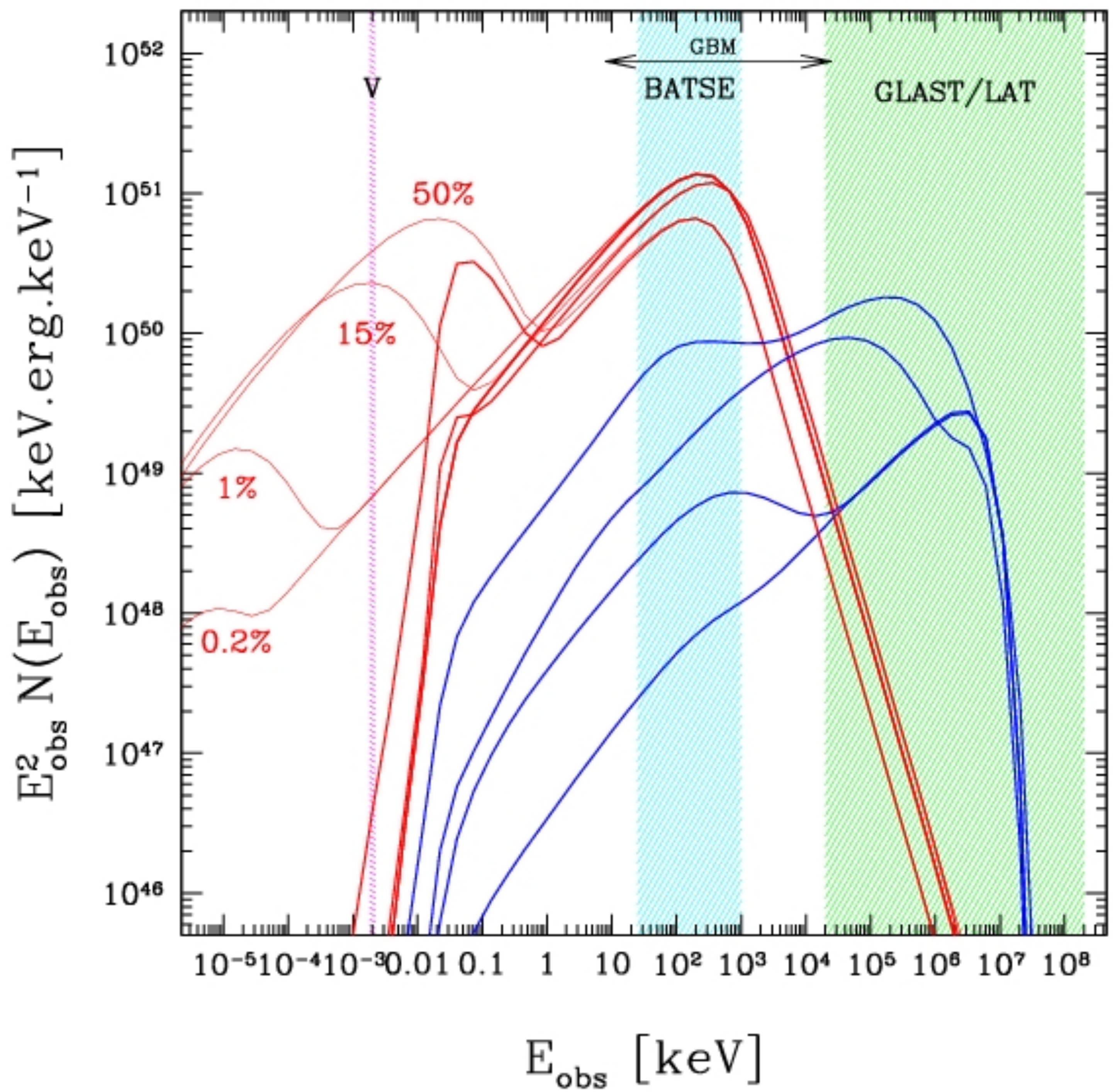

Emission processes and temporal profile: sub MeV range

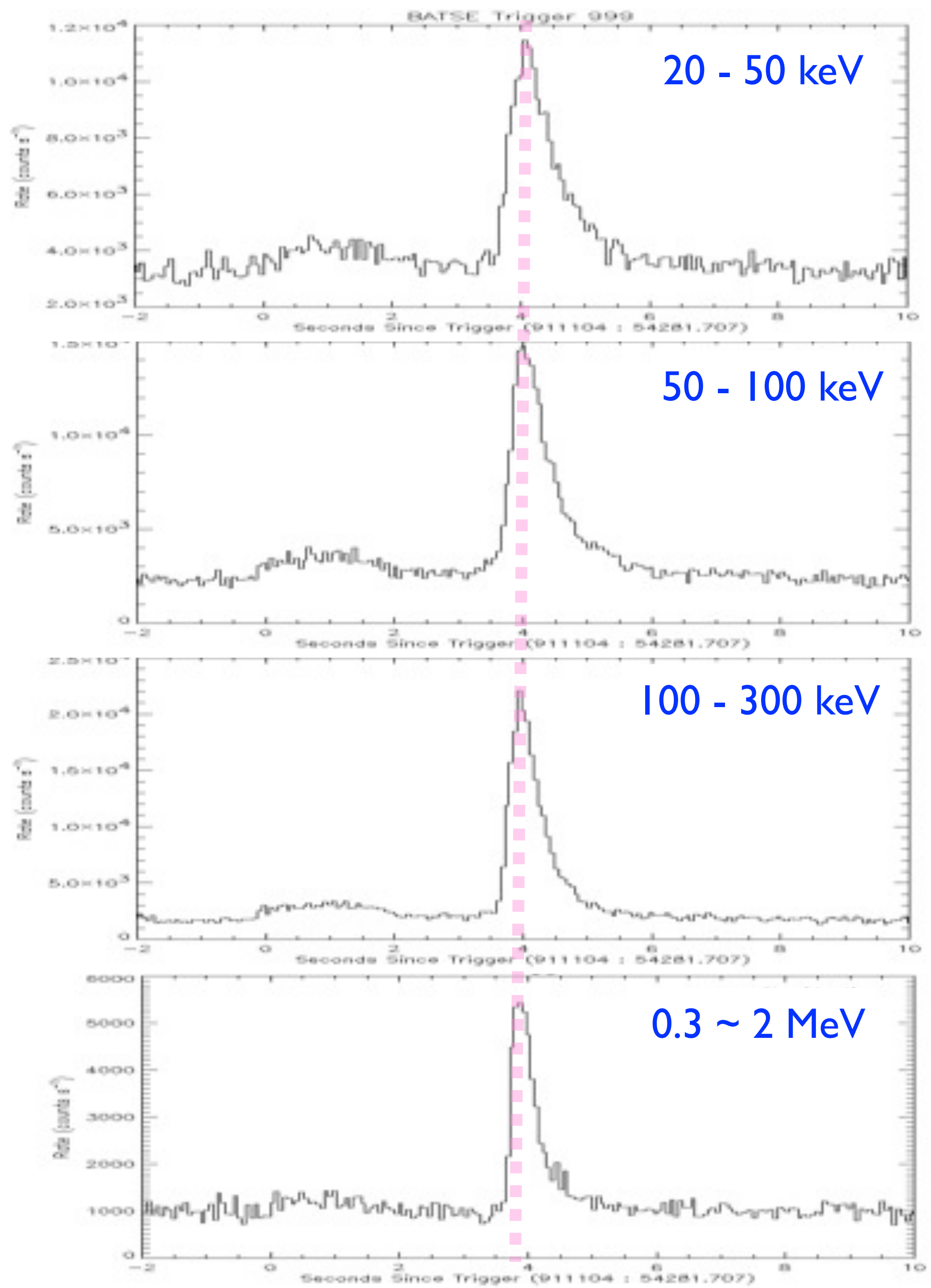

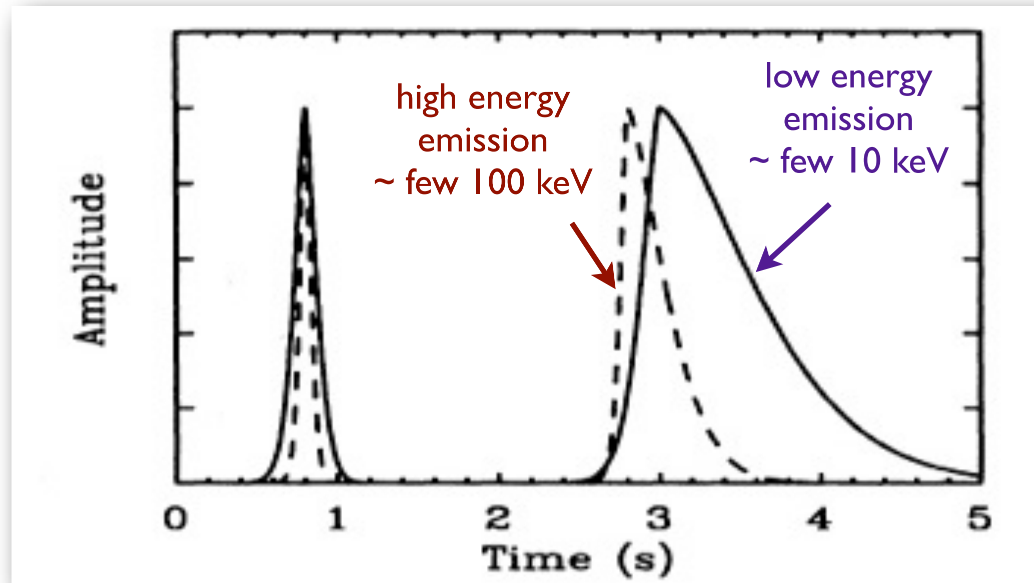

Norris et al. 1996 (BATSE GRBs):
asymmetry/energy-shift paradigm

Emission processes and temporal profile: sub MeV range

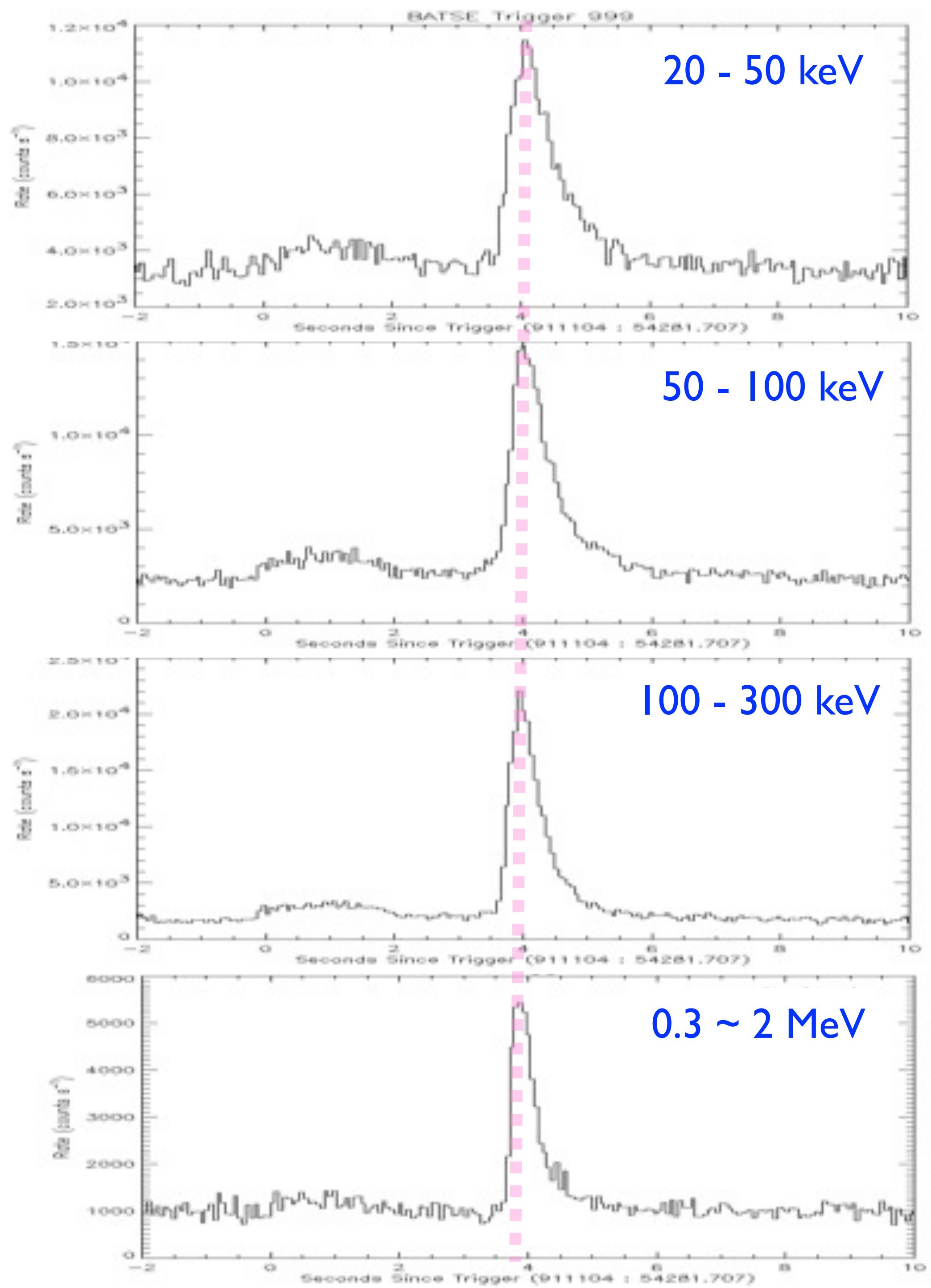

Model: dominant synchrotron emission in sub-MeV range

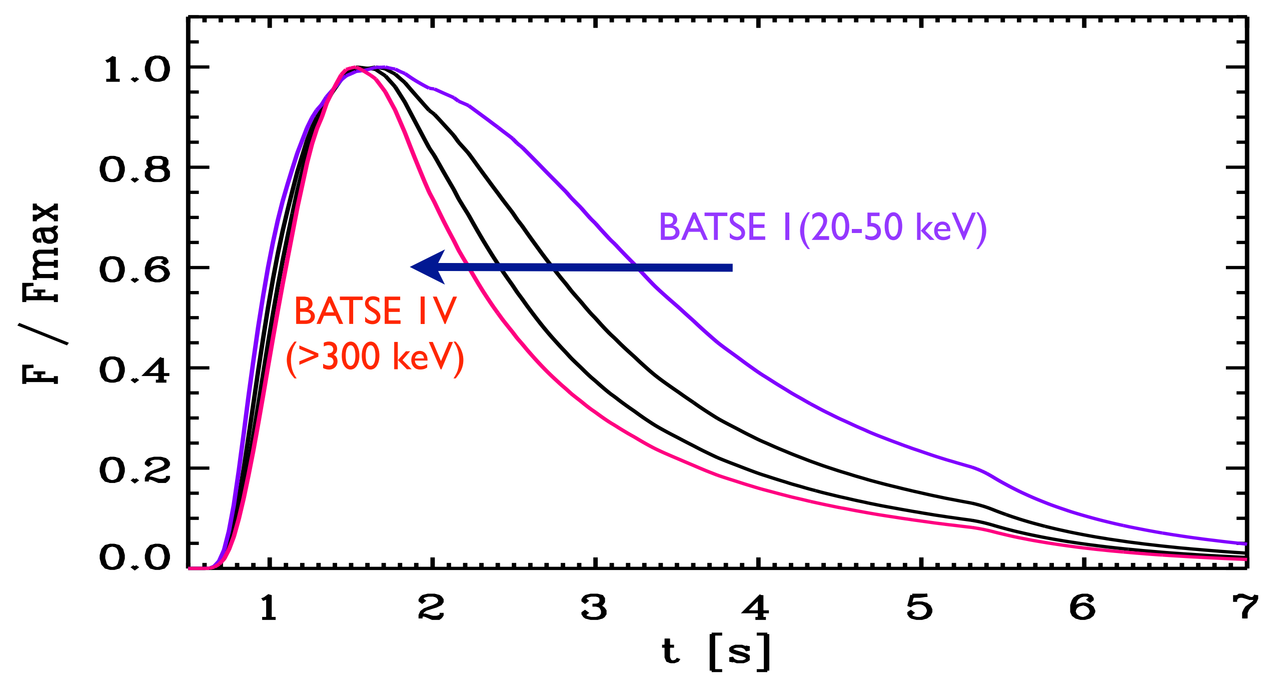

$W(E) \sim E^{-a}$ $\quad a \simeq 0.40$

Fenimore et al 1995
Norris et al 1996
Bissaldi et al. 2011

Emission processes and temporal profile: > 100 MeV bands

Model: in LAT (>100 MeV) energy bands both components present, synchrotron + IC

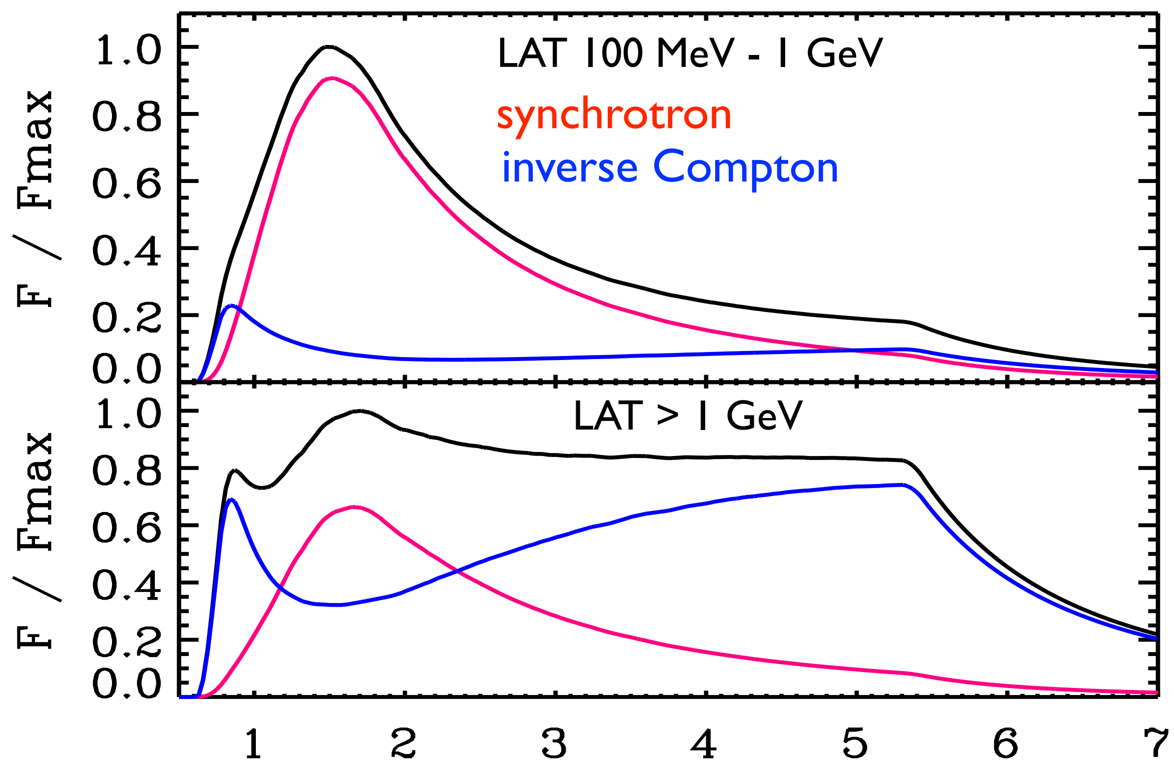

Emission processes and temporal profile: > 100 MeV bands

Model: in LAT (>100 MeV) energy bands both components present, synchrotron + IC

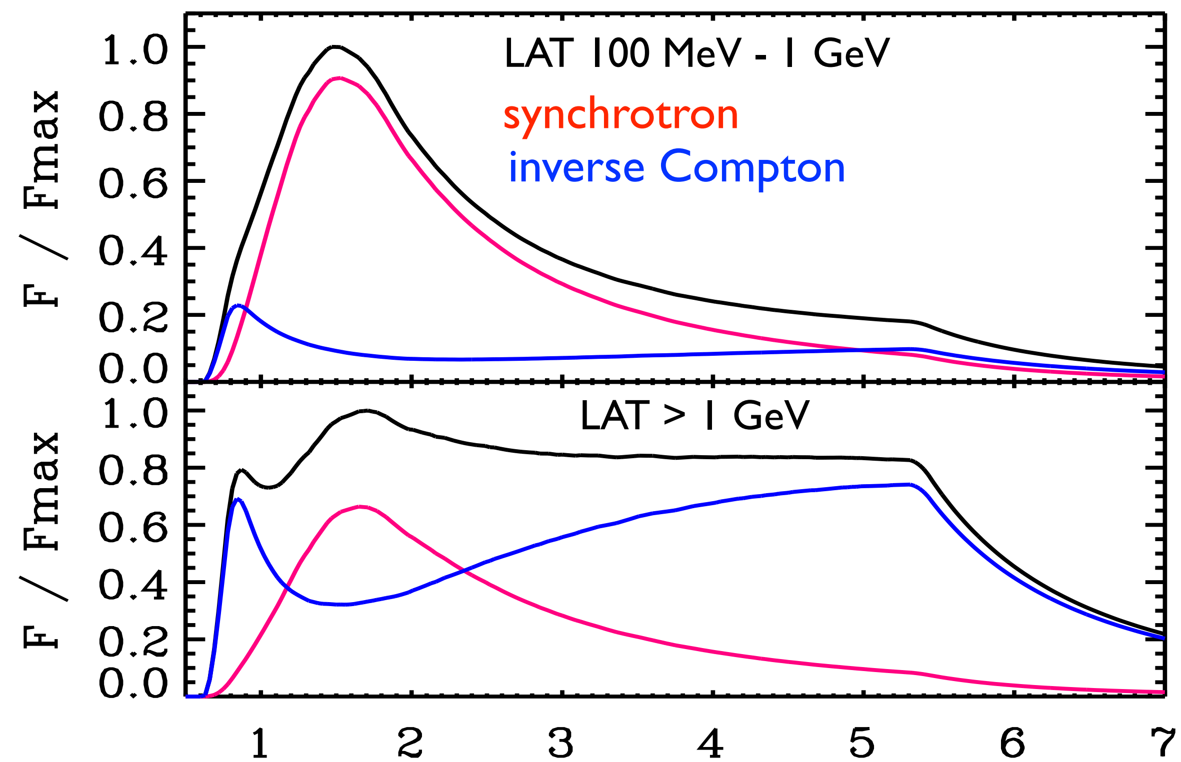

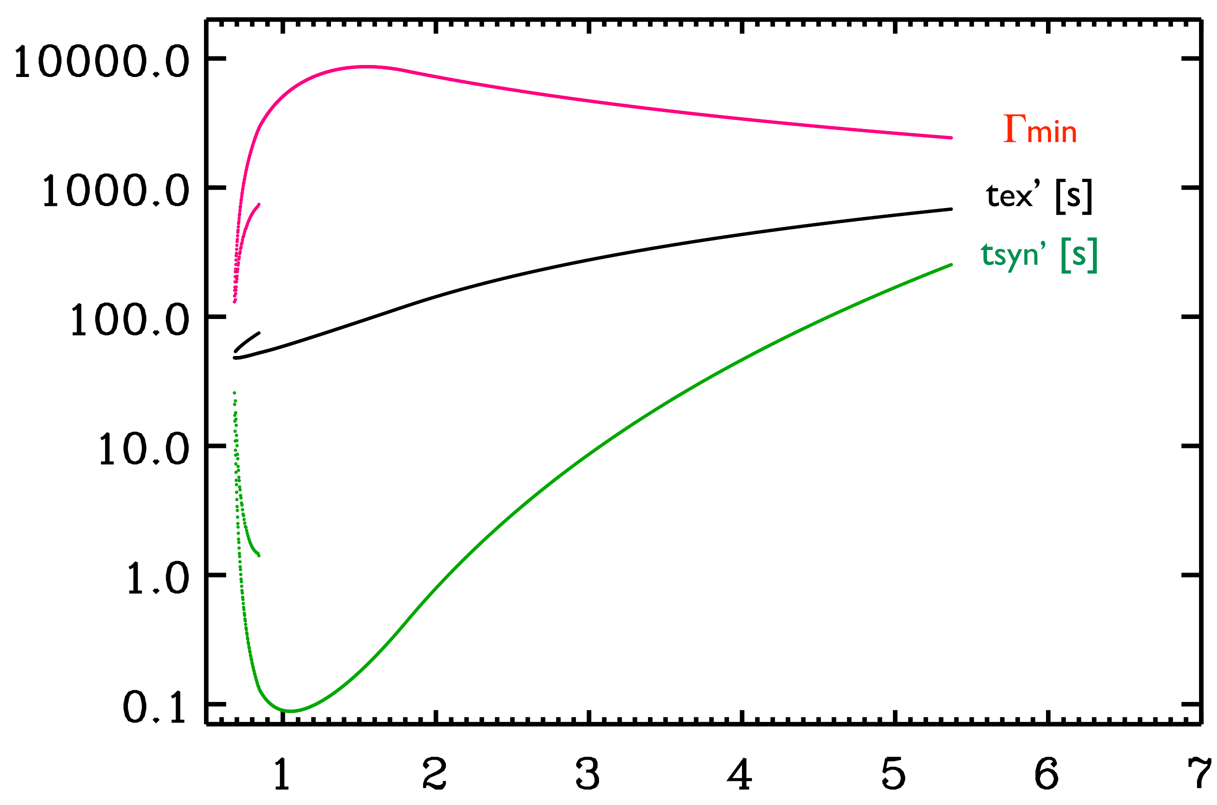

Emission processes and temporal profile: > 100 MeV bands

Model: in LAT (>100 MeV) energy bands both components present, synchrotron + IC

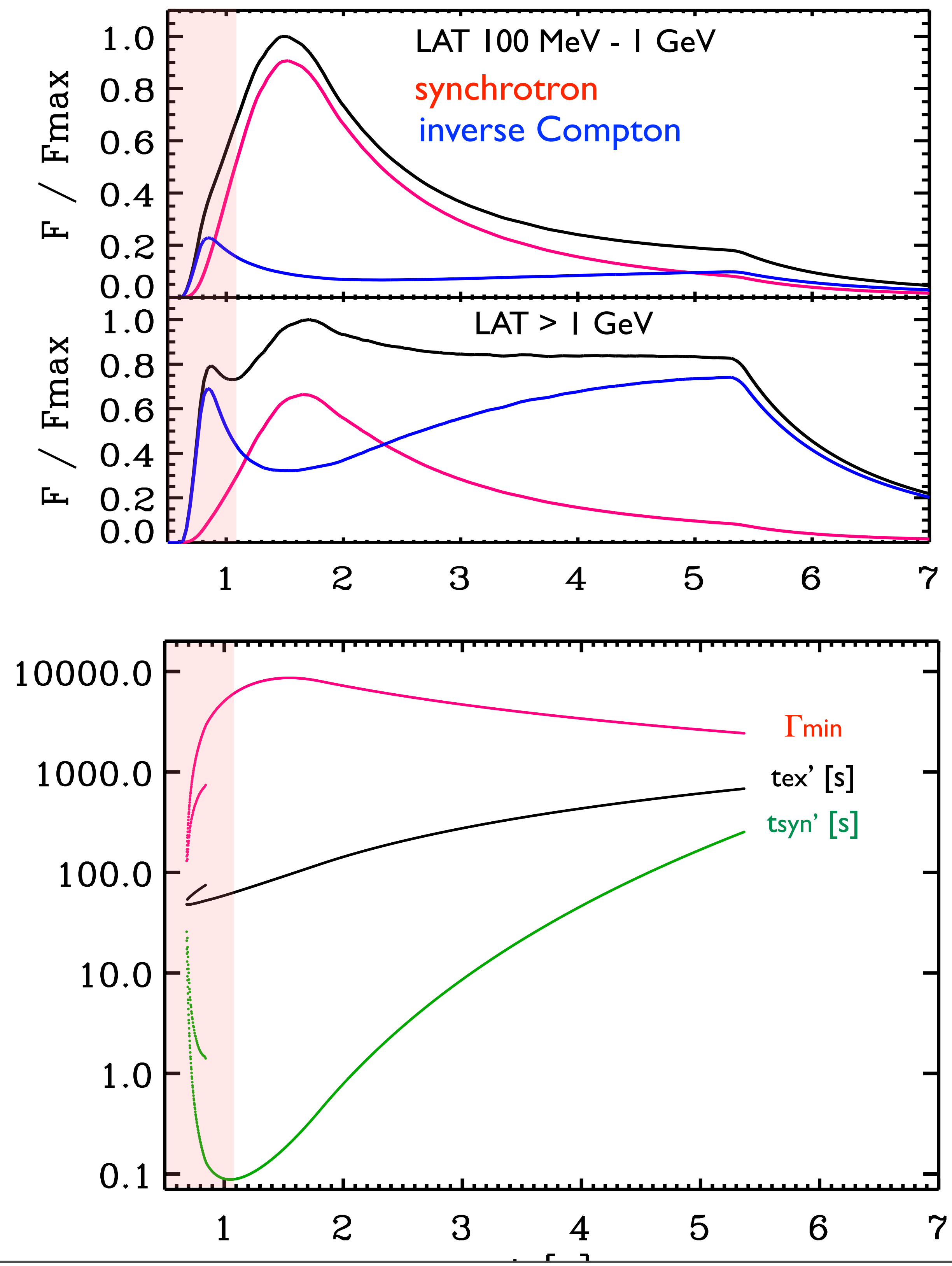

weak shock

ε^* low

moderate $\Gamma_m \Rightarrow$ large t_{syn}'

R small $\Rightarrow t_{ex}' \cong R/\Gamma^* c$ small

$t_{syn}' \leq t_{ex}' \Rightarrow$ large efficiency of IC

Emission processes and temporal profile: > 100 MeV bands

Model: in LAT (>100 MeV) energy bands both components present, synchrotron + IC

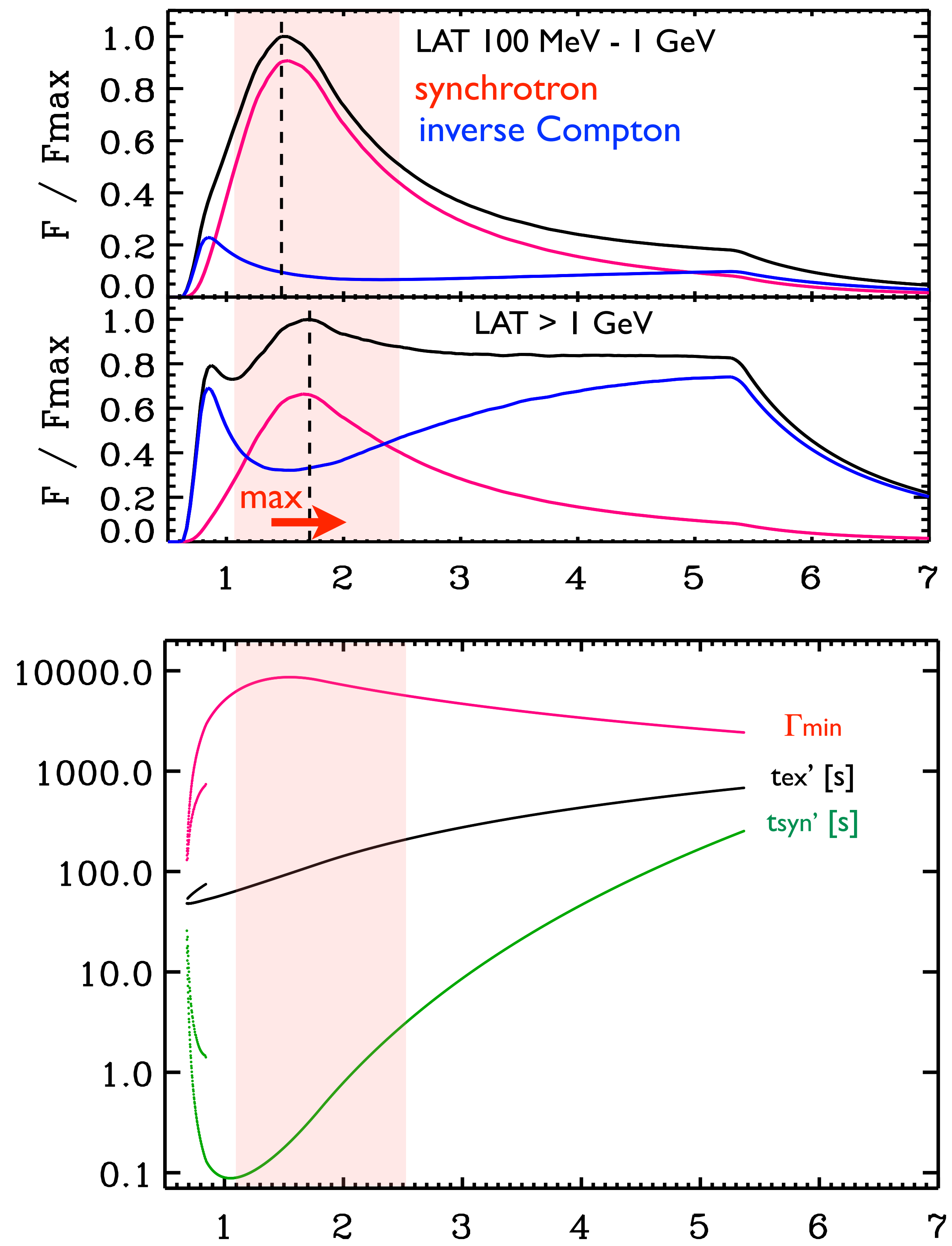

shock becomes stronger

Γ_m increases $\Rightarrow$ t_{syn}' decreases

R, t_{ex}' increase

$t_{syn}' \ll t_{ex}'$ $\Rightarrow$ low efficiency of IC

dominant synchrotron component

Emission processes and temporal profile: > 100 MeV bands

Model: in LAT (>100 MeV) energy bands both components present, synchrotron + IC

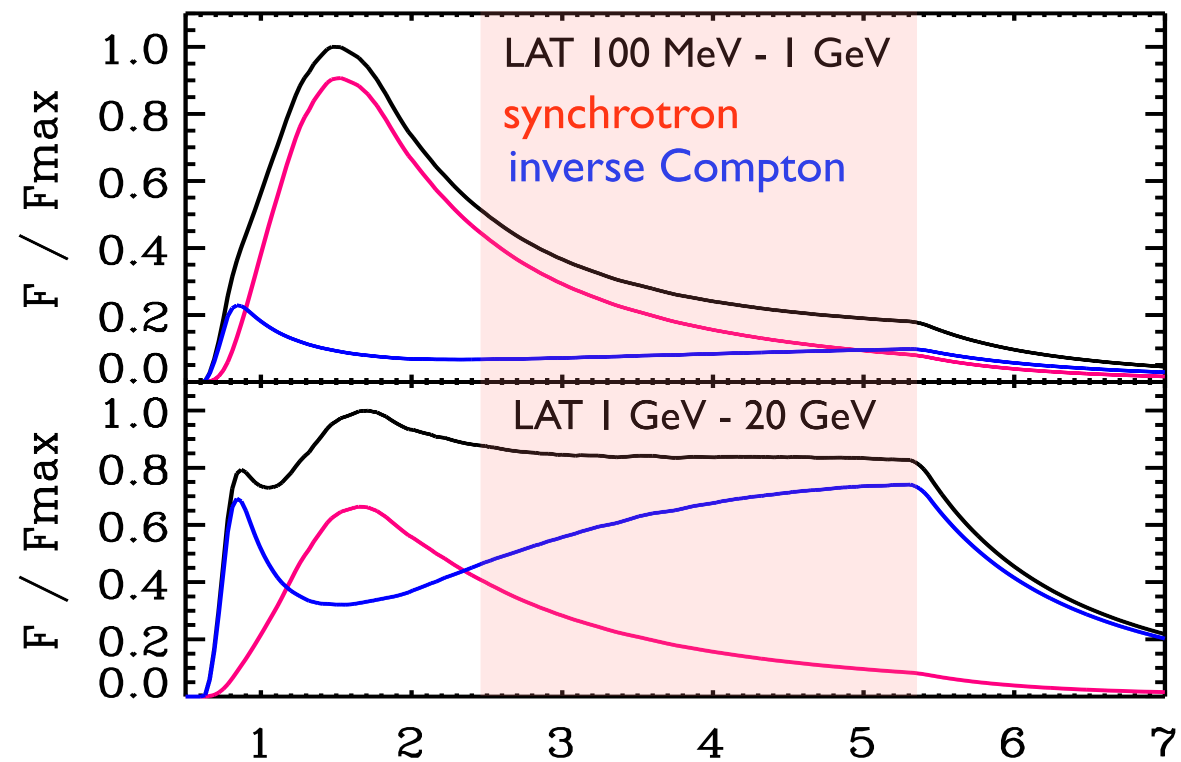

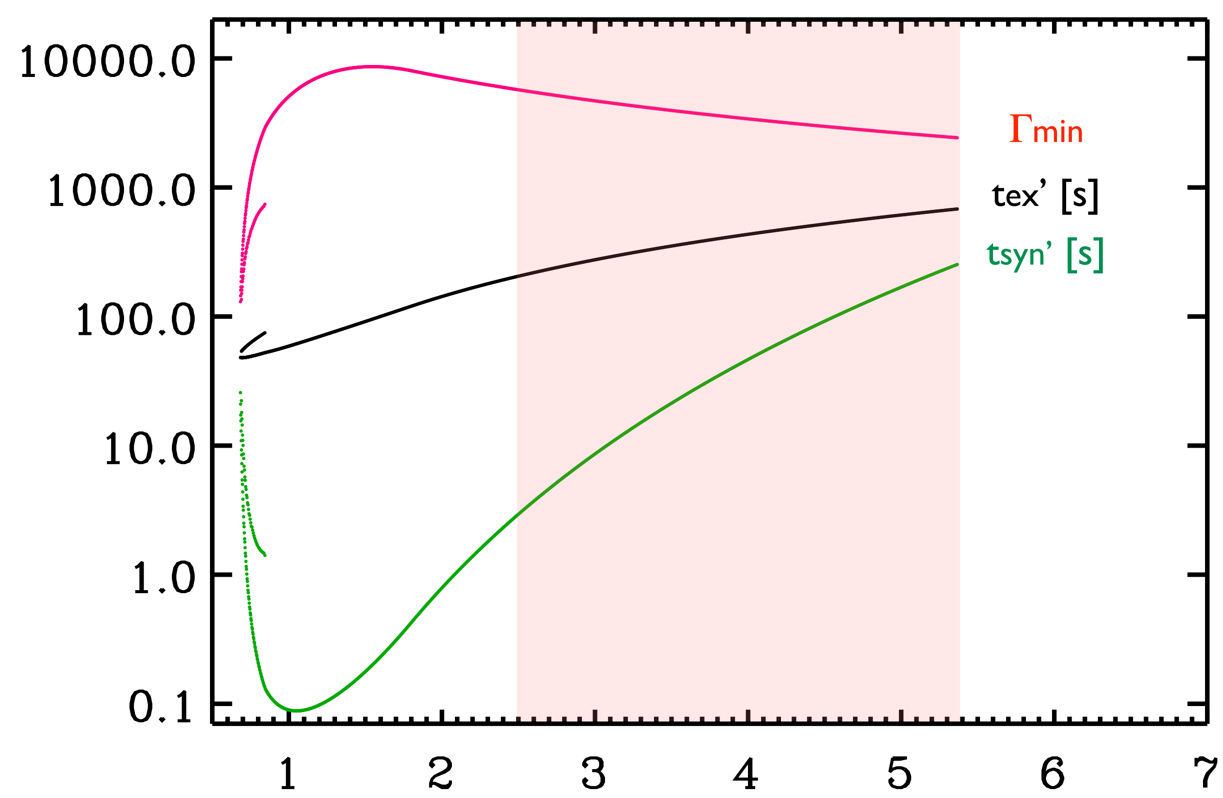

tail of the pulse:

B decreases ⇒ tsyn' increases

tsyn' ≤ tex' ⇒ increased efficiency of IC

IC component dominant in GeV

Emission processes and spectral properties

4-parameters “Band spectrum”
E_p, α, β and normalization
Band et al. 1993

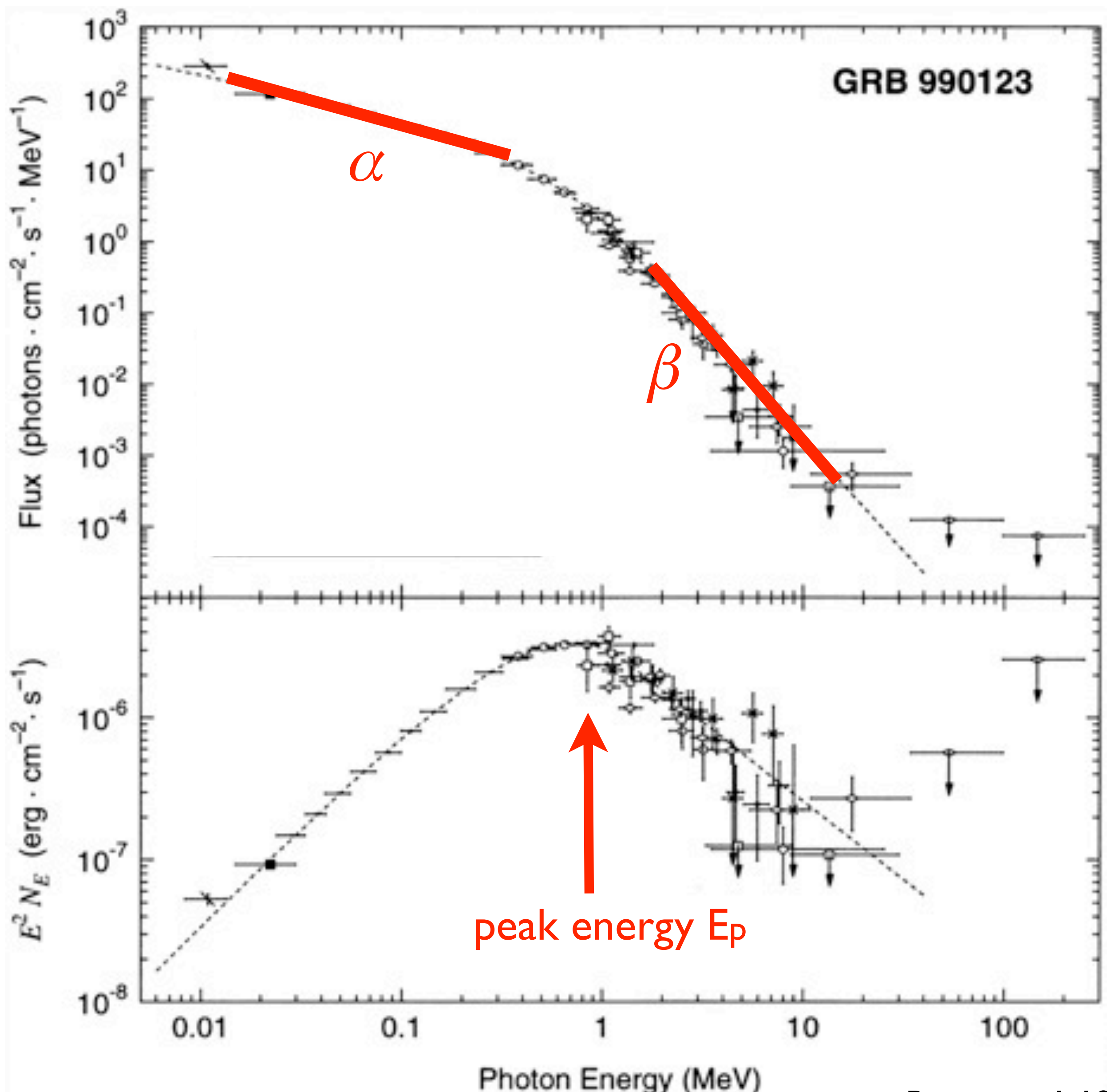

Briggs et al. 1999

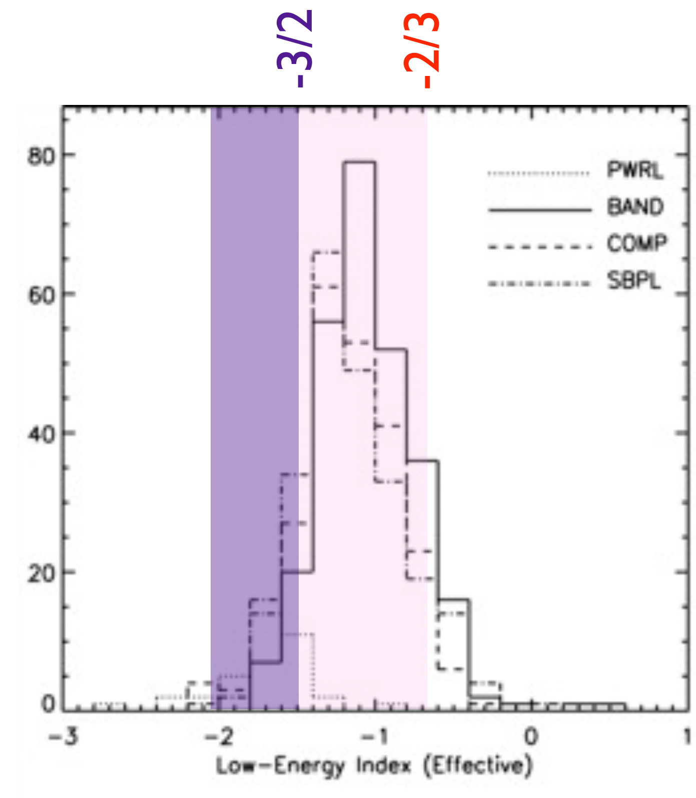

α = -1.02 ± 0.27

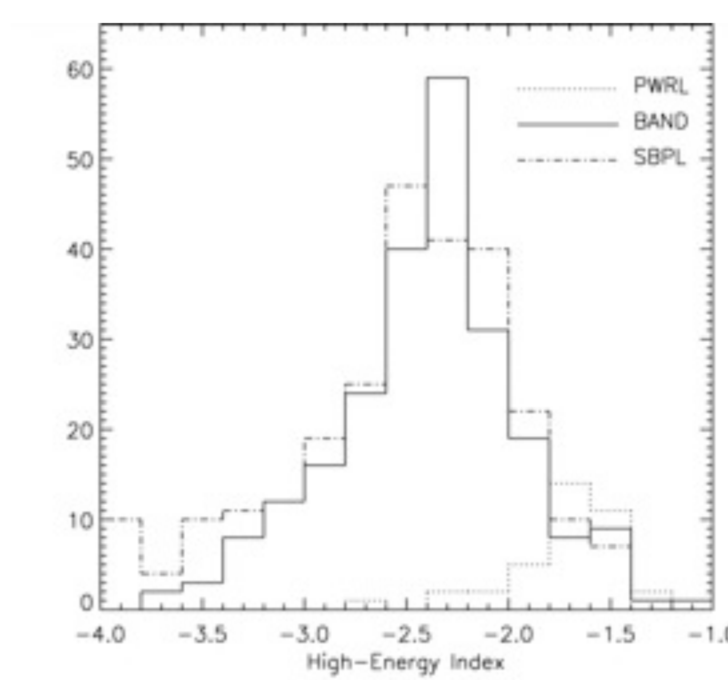

β = -2.35 ± 0.27

Kaneko et al. 2006

Emission processes and spectral properties

Sari, Piran & Narayan 1998

Relativistic electrons:

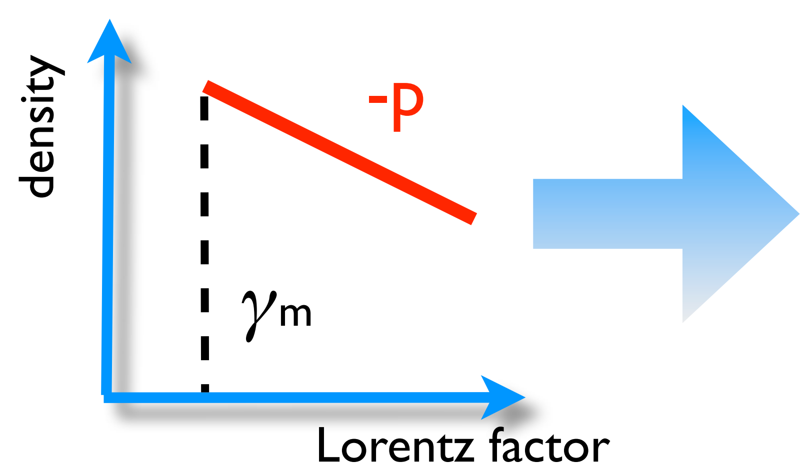

Synchrotron spectrum: fast cooling ($\gamma_c < \gamma_m$)

Synchrotron spectrum: slow cooling ($\gamma_c > \gamma_m$)

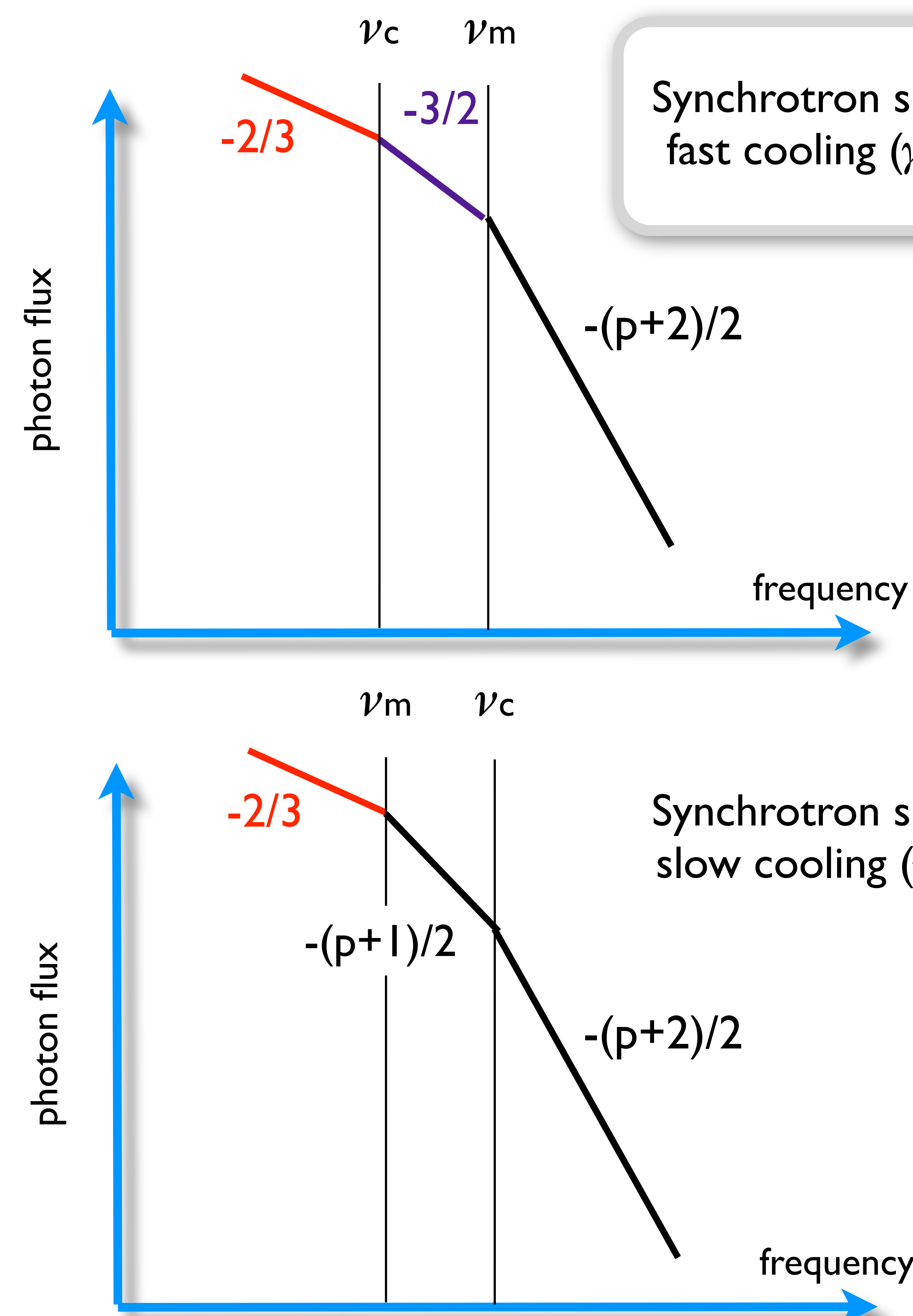

γ_m: minimum Lorentz factor at injection

γ_c: radiative timescale = dynamical timescale

Emission processes and spectral properties

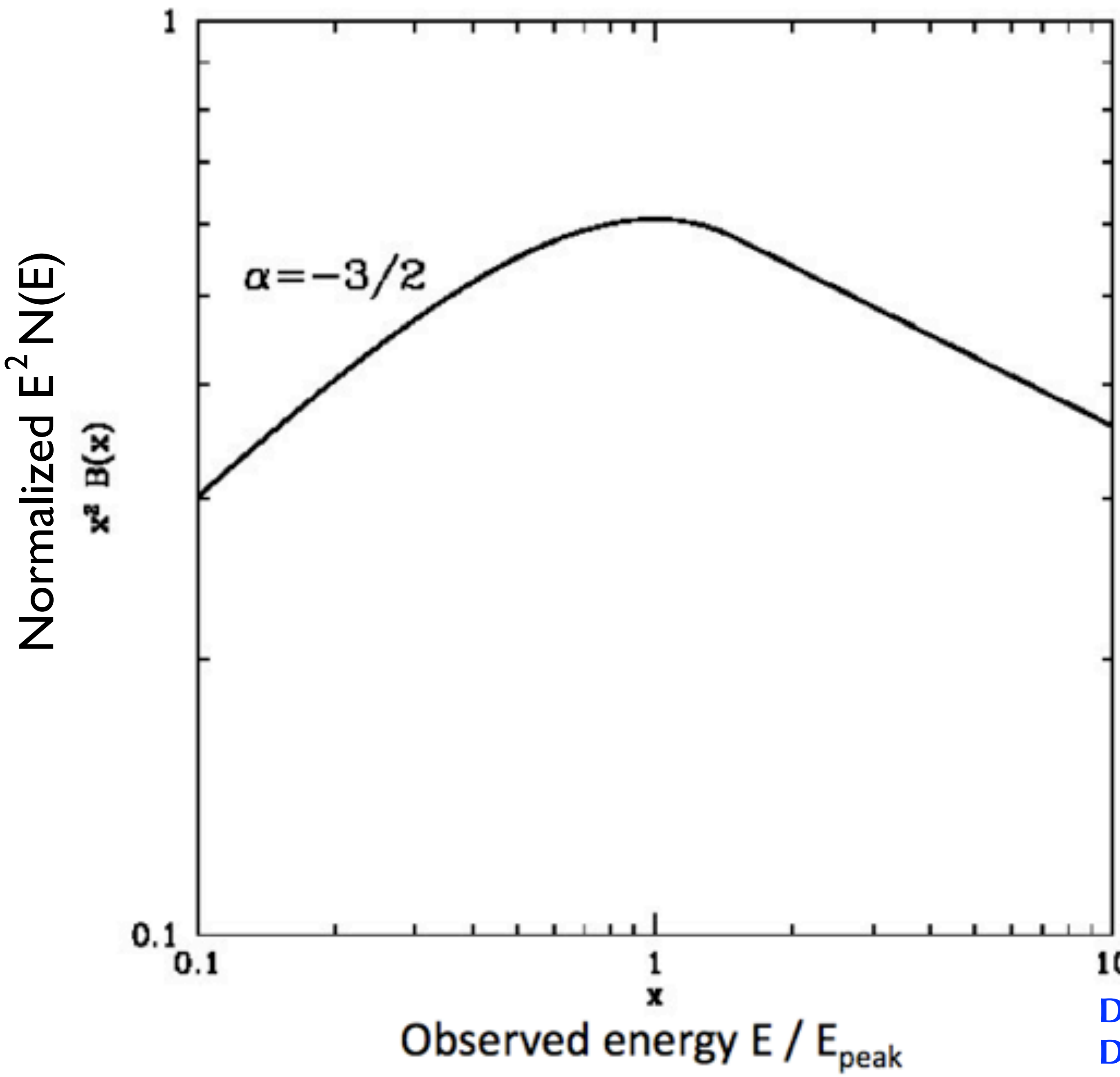

Band function

α = - 1.5
β = - 2.25

Daigne, Bosnjak & Dubus 2011
Derishev 2001

Emission processes and spectral properties

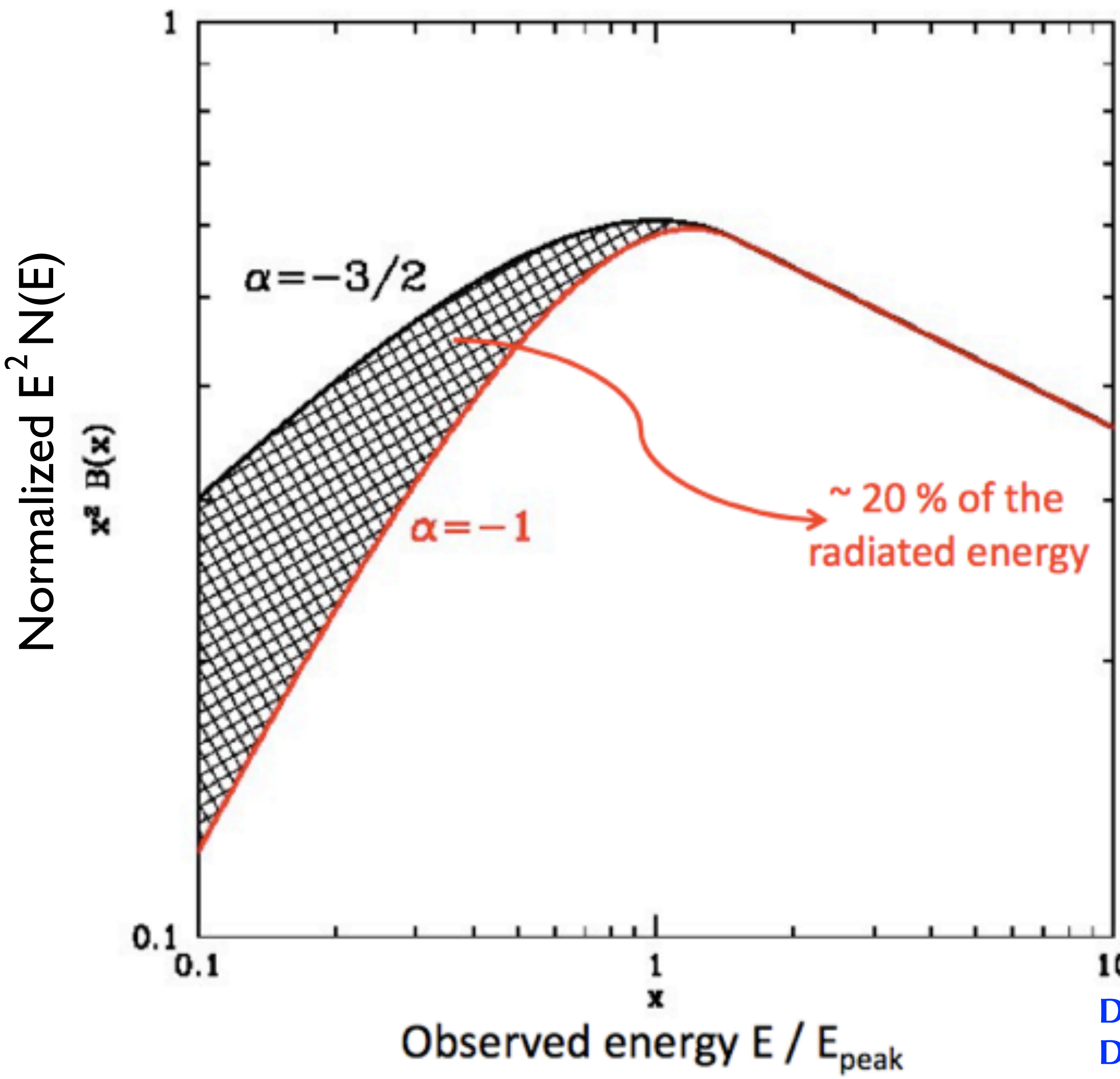

Band function

α = - 1.5 → -1
β = - 2.25

Daigne, Bosnjak & Dubus 2011
Derishev 2001

Inverse Compton scatterings in Klein-Nishina regime have an impact on the synchrotron slope

Emission processes and spectral properties

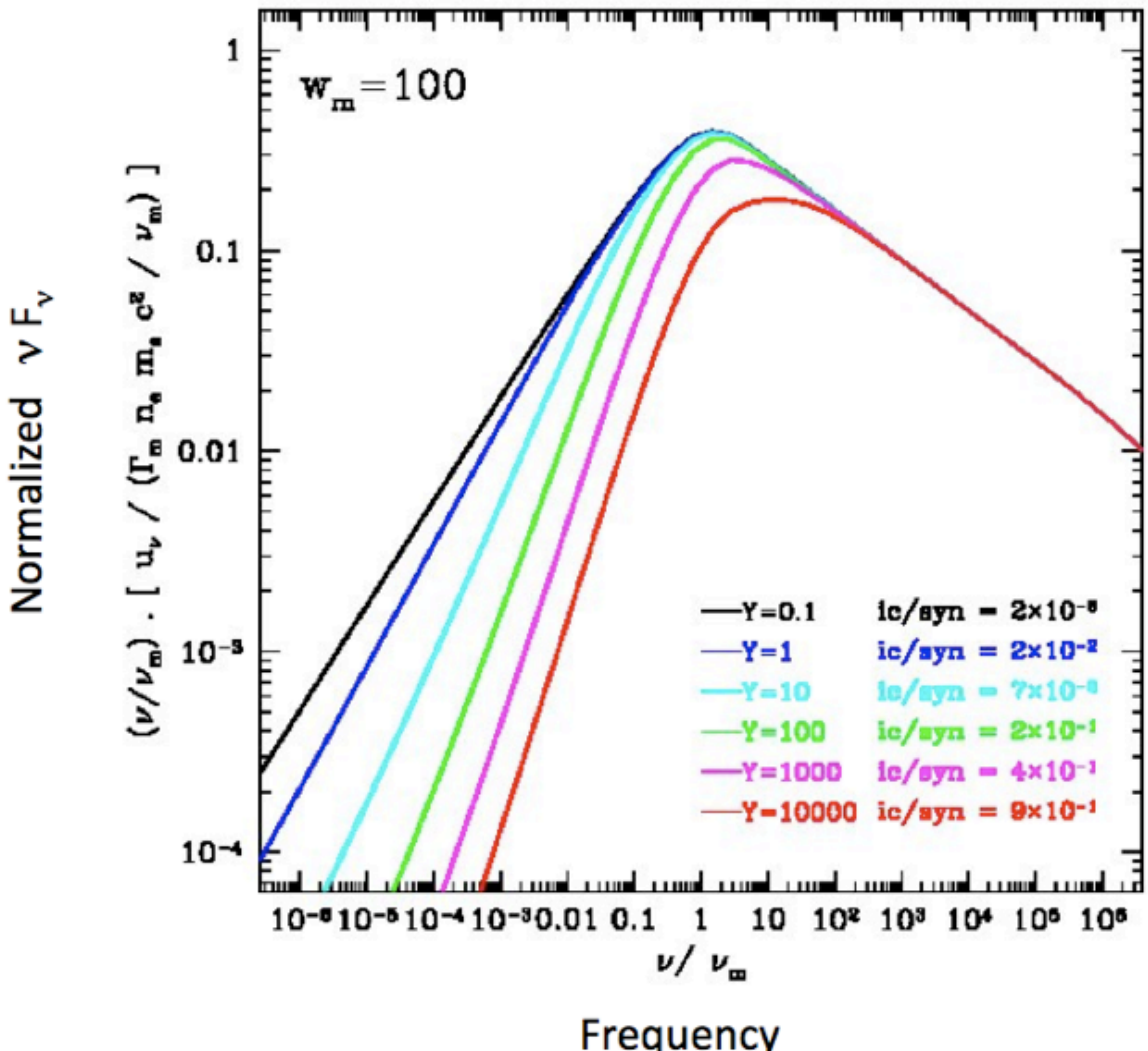

w_m : importance of KN

$$w_m = \Gamma_m \frac{h\nu'_m}{m_e c^2}$$

Y : importance of IC vs syn

$$Y = \frac{4}{3}\tau_T \Gamma_m \Gamma_c \simeq \frac{\epsilon_e}{\epsilon_B}$$

Thomson regime: the electron cooling rate due to IC scatterings remains proportional to γ^2 as for the synchrotron power

KN regime: the electron cooling rate due to IC depends on γ

Exact calculation with synchrotron + IC only
(no adiabatic cooling, synchrotron self-absorption, $\gamma\gamma$ annihilation)

Emission processes and spectral properties

SYNCHROTRON CASE **(B)**

low magnetic field

$dE/dt = 5 \times 10^{53}$ erg s^{-1}, $\varepsilon_B = 0.0005$, $\varepsilon_e = 1/3$, $\zeta = 0.002$, $p = 2.5$, $z=1$

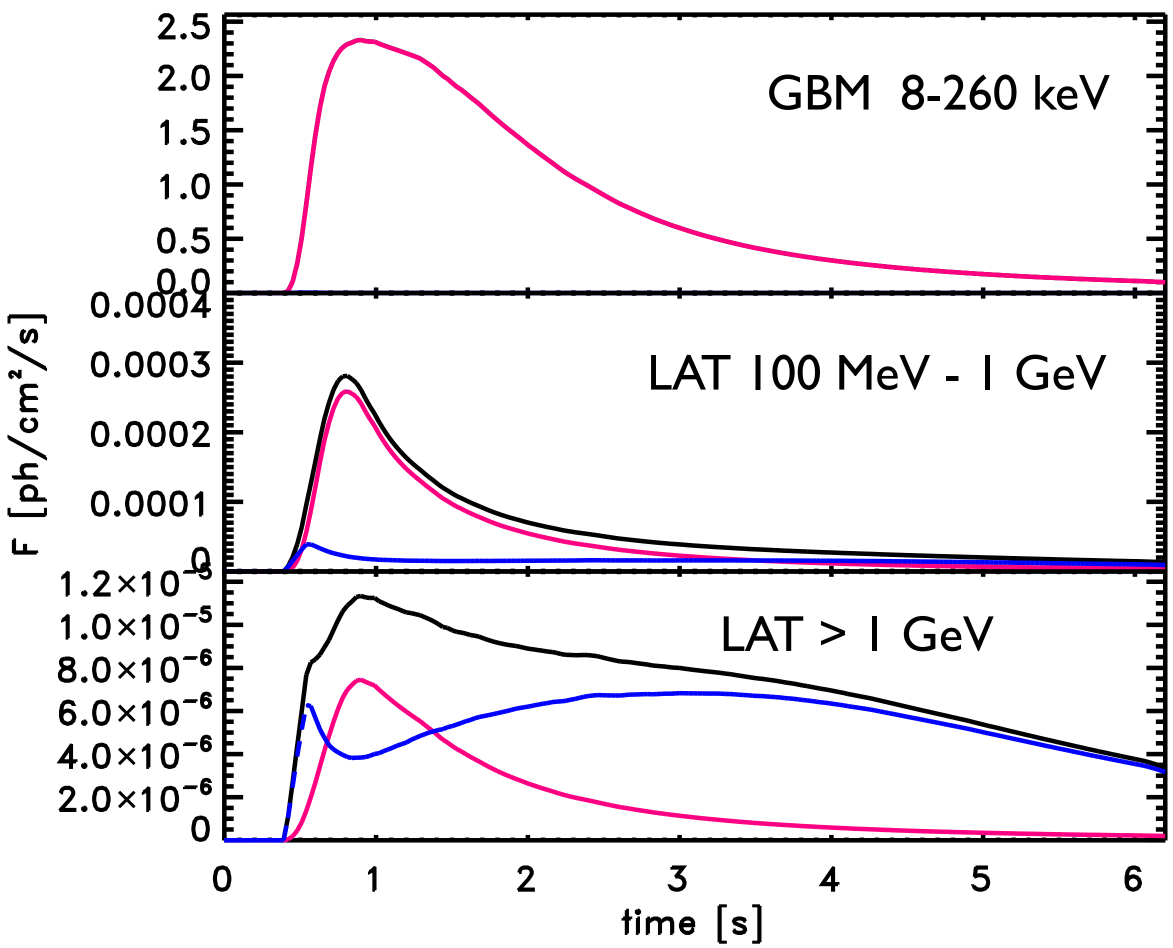

Observed lightcurve

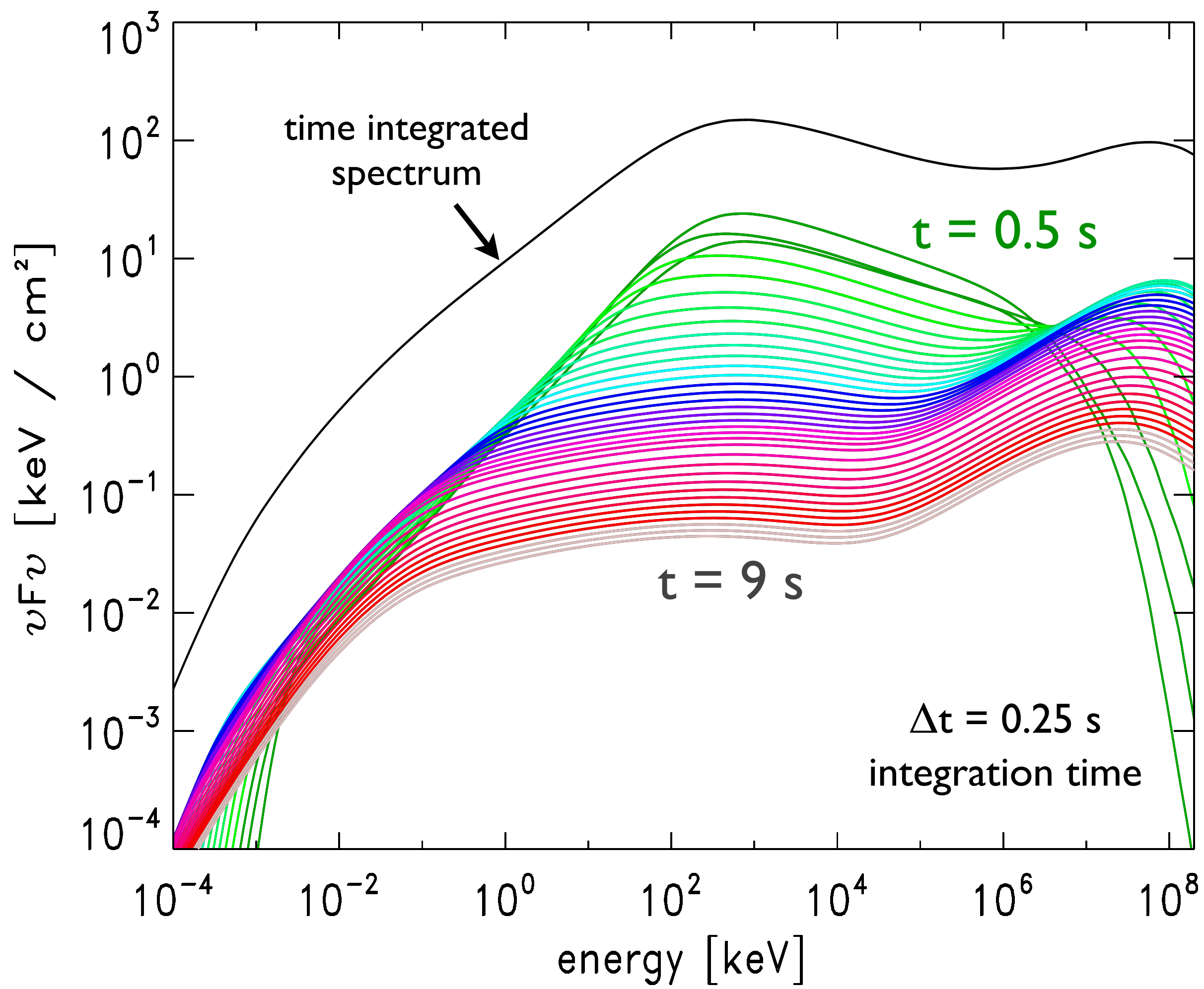

Time resolved spectra

Emission processes and spectral properties

SYNCHROTRON CASE

low magnetic field

dE/dt = 5 x 10^{53} erg s^{-1}, ε_B = 0.0005, ε_e = 1/3, ζ = 0.002, p = 2.5, z=1

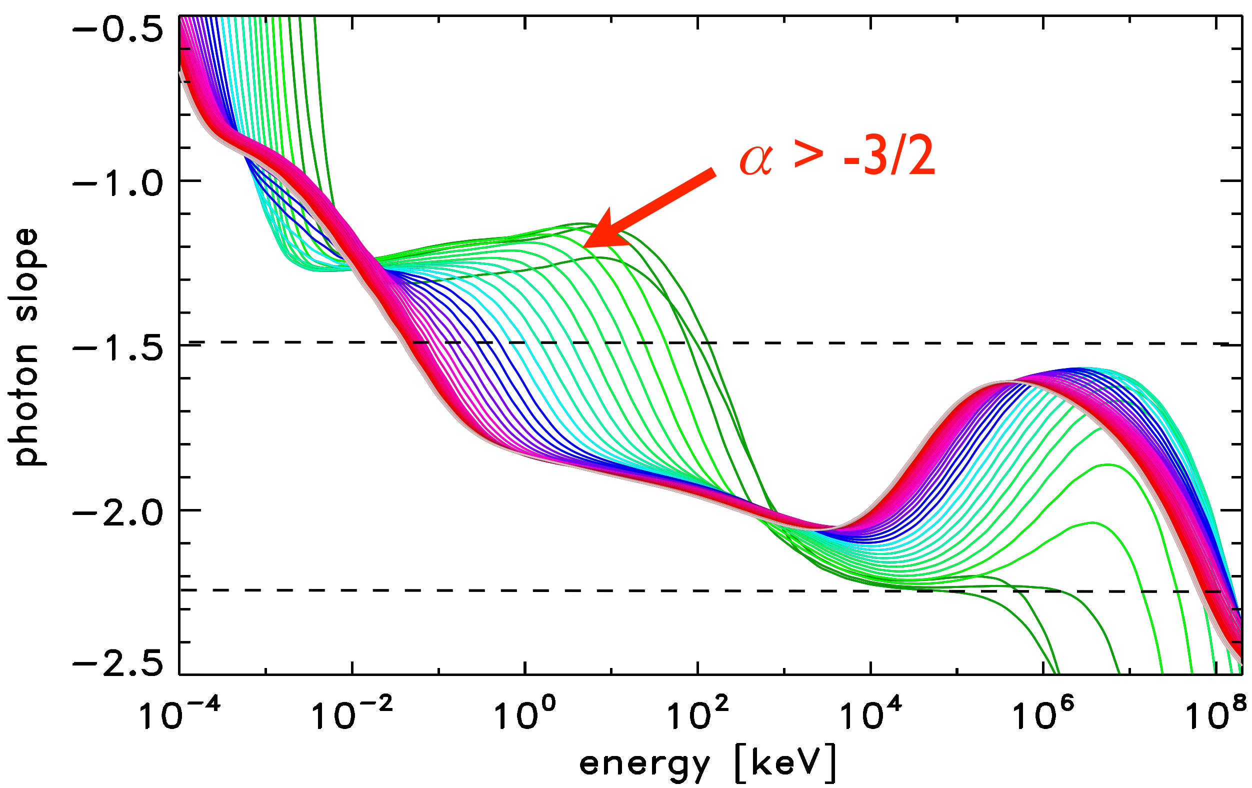

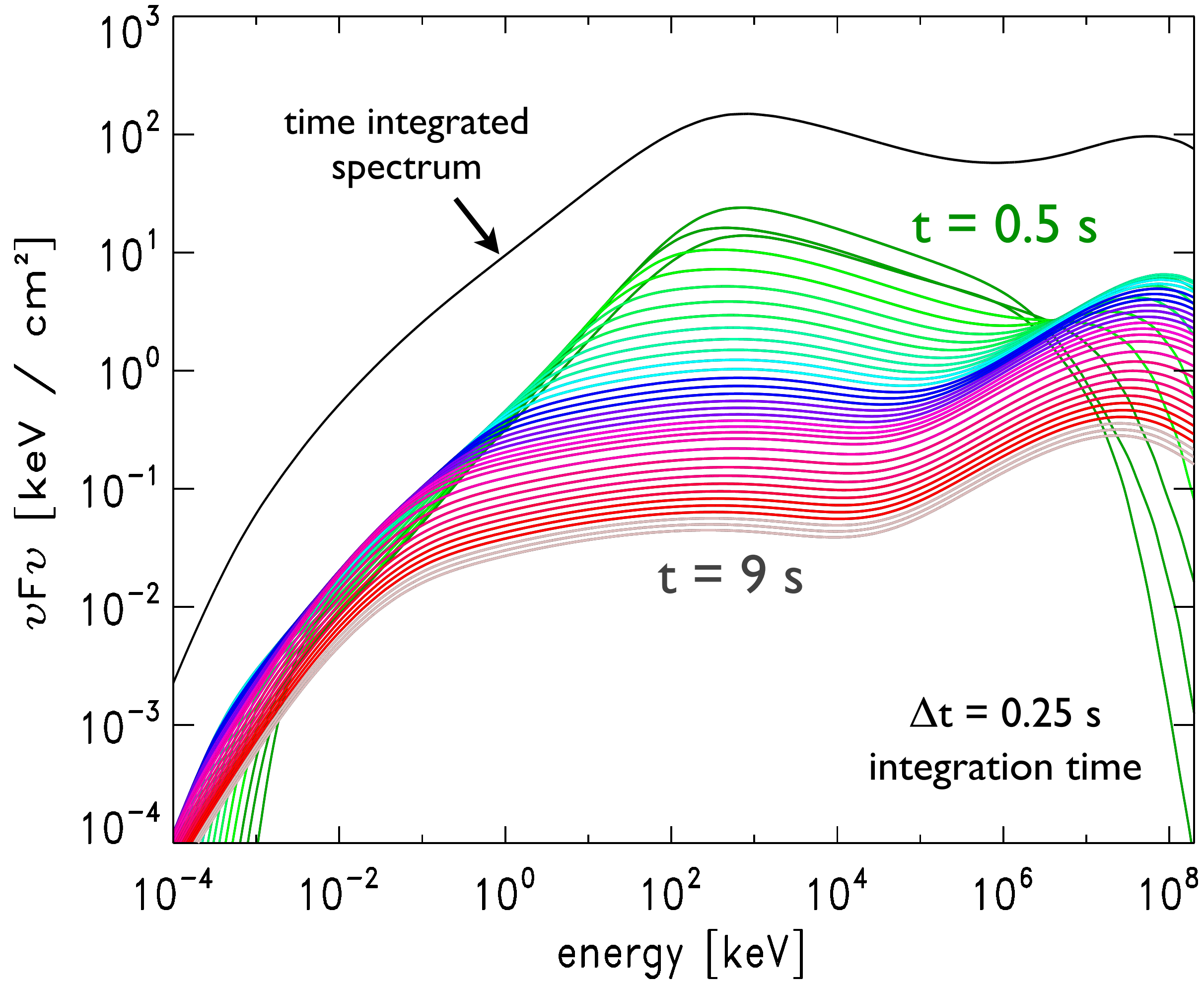

α = -3/2

low energy spectral slope of the fast cooling synchrotron spectrum

Time resolved spectra

Varying the microphysics parameters

SYNCHROTRON CASE

low magnetic field with ζ varying

$dE/dt = 5 \times 10^{53}$ erg s^{-1}, $\varepsilon_B = 0.0005$, $\varepsilon_e = 1/3$, $\zeta_{max} = 0.0025$, $p = 2.5$, $z=1$

We assume $\zeta \sim \varepsilon^*$ (the dissipated energy per proton)

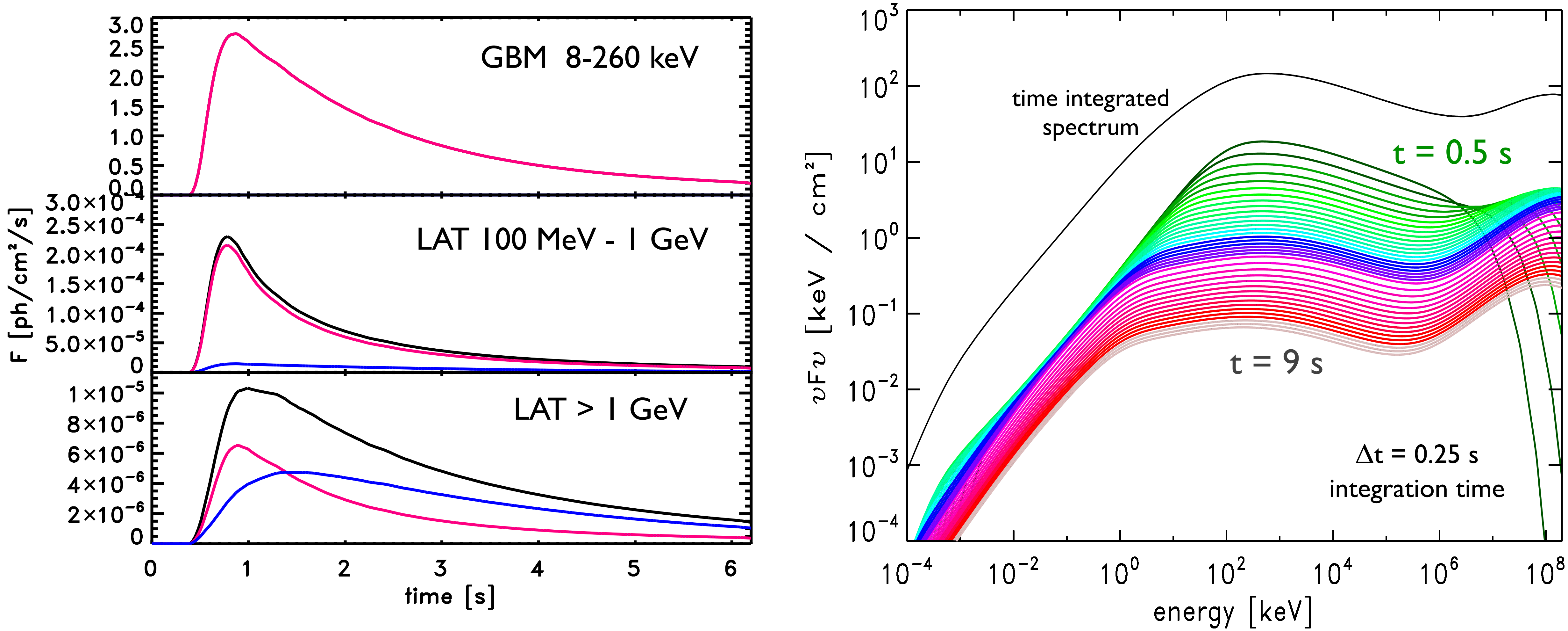

Time resolved spectra

Varying the microphysics parameters

SYNCHROTRON CASE

low magnetic field with ζ varying

$dE/dt = 5 \times 10^{53}$ erg s^{-1}, $\varepsilon_B = 0.0005$, $\varepsilon_e = 1/3$, $\zeta_{max} = 0.0025$, $p = 2.5$, $z=1$

We assume $\zeta \sim \varepsilon^*$ (the dissipated energy per proton)

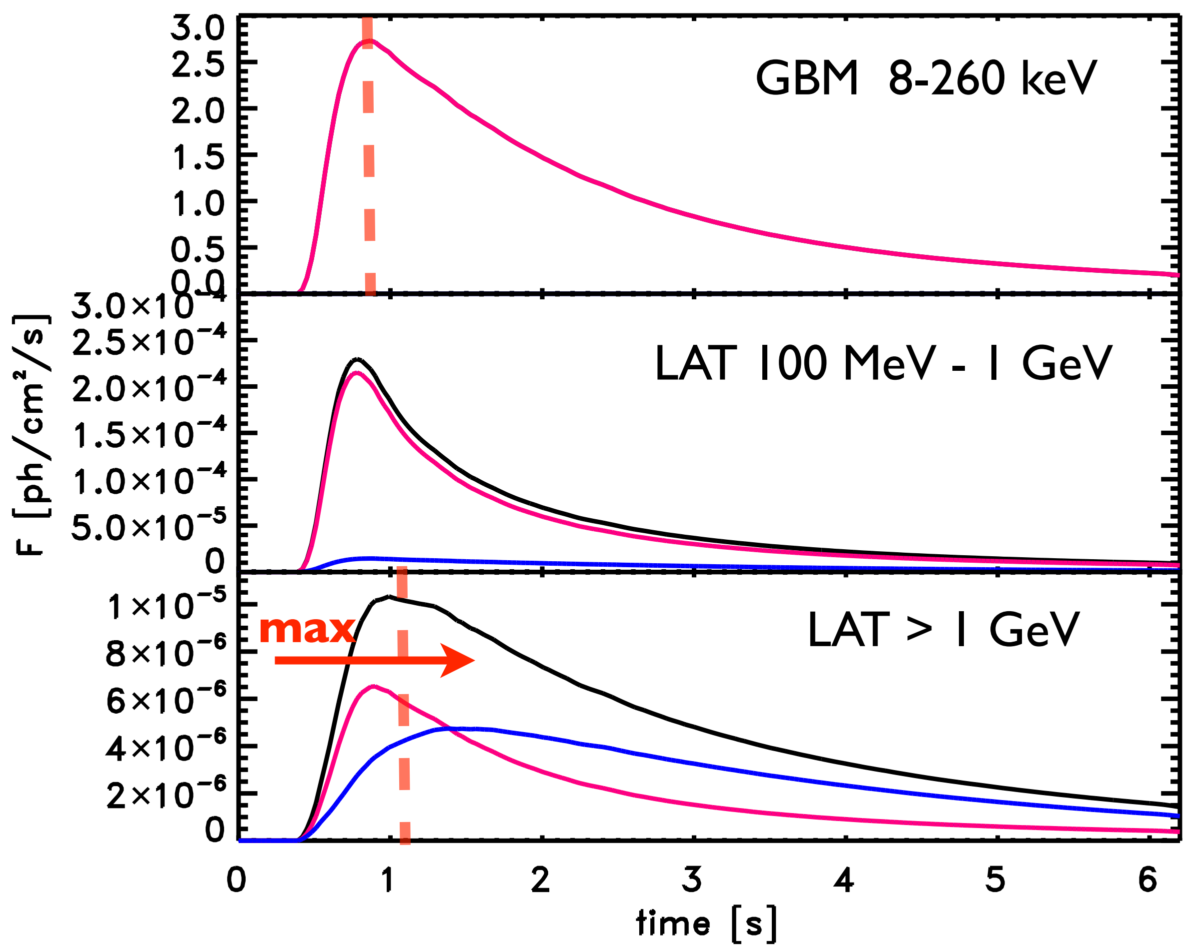

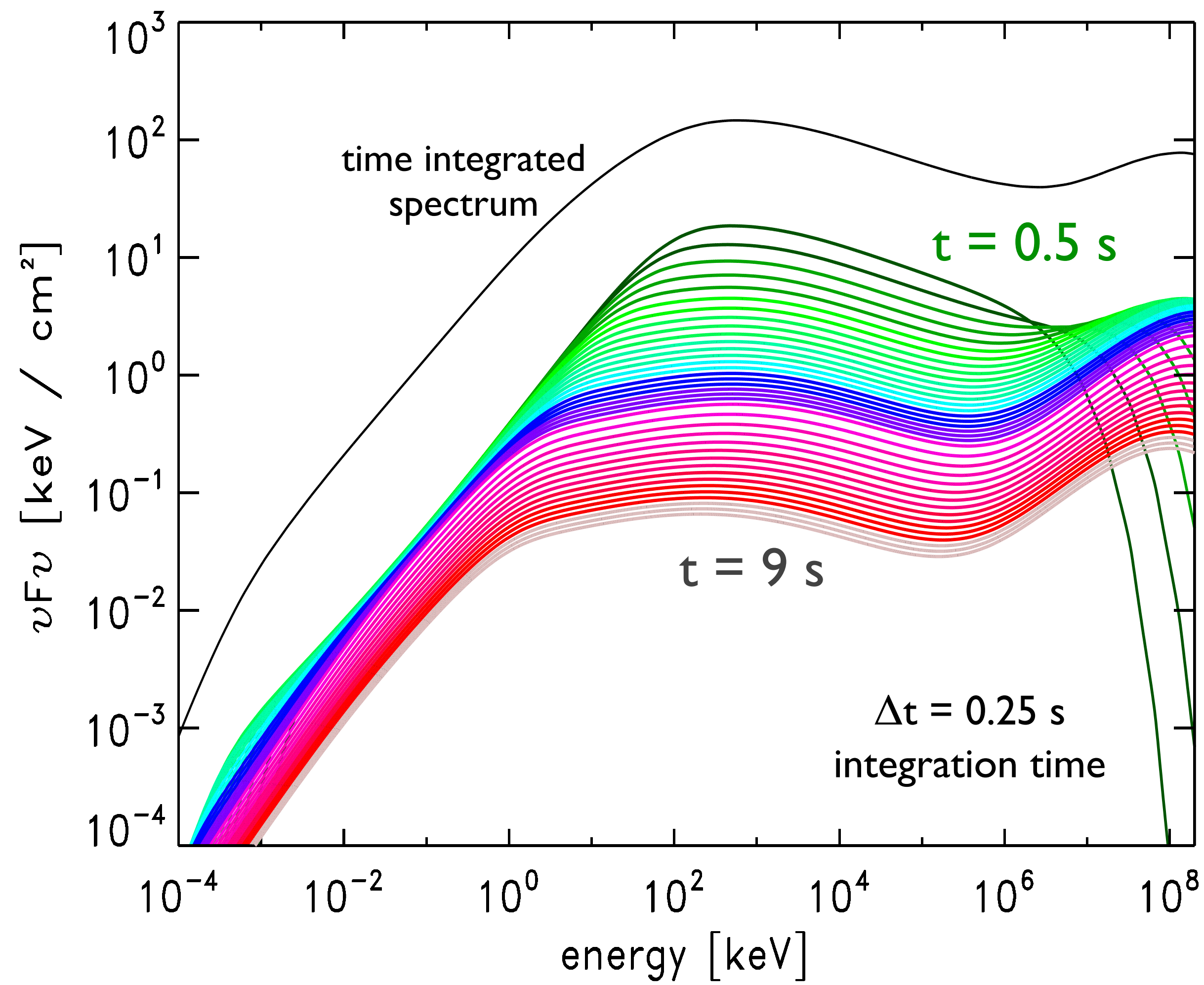

Time resolved spectra

Varying the microphysics parameters

SYNCHROTRON CASE

low magnetic field with ζ varying

dE/dt = 5 x 10^{53} erg s^{-1}, ε_B = 0.0005, ε_e = 1/3, ζ_{max} = 0.0025, p = 2.5, z=1

We assume $\zeta \sim \varepsilon^*$ (the dissipated energy per proton)

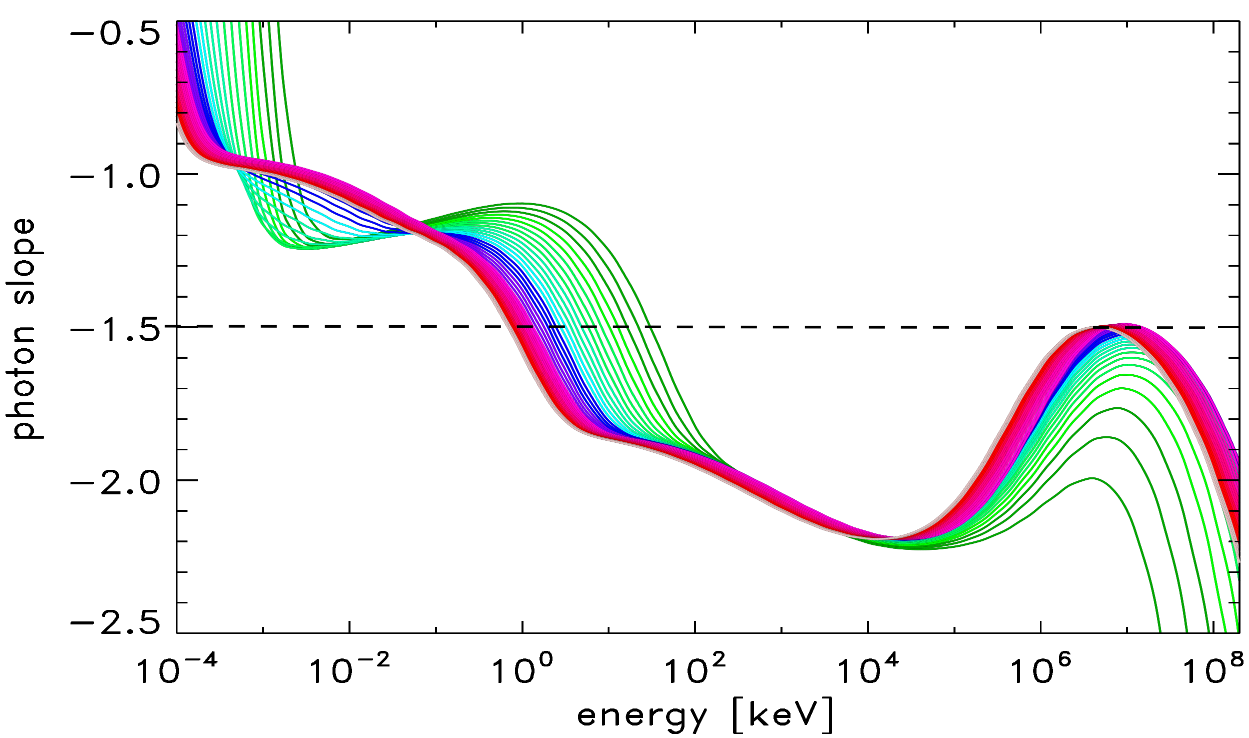

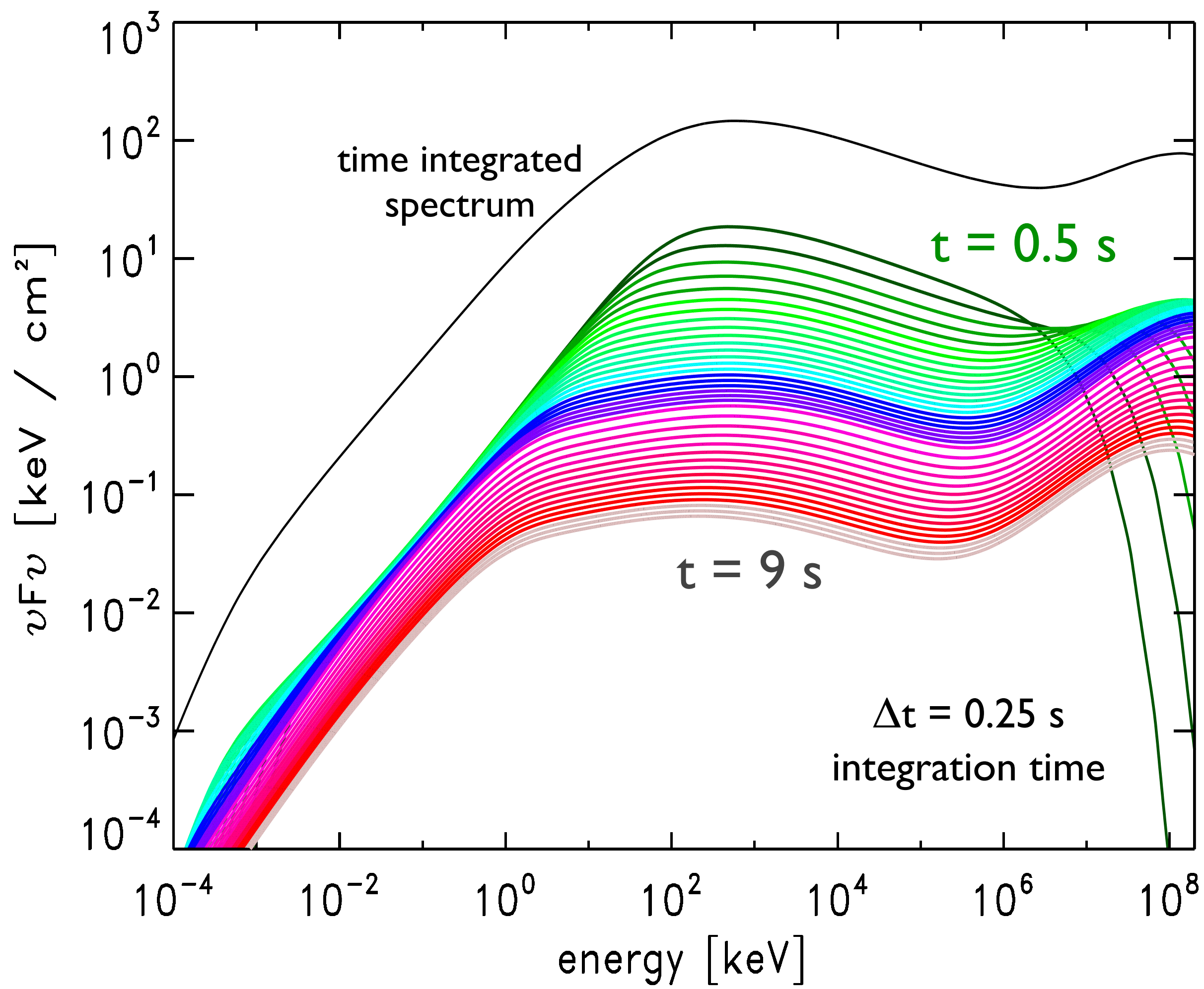

Time resolved spectra

High-energy emission: light curves

Bosnjak & Daigne 2013
submitted

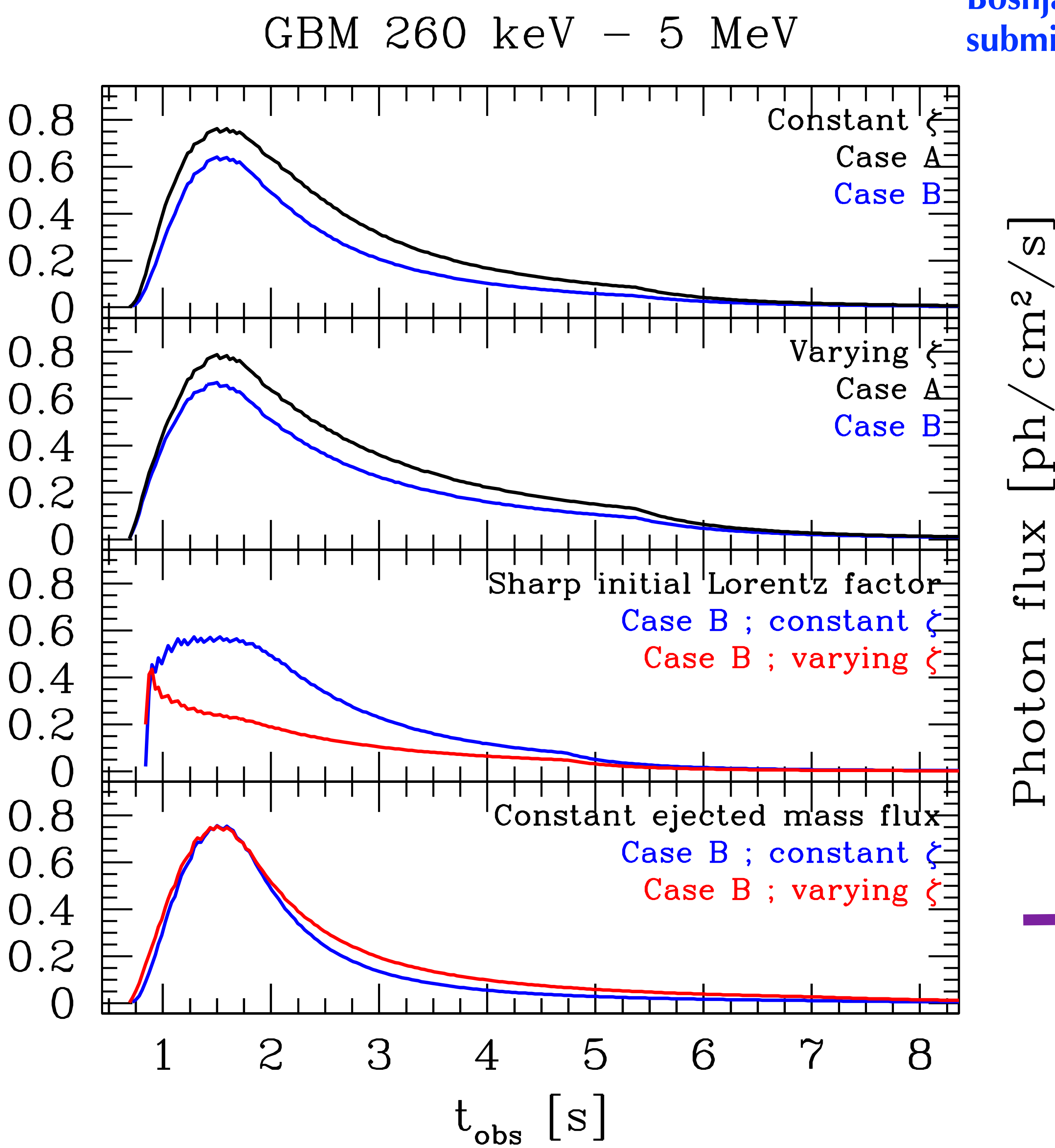

'Sharp' initial Lorentz factor:

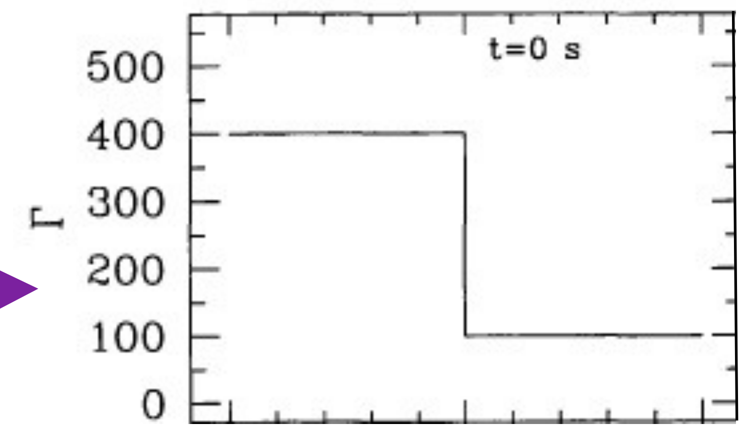

Constant ejected mass flux:
$dE/dt \propto \Gamma$

High-energy emission: light curves

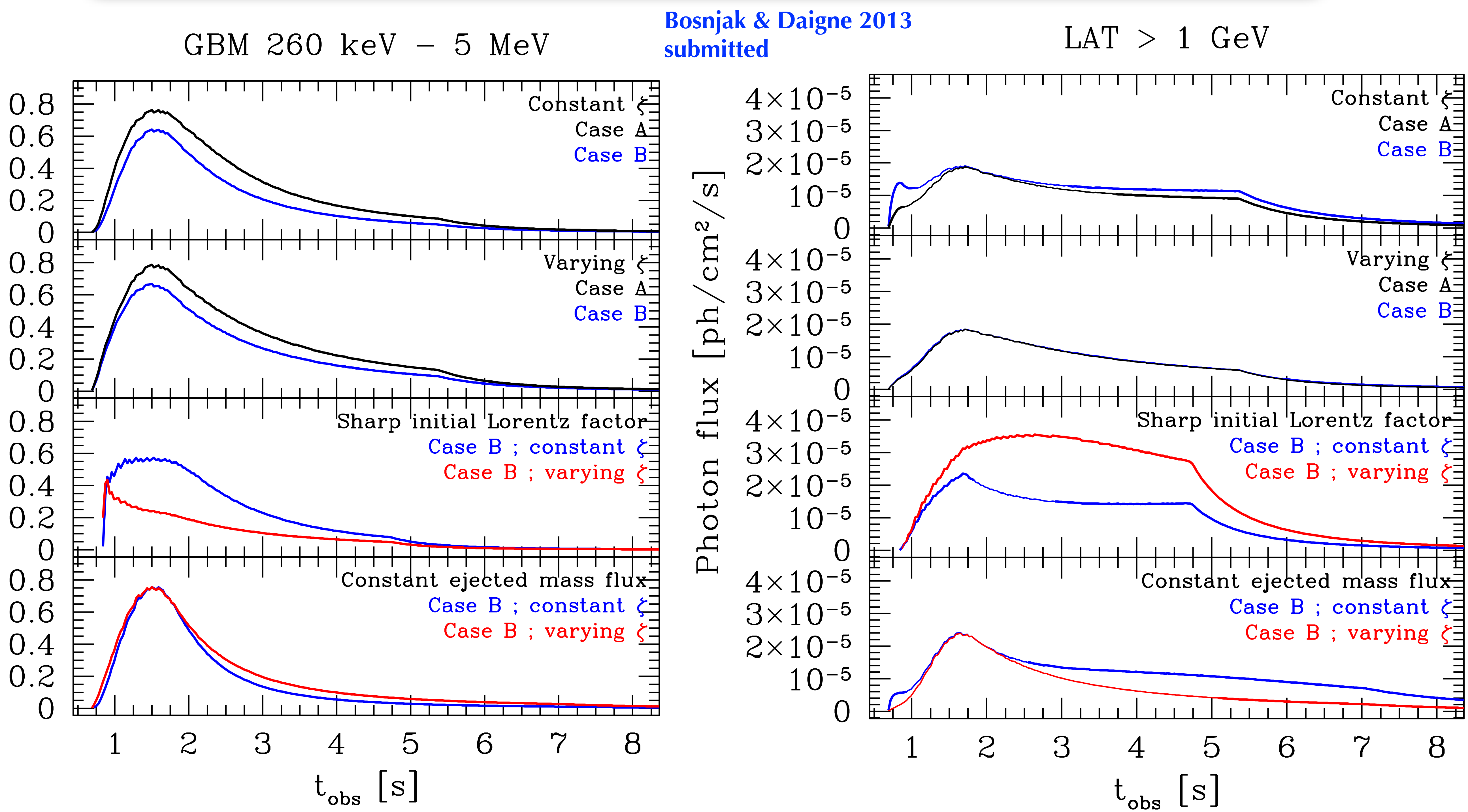

Spectral and temporal behavior: HIC & HFC

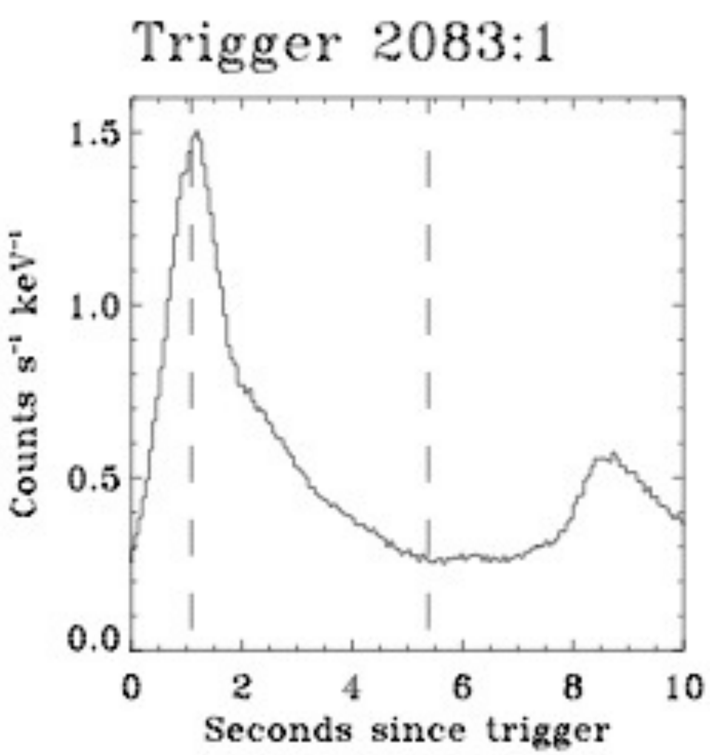

Kargatis 1995
Liang & Kargatis 1996
Ryde & Svensson 2002

Bosnjak & Daigne 2013 submitted

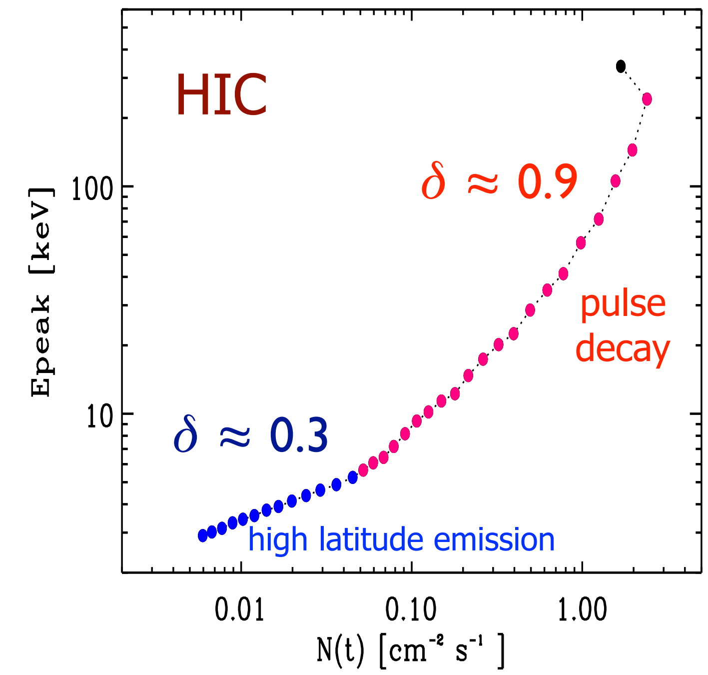

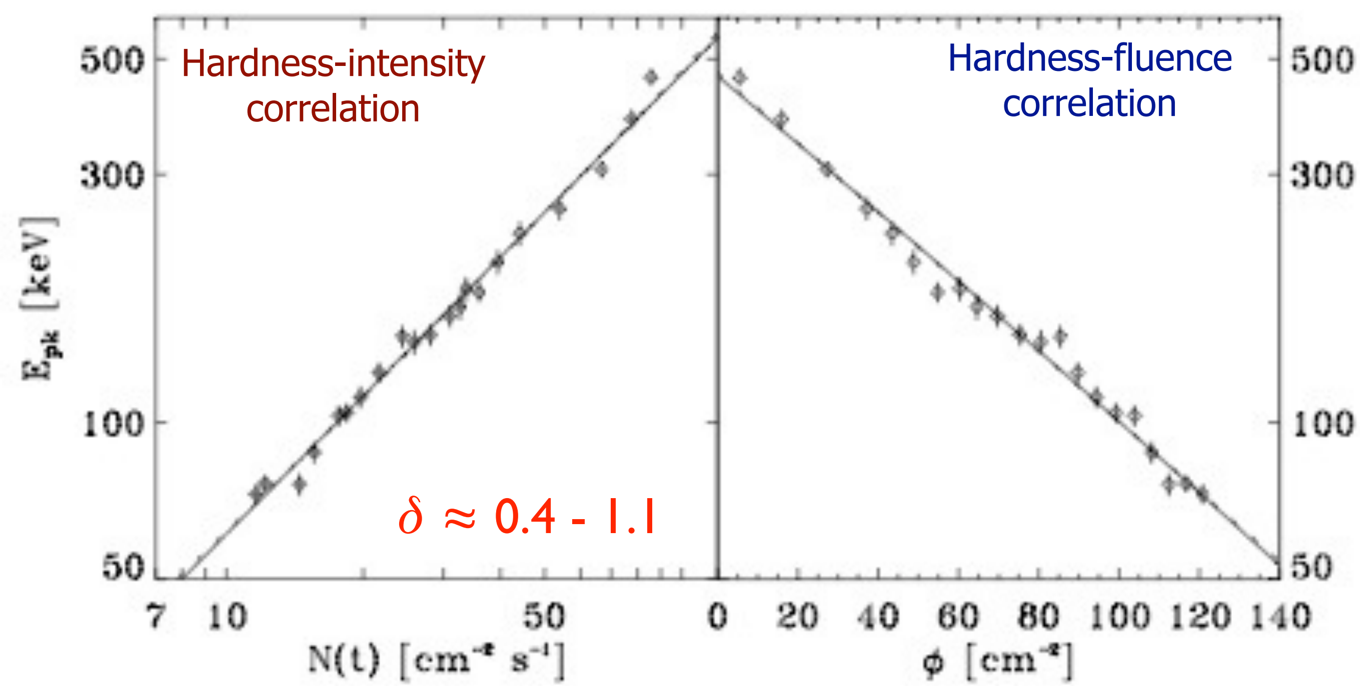

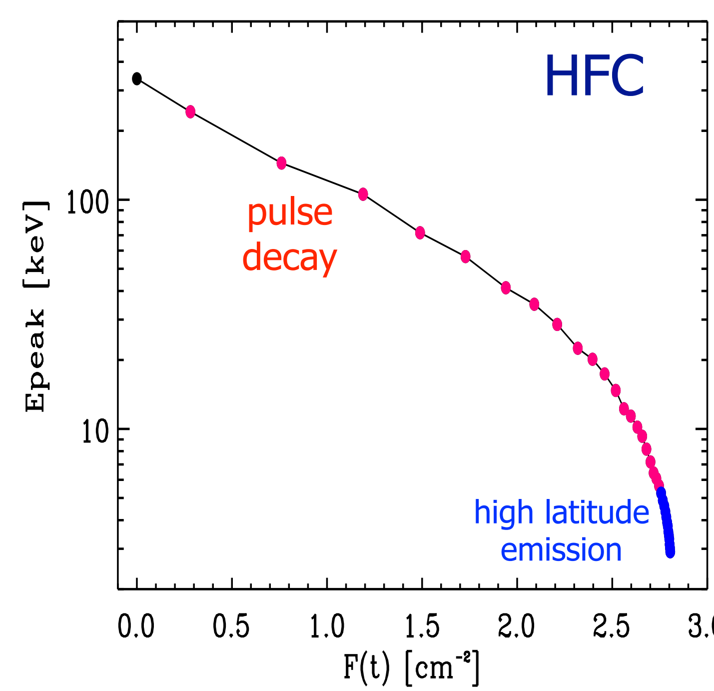

$$E_{pk}(N) = E_{pk,\,0}(N/N_0)^{\delta}$$

$$E_{pk}(\Phi) = E_{pk,\,max}\, e^{-\Phi/\Phi_0}$$

HLE: $E_p \propto 1/\, t_{obs}$

$F_{bol} \propto 1/\, t_{obs}^3$

Spectral and temporal behavior: HIC & HFC

Spectral peak energy is affected by inverse Compton scatterings

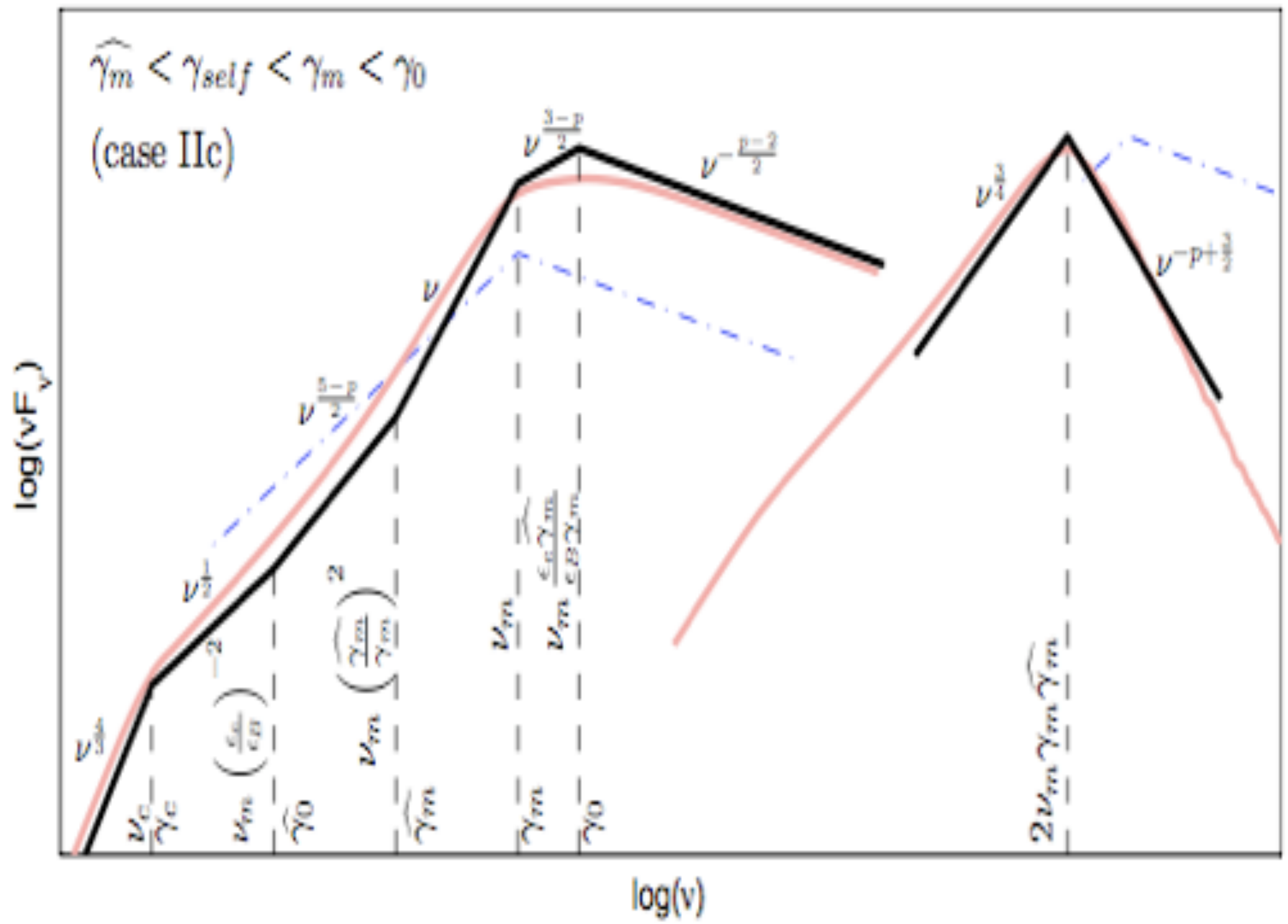

Nakar, Ando & Sari 2009

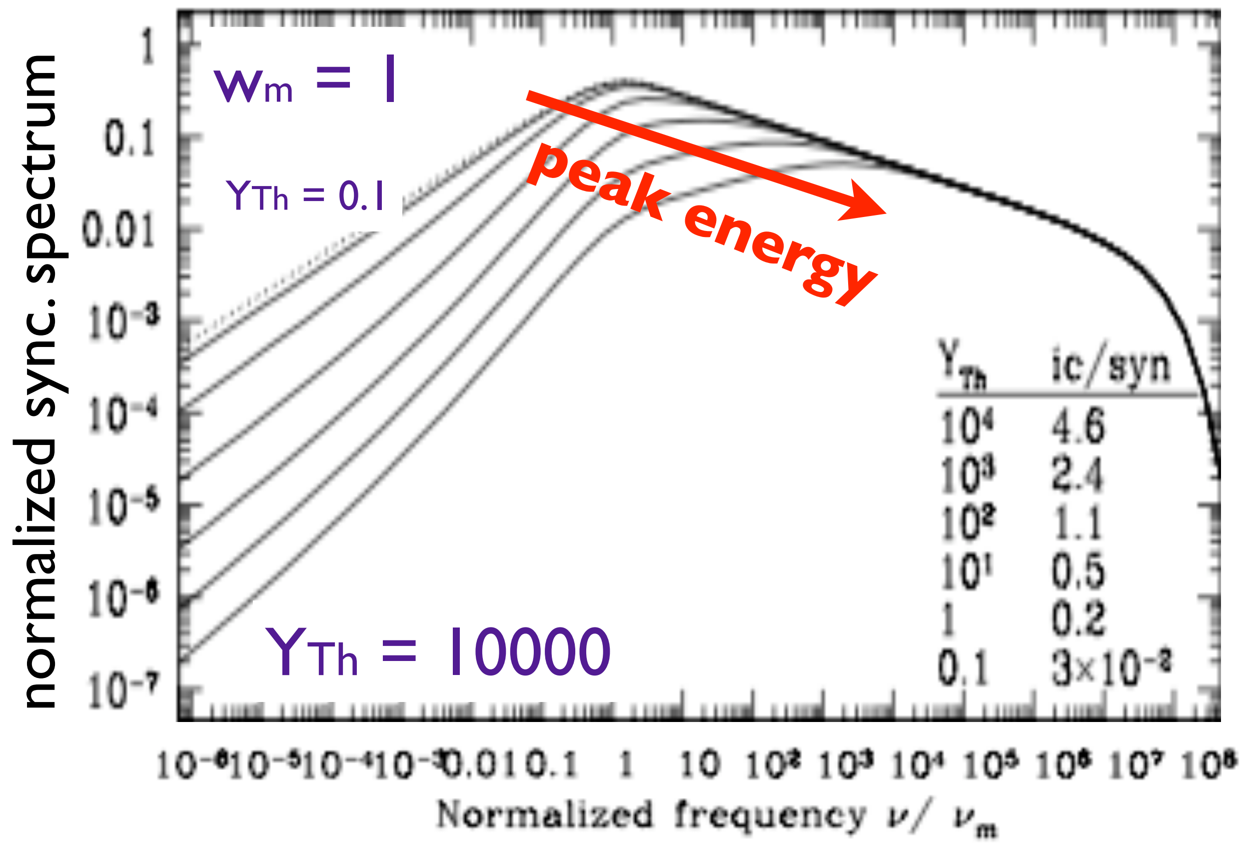

Daigne, Bosnjak & Dubus 2011

Numerical simulations show that this problem can be solved by a steeper slope of the relativistic electron distribution ($p > 2.7\text{-}2.8$) responsible for the emission is adopted (**Bosnjak & Daigne 2013 submitted**).

Spectral and temporal behavior: HIC & HFC

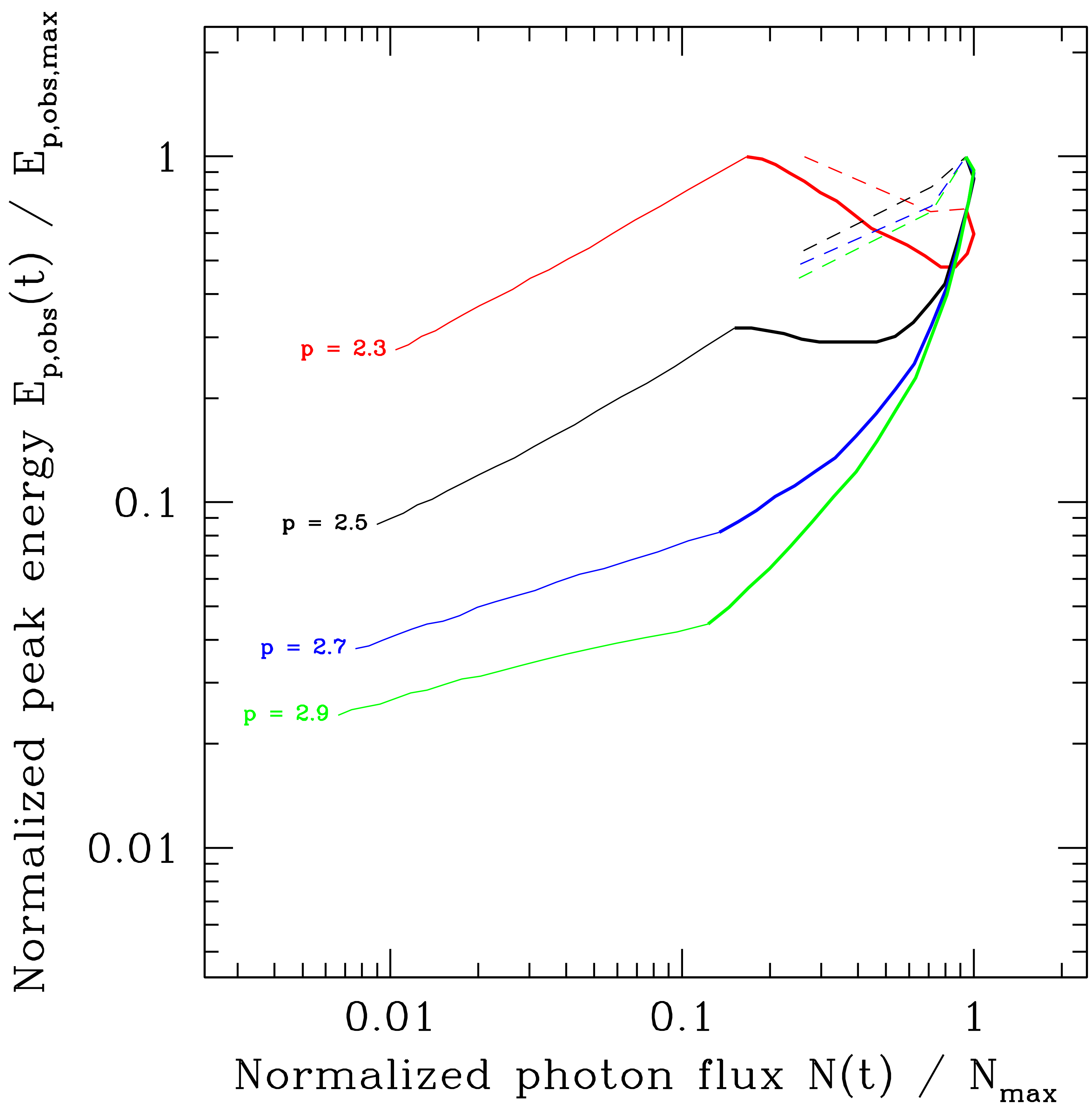

Bosnjak & Daigne 2013 submitted

Modeling of short pulses, multi-peaked bursts..

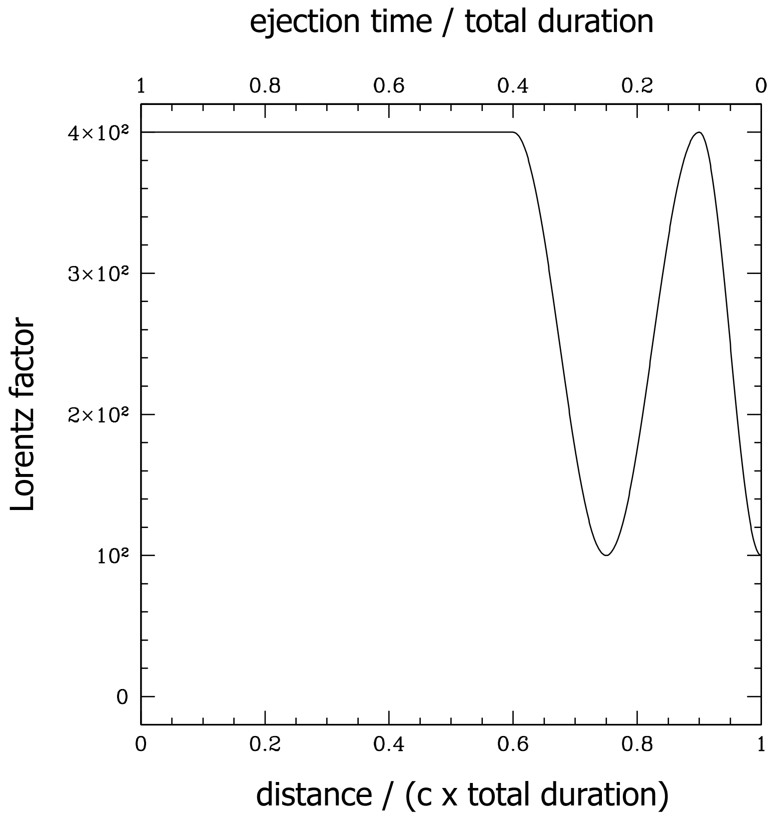

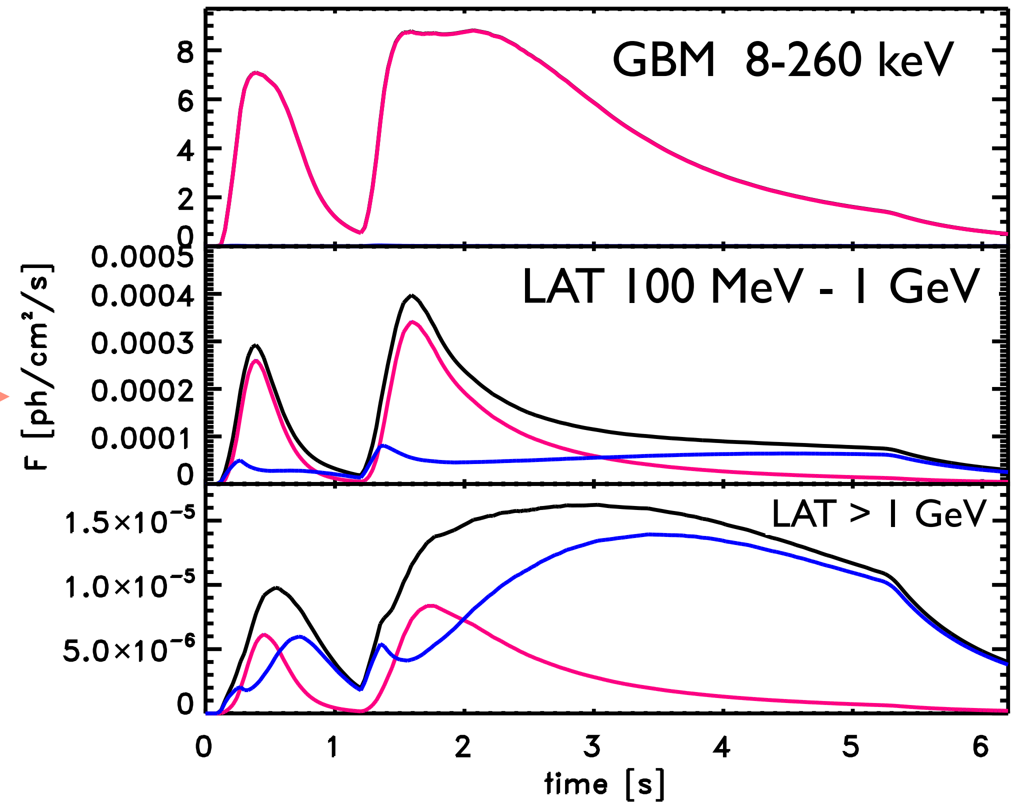

synchrotron
inverse Compton
total

Modeling of short pulses, multi-peaked bursts..

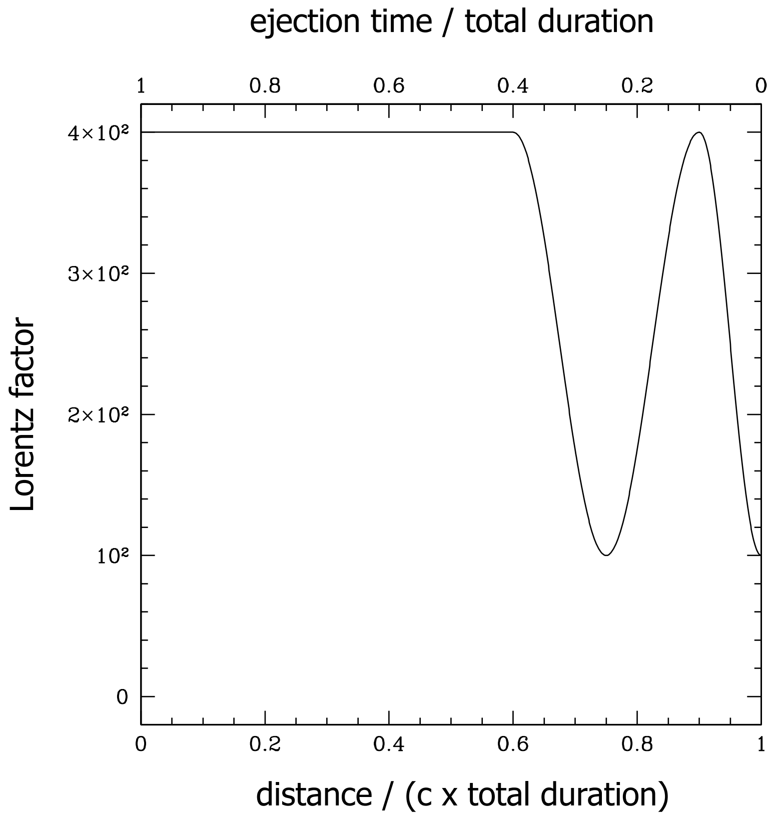

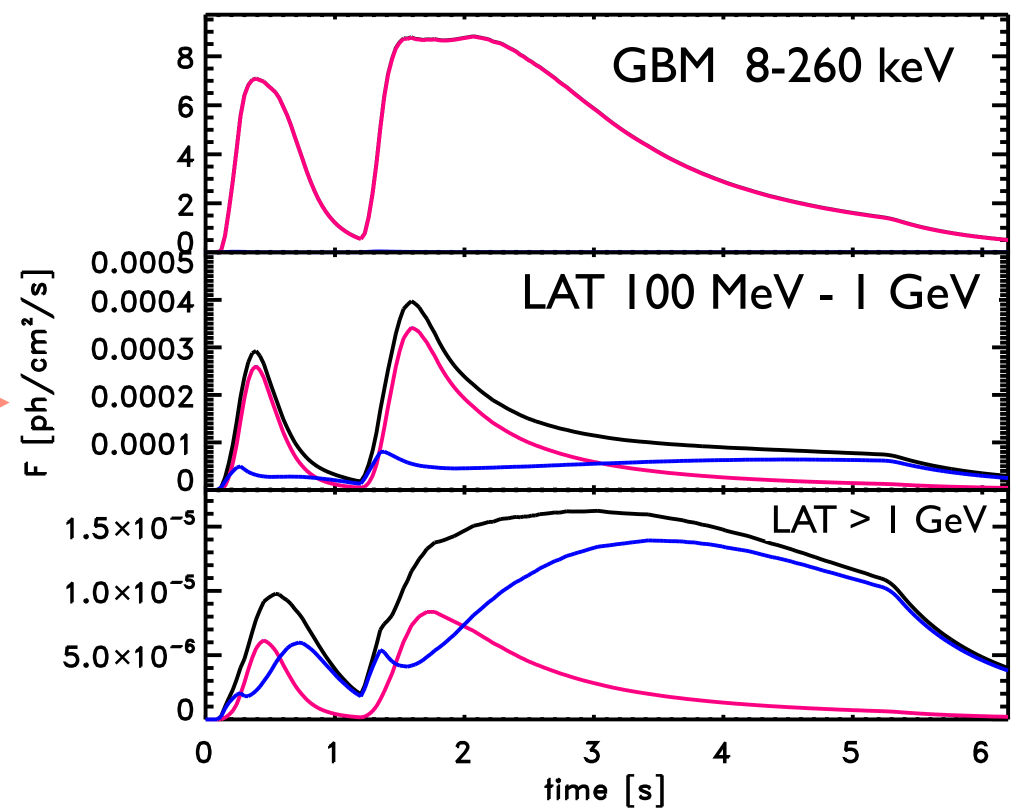

synchrotron
inverse Compton
total

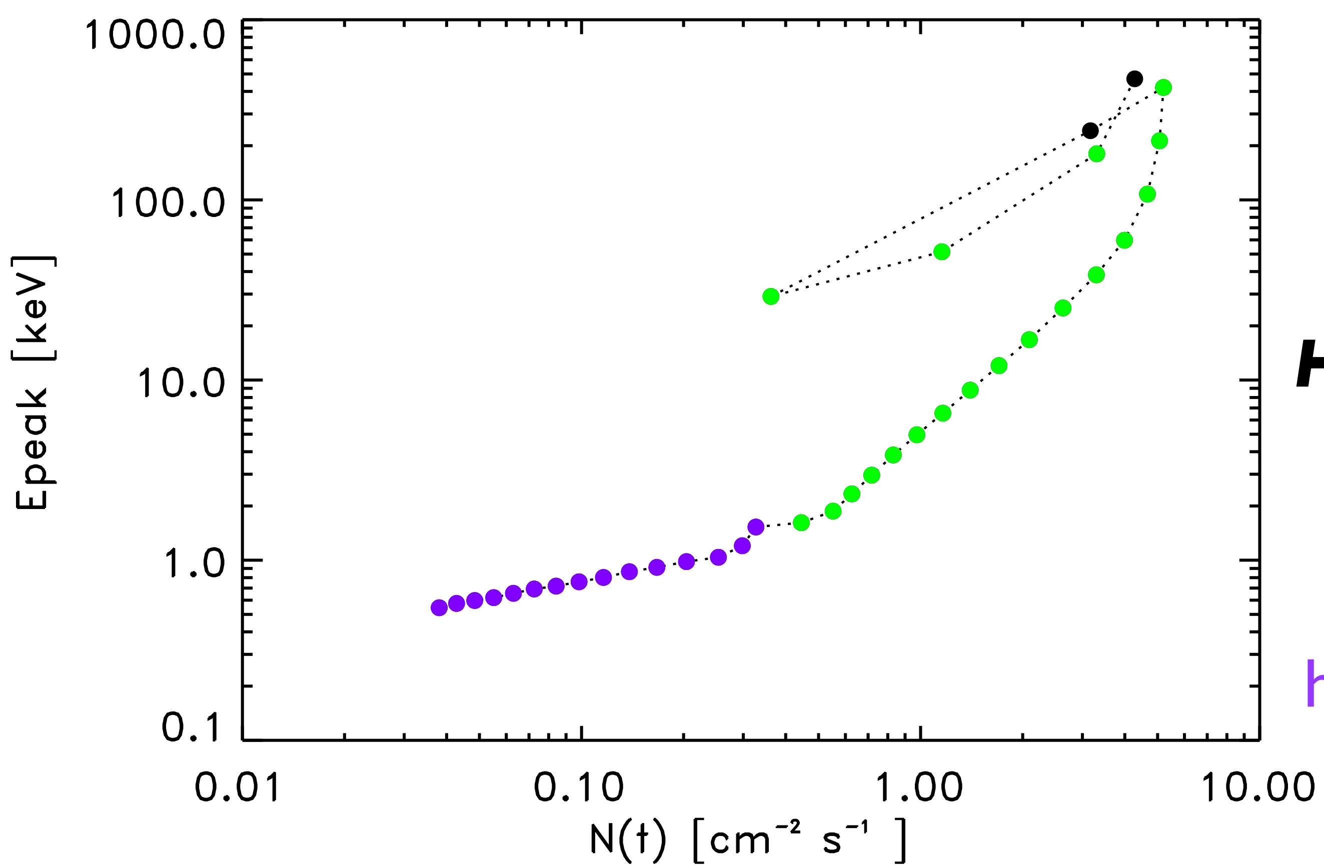

Hardness-intensity correlation:

pulse rise

pulse decay

high latitude emission

Spectral and temporal behavior: effect of the duration of the ejection

Bosnjak & Daigne 2013 submitted

- shorter pulses have higher peak energies

- for short pulses, as the peak energy is above BATSE ch 4, all light curves correspond to the same part of the spectrum and lags are negligible/the pulse has the same width

- the ratio of the rise time over the decay time tends to 1 for the shortest pulses

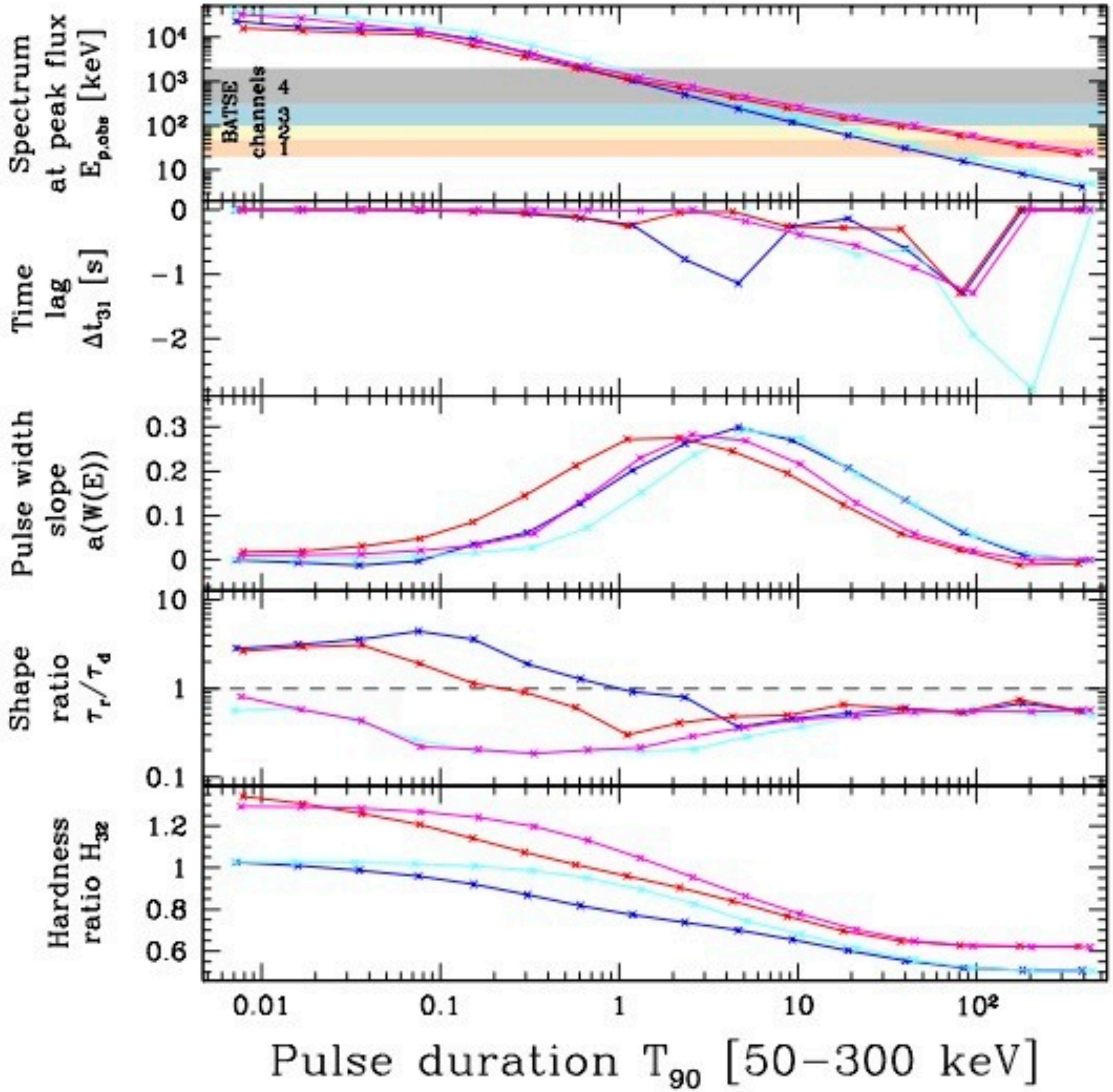

p=2.7

tw : 2 ms - 200s

high B: ζ = cte. ζ varying

low B: ζ = cte. ζ varying

Modeling of short pulses, multi-peaked bursts..

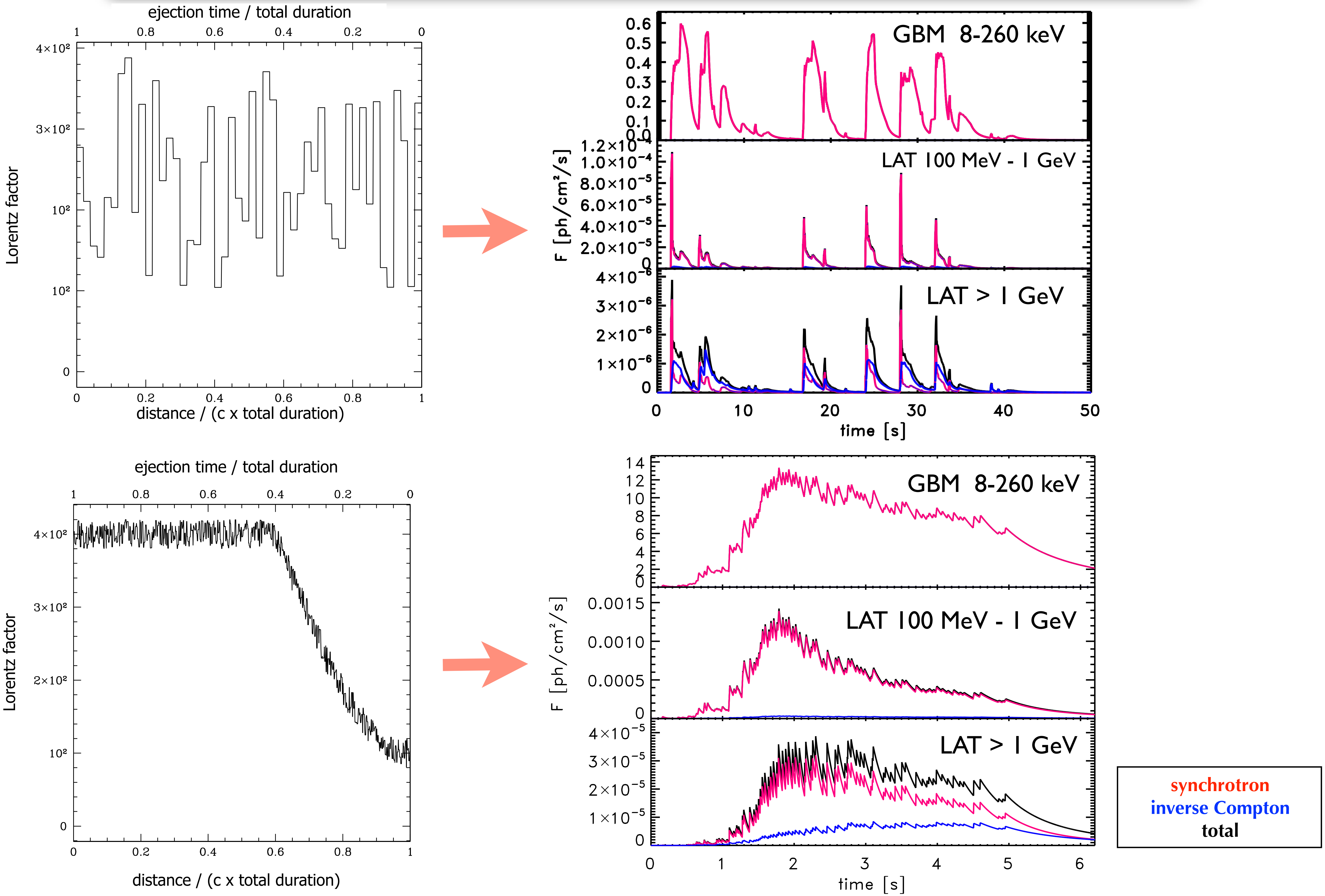

Summary

We developed **modeling tools to compute the GRB prompt emission from internal shocks in a time-dependent way** in different spectral bands, including the high-energy gamma rays

The exploration of the parameter space shows that we can expect two classes of broad-band spectra, which correspond to different physical conditions in the shocked region: **"synchrotron case"** (where the dominant process in Fermi-GBM range is synchrotron radiation) and **"inverse Compton case"** (where the synchrotron component peaks at low energy and dominant process in GBM range is inverse Compton)

Fermi GRB observations favor the **"synchrotron case", with inverse Compton scatterings occurring in Klein-Nishina regime. This scenario reproduces qualitatively the observed spectral evolution (HIC, HFC). We constrain the parameters of the model (p, ϵ_B, ζ) in order to have a quantitative agreement**